

**ANALYSIS OF GENETIC VARIATION OF THE PREGNANE X RECEPTOR
IN PUTATIVE CHOLESTATIC ADVERSE DRUG REACTIONS USING
ARCHIVAL LIVER BIOPSIES: IDENTIFICATION OF A NOVEL
DYSFUNCTIONAL PROTEIN VARIANT.**

Thesis submitted for the degree of
Doctor of Philosophy
at the University of Leicester

by

Daniel Frank Carr BSc (Hons), MSc
Department of Cancer Studies and Molecular Medicine
University of Leicester

June 2005

UMI Number: U204017

All rights reserved

INFORMATION TO ALL USERS

The quality of this reproduction is dependent upon the quality of the copy submitted.

In the unlikely event that the author did not send a complete manuscript and there are missing pages, these will be noted. Also, if material had to be removed, a note will indicate the deletion.



UMI U204017

Published by ProQuest LLC 2014. Copyright in the Dissertation held by the Author.
Microform Edition © ProQuest LLC.

All rights reserved. This work is protected against
unauthorized copying under Title 17, United States Code.



ProQuest LLC
789 East Eisenhower Parkway
P.O. Box 1346
Ann Arbor, MI 48106-1346

particularly drug-induced cholestasis.

Analysis of genetic variation in ADR is problematic due to their rarity and the difficulty in acquisition of a significant cohort. By screening an archive of clinical liver biopsies, 53 patients displaying evidence of cholestatic ADRs have been identified. These liver specimens were formalin-fixed, therefore nucleic acid yield and integrity is compromised. To overcome this, DNA extraction and amplification methods were optimised for sequencing of the open reading frames of the PXR gene allowing as little as 1ng of genomic DNA to be analysed. Simultaneous mRNA extraction and RT-PCR analysis was also developed.

In the majority of cases sequence analysis revealed no significant variants. However, in two cases (3.6%) a non-synonymous T/C base substitution encoding a novel PXR protein variant, C301R, was identified as a heterozygote in. In a normal control cohort of 308 no incidence of C301R was observed ($p=0,023$). Functional analysis using a reporter gene co-transfection assay of this variant discovered an apparent attenuation of ligand (hyperforin and rifampicin)-mediated transcriptional activation, of both ER6 and ER6 CYP3A response elements compared to the wild-type human PXR. The C301R variant displayed no loss of DNA response element binding compared to wild-type PXR.

The identification of this variant protein at a significantly increased frequency compared to a normal population, in a hepatic ADR cohort, would suggest that this apparently functional PXR variant may be one single predisposing factor to ADR. Similar utilisation of archival biopsies could be used to identify further candidate genes associated to ADR pre-disposition.

Acknowledgements

I would like to acknowledge and say a huge thank you to the following people for their important contributions to this study:

My supervisors, Dr Howard Pringle and Dr Jonathan Tugwood, for their knowledge support and help throughout the three years of this project. The experience and skills I have learnt through them will prove invaluable to me in the future.

Dr James Sidaway whose ideas and enthusiasm for the subject were what enabled this project to be initiated.

Mrs Linda Potter for her considerable assistance in optimising nucleic acid extraction protocols and performing “rapid” DNA extractions on the control tissue biopsy samples.

Mrs Johanna Loughlin for her huge assistance in performing the reporter gene assays and assisting with electrophoretic mobility shift assays. Her enthusiasm and patience knows no bounds.

The R&D Genetics department at AstraZeneca Pharmaceuticals, Alderley Park, particularly Miss Rachael Moore, for undertaken sequencing of PCR products and assisting in the analysis of sequence data.

Dr Angus McGregor for undertaking the histopathology assessment of the ADR hepatic biopsy specimens and providing his expertise to obtain the microscopic images within this study.

All members of the Cell Signalling and Interaction Group, Department of Cancer Studies and Molecular Medicine, University of Leicester for making my time in the department so enjoyable.

My family for their support and my parents, Frank and Teresa for giving me all the opportunities in life I could ever wish for.

Last but by no means least; I’d like to thank Charlotte Fraser, my best friend and soul mate for her continued love, support and belief in me.

All other work within this thesis was undertaken by me (Daniel F. Carr)

Abbreviations

ABC	ATP-Binding Cassette
ADR	Adverse Drug Reaction
ALF	Acute Liver failure
ALP	Alkaline Phosphatase
ALT	Alanine Transaminase
B2M	Beta-2-Macroglobulin
BSEP	Bile Salt Export Pump
cDNA	Complimentary Deoxyribonucleic Acid
CYP	Cytochrome P450
DBD	DNA Binding Domain
DMSO	Dimethyl Sulphoxide
DNA	Deoxyribonucleic Acid
DTT	Dithiotheritol
DOP	Degenerate Oligonucleotide Primer
EDTA	Ethylenediamine Tetraacetic Acid
EMSA	Electrophoretic Mobility Shift Assay
FGA	Fibrinogen A
FXR	Farnesoid X Receptor
GE	Gel Electrophoresis
GPA	Global Polyadenylation
GR	Glucocorticoid Receptor
GST	Glutathione S-Transferase
H&E	Haematoxylin and Eosin
HFE	Human Haemochromatosis
HNF	Hepatocyte Nuclear Factor
HypF	Hyperforin
IPEP	Improved Primer Extension Preamplification
LBD	Ligand Binding Domain
LCA	Lithocholic Acid
LFT	Liver Function Test
LRH	Liver Receptor Homologue

MCA	Medicine Control Agency
MDR	Multidrug Resistance
MDR	Multi-Drug Resistance
mRNA	Messenger Ribonucleic Acid
NCBI	National Centre for Biotechnology
NTCP	Sodium Taurocholate Co-transporting Protein
OATP	Organic Anion Transporting Polypeptide
PAPSS	3'-phosphoadenosine 5'-phosphosulfate synthetase
PBC	Primary Biliary Cirrhosis
PCN	Pregnenolone 16 α -Carbonitrile
PCR	Polymerase Chain reaction
PFIC	Progressive Familial Intrahepatic Cholestasis
PR	Progesterone Receptor
PSC	Primary Sclerosing Cholangitis
PPAR	Peroxisome Proliferator Activated Receptor
PXR	Pregnane X Receptor
QPCR	Quantitative Polymerase Chain Reaction
RIF	Rifampicin
RNA	Ribonucleic Acid
RT-PCR	Reverse Transcriptase-PCR
RU486	Mifepristone
RXR	Retinoid X Receptor
SAP	Shrimp Alkaline Phosphatase
SDS	Sodium Dodecyl Sulphate
SHP-1	Short Heterodimer Partner 1
SNP	Single Nucleotide Polymorphism
sPGP	Sister of P-Glycoprotein
SSCP	Single Strand Conformation Polymorphism
STD	Dehydroepiandrosterone Sulfotransferase
STR	Short Tandem Repeat
SXR	Steroid X Receptor
TAE	Tris Acetate EDTA
TBE	Tris Borate EDTA

TBS	Tris-Buffered Saline
TDT	Terminal Deoxynucleotidyl Transferase
TEMED	Tetramethylethylenediamine
UGT	Uridine diphosphate-glucuronosyltransferase
ULN	Upper Normal Limit
UTR	Untranslated Region
VBDS	Vanishing Bile Duct syndrome
WGA	Whole Genome Amplification

Content

	<u>Page</u>
Abstract	1
Acknowledgements	2
Abbreviations	3
Table of Contents	6
List of Figures	12
List of Tables	15
Chapter 1: Introduction	16
1.1 Drug-Induced Liver Injury (DILI).	17
<i>1.1.1 Genetic Susceptibility to DILI</i>	<i>20</i>
1.2 Drug-induced Cholestasis.	22
<i>1.2.1 Pure Cholestasis</i>	<i>22</i>
<i>1.2.2 Genetic Susceptibility to Cholestatic Liver Disease</i>	<i>23</i>
1.3 Nuclear Hormone Receptor Super Family.	26
<i>1.3.1 Response element and DBD.</i>	<i>26</i>
<i>1.3.2 Ligand-Binding and Activation</i>	<i>26</i>
1.4 Pregnane X Receptor (PXR).	27
<i>1.4.1 Activation of hPXR by a diverse range of xenobiotics</i>	<i>28</i>
<i>1.4.2 Genetic variation of hPXR</i>	<i>30</i>
<i>1.4.3 Transcriptional variation of hPXR.</i>	<i>33</i>
<i>1.4.4 Regulation of Hepatic Detoxification pathways by hPXR</i>	<i>35</i>
1.5 Farnesoid X Receptor (FXR).	36
1.6 Role of PXR and FXR in Bile Acid Homeostasis.	37
<i>1.6.1 Regulation of Hepatobiliary Transport by PXR and FXR.</i>	<i>38</i>
<i>1.6.2 Regulation of Cholesterol Catabolism by PXR and FXR.</i>	<i>41</i>
1.7 Aims and Objectives.	44
Chapter 2: Materials and Methods	46

2.1	Materials	47
2.1.1	<i>Chemicals and kits</i>	47
2.1.2	<i>Enzymes</i>	49
2.1.3	<i>Plasmids</i>	50
2.1.4	<i>Buffers, Solutions and other agents</i>	50
2.1.5	<i>Control Liver DNA</i>	54
2.2	Methods	54
2.2.1	<i>Nucleic Acid Extraction</i>	54
2.2.1.1	RNA Isolation.	55
2.2.1.2	DNA Isolation.	55
2.2.1.3	“Rapid” DNA Isolation	55
2.2.1.4	DNA Quantification by PicoGreen™ Fluorescence Assay.	56
2.2.2	<i>Whole Genome Amplification (WGA).</i>	56
2.2.2.1	Global Polyadenylation (GPA) PCR	56
2.2.2.2	Improved Primer Extension Preamplification (IPEP).	57
2.2.2.3	Specific Target PCR amplification of WGA products	57
2.2.3	<i>Multiplex Nested PCR Amplification</i>	58
2.2.3.1	Modified Multiplex Nested PCR Amplification	59
2.2.4	<i>Reverse Transcriptase PCR</i>	61
2.2.4.1	cDNA Synthesis	61
2.2.4.2	PCR amplification of cDNA	61
2.2.4.3	Primer Design for cDNA amplification	61
2.2.5	<i>Restriction Endonuclease Digestion of PCR Products</i>	62
2.2.5.1	BccI Restriction Endonuclease	62
2.2.5.2	MwoI Restriction Endonuclease	62
2.2.6	<i>Gel Electrophoresis (GE)</i>	62
2.2.6.1	<u>Agarose Gel Electrophoresis</u>	62
2.2.6.2	Polyacrylamide Gel Electrophoresis And Silver Staining	63
2.2.7	<i>DNA Sequencing</i>	63
2.2.8	<i>In vitro mutagenesis</i>	64
2.2.9	<i>Western Blotting</i>	64
2.2.9.1	In vitro coupled transcription/ translation	64
2.2.9.2	Preparation and quantification of HeLa cell protein lysates	65

2.2.9.3	Sodium Dodecyl Sulphate-Polyacrylamide Gel Electrophoresis (SDS-PAGE)	65
2.2.9.4	Transfer and Blocking	65
2.2.9.5	Antibody Labelling	66
2.2.10	<i>Reporter gene co-transfection assay</i>	66
2.2.10.1	Preparation of HeLa cell lysates for mRNA analysis.	67
2.2.11	<i>Electrophoretic mobility shift assay</i>	68
2.2.11.1	$\gamma^{32}\text{P}$ Radio-labelling of Double-Stranded Oligonucleotide	68
2.2.11.2	EMSA DNA/Protein Complex Binding Reaction	68
2.2.11.3	Biotinylated EMSA complex detection.	69
2.2.12	<i>Other protocols.</i>	69
2.2.12.1	Preparation of charcoal-stripped foetal calf serum.	69
2.2.13	<i>Statistical Analysis</i>	70

Chapter 3: Identification and characterization of a hepatic ADR cohort from the clinical tissue archive. **71**

3.1	Adverse Drug Reaction Cohort Identification.	72
3.2	Blood Serum Liver Function Test Data for ADR Cohort.	75
3.3	Morphological Assessment and Classification.	77
3.4	Discussion	82
3.4.1	<i>Selection of hepatic ADRs from the archival collection.</i>	82
3.4.2	<i>Evaluation of LFT data from ADR cohort selection.</i>	83
3.4.3	<i>Relationship of serum LFT data with reassessed histology.</i>	84
3.4.4	<i>Could altered PXR functionality be a predisposing factor in the drug-induced aetiology of the ADR cases?</i>	84
3.4.5	<i>Conclusions</i>	85

Chapter 4: Whole Genome Amplification and Nested PCR Pre-Amplification for Analysis of DNA from low yield formalin-fixed tissue.

4.1 Introduction	87
4.1.1 <i>Formalin Fixation</i>	87
4.1.2 <i>Whole Genome Amplification</i>	88
4.2 DNA Pre-amplification	91
4.2.1 <i>Whole Genome Amplification</i>	91
4.2.2.1 <i>Global polyadenylation PCR</i>	91
4.2.2.2 <i>Improved primer extension pre-amplification</i>	94
4.2.2 <i>Multiplex Nested Pre-amplification (MNP)-PCR</i>	99
4.3 Intersample variability of formalin-induced DNA degradation	102
4.4 Inter-sample contamination controls	105
4.4.1 <i>Sample discrimination by use of the fibrinogen A short tandem repeat (STR) locus.</i>	106
4.4.2 <i>Allele frequency comparison with a published SNP</i>	110
4.5 mRNA expression analysis from formalin-fixed liver biopsies.	114
4.6 Discussion	116
4.6.1 <i>Pre-amplification of DNA from formalin fixed tissue.</i>	116
4.6.2 <i>Multiplex PCR for pre-amplification of DNA from formalin-fixed tissue.</i>	117
4.6.3 <i>Internal controls for evaluation of inter-sample contamination of multiplex PCR pre-amplification.</i>	118
4.6.4 <i>Simultaneous gene expression and sequence analysis from formalin-fixed tissue.</i>	120
4.6.5 <i>Conclusions</i>	121

Chapter 5: Sequence variation of the hPXR Gene within an Adverse Drug Reaction Cohort.

5.1 Identification of a potential novel SNP within the hPXR-LBD.	124
5.1.1 <i>In silico prediction of structure and function of C301R variant</i>	125
5.1.2 <i>Determination of C301R allelic frequency</i>	127

5.2	Creation of a C301R variant human PXR cDNA clone.	130
5.3	Reporter gene co-transfection assay of C301R basal and drug-induced activation of downstream proximal promoter response elements.	134
5.3.1	<i>Selection of a host cell-line for PXR transfection assay.</i>	134
5.3.2	<i>Confirmation of expression of transfected wild-type and C301R variant PXR in a HeLa cell system.</i>	136
5.3.3	<i>Effect of the C301R protein variation on hyperforin-induced PXR activation.</i>	138
5.3.4	<i>Effect of the C301R protein variation on rifampicin--induced PXR activation.</i>	142
5.3.5	<i>Effect of the C301R protein variation on lithocholic acid-induced PXR activation.</i>	144
5.4	Does the C301R variant confer human PXR with rodent PXR-like ligand-binding and activation properties?	146
5.4.1	<i>Effect of the C301R protein variation on dexamethasone-induced PXR activation.</i>	147
5.4.2	<i>Effect of the C301R protein variation on PCN-induced PXR activation.</i>	147
5.5	Effect of C301R variation on PXR heterodimerisation with RXR and subsequent ER6 and DR3 response element.	144
5.6	Does the presence of the C301R variant exert an attenuation of wild-type PXR basal and hyperforin-mediated activation?	157
5.7	Hepatic histology of the two C301R positive ADR cases	160
5.8	Discussion	160
5.8.1	<i>Identification of the C301R variant allele.</i>	160
5.8.2	<i>Frequency of C301R in ADR and control populations.</i>	163
5.8.3	<i>Creation of C301R mutant PXR cDNA clone.</i>	164
5.8.4	<i>C301R induces a significant attenuation of ligand-modulated PXR activation.</i>	165
5.8.5	<i>Mutation of residue 301 does not infer PXR within rodent PXR-like activation properties.</i>	167
		168

5.8.6	<i>C301R exhibits no alteration in the DNA binding activity of human PXR</i>	169
5.8.7	<i>Wild-type PXR activation, in the presence of the C301R variant is significantly impaired.</i>	169
5.8.8	<i>Concurrence of C301R functionality with liver histology and LFT data.</i>	170
5.8.9	<i>Conclusions</i>	
Chapter 6:	General Discussion.	171
6.1	Identification and characterisation of an ADR cohort.	172
6.2	Use of DNA preamplification in genotypic analysis of formalin-fixed archival tissue.	173
6.3	PXR protein variant C301R demonstrates significantly increased frequency in an ADR cohort and attenuated functionality.	175
6.4	Possible Future Work	179
6.5	Conclusions	181
	References	183
	Appendices	200

List of Figures

	<u>Page</u>
1.1 Bland cholestasis in a 5 μ m liver core needle biopsy.	25
1.2 The genomic organisation and schematic structure of the hPXR gene.	29
1.3 Reported non-synonymous variant human PXR alleles.	32
1.4 Splice variation of human PXR gene transcripts.	34
1.5 PXR and FXR mediate bile acid-activated transcription of genes involves in hepatic bile acid clearance.	39
1.6 Regulation of Bile acid homeostasis and cholesterol catabolism by FXR and PXR.	42
2.1 Primer design strategy for multiplex nested PCR amplification of the human PXR gene exonic regions.	60
3.1 Identification of a Hepatic ADR cohort from a clinical archive of core needle liver biopsies.	70
3.2 Blood serum liver function test levels in the ADR patient cohort.	72
3.4 Representative (H&E) stained liver histology from ADR patients exhibiting cholestatic injury.	75
3.5 Representative (H&E) stained liver histology from ADR patients exhibiting fatty change (steatosis).	76
3.6 Bile duct injury associated with hepatic adverse drug reactions.	77
4.1 An Hepatic Core Needle Biopsy.	89
4.2 Global Polyadenylation-PCR DNA yield from varying amounts of input formalin-fixed liver DNA.	92
4.3 PCR amplification of the hPXR functional domain from the product of DNA globally pre-amplified by GPA-PCR.	93
4.4 PCR amplification of the hPXR functional domain from the IPEP-PCR product of 25ng formalin-fixed DNA extracted from a 5 μ m true cut liver biopsy section.	95
4.5 Improved Primer Extension Preamplification-PCR DNA yield from varying amounts of input formalin-fixed liver DNA.	97

4.6	PCR amplification of amplicons spanning the hPXR 5'UTR from IPEP-PCR products preamplified from varying amounts of input DNA.	98
4.7	Multiplex Nested PCR preamplification yield from varying amounts of input formalin-fixed liver DNA from a single 5µm true cut biopsy section.	100
4.8	PCR amplification of amplicons within the hPXR functional domain from the product of multiplex nested-PCR preamplification.	101
4.9	Multiplex nested PCR amplification of hPXR exons from DNA extracted from hepatic core-needle biopsy tissue (patient 26 of the ADR cohort).	104
4.10	Multiplex nested PCR amplification of the FGA STR locus from DNA extracted from hepatic tissue samples of the ADR cohort.	107
4.11	STR profile of a multiplex nested preamplification of formalin-fixed DNA from an ADR cohort liver biopsy.	109
4.12	BccI restriction digestion of Exon 7, product A, for determination of rs227678 SNP in 12 hepatic tissue samples from the ADR cohort.	111
4.13	Percentage frequency of variant alleles for the rs2276708 SNP in the normal, metastatic and ADR cohorts	112
4.14	mRNA expression analysis PXR and downstream target genes from a single 5µM hepatic core needle biopsy section.	115
5.1	Sequence analysis of a potential novel SNP in the hPXR-LBD of an individual within the ADR cohort.	120
5.2	Confirmation of 2 members of the ADR cohort possessing the C301R human PXR variant allele	126
5.3	<i>In vitro</i> mutagenesis of the wild-type human PXR cDNA clone.	128

5.4	Sequencing confirmation of <i>in vitro</i> mutagenesis to introduce the C301R mutation into the wildtype human PXR cDNA clone	132
5.5	<i>In vitro</i> transcription and translation of wildtype and C301R human PXR cDNA clones.	133
5.6	Basal activation of human wild-type and C301R PXR variants.	135
5.7	mRNA and protein expression levels of human PXR in HeLa cells transfected with PXR cDNA clones.	137
5.8	Hyperforin-induced activation of wild-type and C301R PXR variants in a HeLa cell co-transfection assay with a DR3-response element reporter gene.	139
5.9	Hyperforin-induced activation of human wild-type and C301R PXR variants in HeLa cell co-transfection assay with an ER6-response element reporter gene.	141
5.10	Rifampicin-induced activation of human wild-type and C301R PXR variants in a HeLa cell co-transfection assay with a DR3 and ER6)-response element reporter gene.	143
5.11	Lithocholic Acid-induced activation of human wild-type and C301R PXR variants in a HeLa cell co-transfection assay with a DR3 and ER6-response element reporter gene.	145
5.12	Dexamethasone-induced activation of rat PXR and human wild-type and C301R PXR variants in a HeLa cell co-transfection assay.	148
5.13	PCN-induced activation of rat PXR and human wild-type and C301R PXR variants in a HeLa cell co-transfection assay.	149
5.14	Electrophoretic mobility shift assay of PXR/RXR/ER6 CYP3A4 response element by wild-type and C301R PXR variants.	151
5.15	Initial radio-labelled electrophoretic mobility shift assay of PXR/RXR/ER6 CYP3A4 response element by wild-type and C301R PXR variants.	153
5.16	Electrophoretic mobility shift assay of PXR/RXR/ER6 CYP3A4 response element by wild-type and C301R PXR variants.	154

5.17	Electrophoretic mobility shift assay of PXR/RXR/DR3 CYP3A4 response element by wild-type and C301R PXR variants.	156
5.18	Effect of C301R co-transfection on wild-type PXR basal and hyperforin activation.	158
5.19	Liver Histology of ADR patient number 4, a PXR C301R positive patient.	161
5.20	Liver Histology of ADR patient number 10, a PXR C301R positive patient.	162

List of Tables

3.1	Classification of the morphology of hepatic biopsy sections from the ADR patient cohort.	74
4.1	Statistical analysis of rs2276708 SNP genotype within normal, metastatic and ADR liver biopsy cohorts	113
5.1	Frequency of the C301R PXR variant allele in the ADR, normal and metastatic populations as determined by the MwoI restriction digest screen.	129

Chapter 1: Introduction

Introduction

“A diamond with a flaw is worth more than a pebble without imperfections”
(Chinese Proverb)

Within the population, idiosyncratic drug reactions occur. As the name suggests predicting individual responses (both pharmacological and toxicological) is a challenge. However of such reactions are rare and the frequency of individuals carrying any given specific genetic predisposition is even lower. This study seeks to isolate the “diamonds” (individuals predisposed to adverse drug reactions) from the “pebbles” (general population) in order to identify and characterise the “flaws” (genetic predispositions).

1.1 Drug-Induced Liver Injury (DILI).

The pathology of drug-induced liver injury covers a broad spectrum. Though commonly manifesting as hepatitis and/or cholestasis, virtually any pattern of acute or chronic liver disease can occur. Particular drugs are often associated with characteristic types of liver injury. The antiarrhythmic amiodarone is associated with incidence of macrovesicular steatosis (hepatic fatty accumulation) and phospholipidosis (phospholipid accumulation) (Pessayre *et al.*, 1999). Diclofenac, a widely-used anti-inflammatory is commonly associated with incidence of hepatocellular hepatitis, though a number of cholestatic or mixed injury cases have been observed (Pessayre *et al.*, 1999). A large number of drugs are associated with a mixed pattern of disease, characterised by the presence of both hepatocellular necrosis and cholestatic liver injury. Examples of such drugs are diverse and include the anticonvulsant carbamazepine where hepatitis with acute cholangitis has been

observed (Larrey *et al.*, 1987), and the tricyclic antidepressant, amitriptyline (Pessayre *et al.*, 1999).

The most severe pattern of injury is massive necrosis, presenting as acute liver failure (ALF). In the United States 2,000 cases of ALF occur annually, 16% of which are due to idiosyncratic drug reactions (Bissell *et al.*, 2001). The infrequent occurrence of such reactions is further highlighted by data from a group from Newcastle, UK who identified, clinically and histologically, just 44 cases of idiosyncratic drug reactions over an 18-year period (Aithal and Day, 1999). Initially this study considered 110 cases but the final cohort of 44 was arrived at by discriminating against cases where overdoses or non-drug causes were suspected or where no suspect drug therapy could be identified. Such drug-induced liver injury cases represent the more severe “tip of the iceberg”, since many other drug effects are milder and do not justify an intrusive liver biopsy procedure. There is also evidence that only a small minority of hepatic adverse drug reactions are actually reported to regulatory bodies. A French population-study obtained 34 hepatic ADRs over a period of three years amounting to an incidence of 13.9 ± 2.4 per 100,000 people (Sgro *et al.*, 2002). This study concluded that the actual incidence of hepatic ADR in the French population was actually 16 times greater than that spontaneously reported to regulators. A South Wales population study of cases of clinically obvious jaundice (Whitehead *et al.*, 2001) observed drug toxicity as the cause in 7/121 cases (5.7%) with a total incidence of 7 in approximately 369,000 (1.8 in 100,000). There is also some suggestion that of misdiagnosis of hepatic ADRs. As well as suggesting under-reporting of hepatic ADRs via the British yellow-card reporting system, (Aithal *et al.*, 1999) suggest that almost half of reported hepatic ADRs are almost certainly unrelated to the incriminated drug. This could cause delay in obtaining correct diagnosis and

withdrawal of the offending compound. (Aithal *et al.*, 1999) found that misdiagnosis of hepatic ADR had occurred in 65/138 cases (47%) with a further 21 (15%) undetermined.

At present there are no diagnostic markers for drug-induced liver injury and therefore assessment is often based on circumstantial evidence. This can lead to variability in case causality assessment. A number of consensus meetings have endeavoured to address this issue (Danan, 1988) and in 1990 a series of international consensus criteria were agreed upon (Benichou, 1990). These criteria ultimately categorise cases in drug-related, non-drug-related and indeterminate. More recently a clinical diagnostic scale (CDS) for diagnosis of drug-induced liver injury has been developed (Maria and Victorino, 1997). CDS scoring has been assessed (Aithal *et al.*, 2000) and appears to correlate well with the international consensus criteria. The CDS is able to apply a numerical score to each case and by applying a “cut-off” score allows for easier clinical application (Aithal *et al.*, 2000).

The frequency and economic impact of idiosyncratic drug reactions are a long-standing challenge to both the pharmaceutical industry and regulatory bodies. These problems have recently been highlighted by cases of troglitazone-associated idiosyncratic drug reactions (Kohlroser *et al.*, 2000; Murphy *et al.*, 2000).

Troglitazone, a peroxisome proliferator-activated receptor gamma (PPAR γ) agonist, was an approved drug for the treatment of diabetes mellitus. Estimates suggest that 1:1250 patients taking troglitazone developed jaundice and 1:40,000 to 1:50,000 developed irreversible liver failure leading to death or transplantation (Bissell *et al.*, 2001). Medicine Control Agency (MCA) approval was subsequently revoked in December 1997 and the manufacturers (Warner-Lambert) felt it necessary to

voluntarily withdraw troglitazone from the market in Europe with the US following suit in March 2000.

The reasons for such a drug receiving approval, and being able to cause such injury, lies within the limitations of hepatotoxicity assessment prior to approval (Lee, 2000). For example, if 5000 patients participate in a clinical trial, the observed incidence of troglitazone-induced jaundice is likely to be at a frequency of approximately 4 individuals. However drug reaction causing irreversible liver failure occurring in a cohort of 5000 is highly unlikely to be demonstrable.

The elucidation of the mechanisms associated with such idiosyncratic drug reactions is still a major barrier to overcome. However, the fast evolving field of pharmacogenetics has provided a new approach to the problem. Given a finite number of pharmacokinetic processes and pathways of hepatotoxicity, it should be possible, in the future, to prepare genetic profiles associated with increased risk of various drug-induced reactions. Thus an individual's risk for hepatotoxicity following drug administration could be predicted (McCarthy and Hilfiker, 2000).

1.1.1 Genetic Susceptibility to DILI

A number of studies have been undertaken which demonstrate an association between specific drug-induced hepatotoxicity and polymorphisms of both the immune system and drug metabolising pathways. In the case of the anti-inflammatory diclofenac, (Aithal *et al.*, 2000) noted that variant alleles of the CYP2C9 gene, termed CYP2C9*2 and *3 were not a determinant of diclofenac-induced hepatotoxicity, though CYP2C9*3 demonstrated reduced 4'-hydroxylation activity compared to wild-type. These same two variant alleles have previously been associated with altered pharmacokinetics of the anti-coagulant warfarin (Aithal *et al.*, 1999). CYP2C9*2 and

*3 are both associated with lower warfarin dose requirement and bleeding complications in patients. Further studies by (Aithal *et al.*, 2004) suggest cytokine polymorphisms, specifically IL-4 and IL-10, are associated with diclofenac hepatotoxicity. A possible association with HLA (human leukocyte antigen)-11 has also been reported (Berson *et al.*, 1994). Studies have also shown an association between a specific HLA-DRB haplotype and hepatotoxicity induced by the antibiotic co-amoxiclav (Hautekeete *et al.*, 1999; O'Donohue *et al.*, 2000). (Sharma *et al.*, 2002) also described an association between HLA-DQ genotype and development of hepatotoxicity by administration of the antituberculosis therapy, isoniazid. These, and other studies, suggest an important role for the immune system in determining susceptibility to drug-induced toxicity by a number of compounds.

Drug-induced liver injury has, however, been associated with polymorphisms of a number of both phase 1 and 2 xenobiotic metabolising enzymes. Other isoniazid hepatotoxicity-associated susceptibility risks, for instance, include polymorphisms of the N-acetyltransferase 2 gene and a CYP2E1 c1 genotype (Huang *et al.*, 2003; Huang *et al.*, 2002). An association between troglitazone hepatotoxicity and a double-null GSTM1 and T1 genotype has been proposed (Watanabe *et al.*, 2003). (Simon *et al.*, 2000) also proposed this combination as a risk factor in transaminitis induced by administration of the acetylcholinesterase inhibitor tacrine. The studies described here highlight examples of the diversity of the genetic susceptibility factors associated with drug-induced liver injury. The diversity of genetic factors coupled with the range of observed patterns of drug-induced liver injury highlights the complex and heterogeneous nature of this disease state.

1.2 Drug-induced Cholestasis.

Classically defined as impairment in bile formation and/or flow, cholestasis is a common manifestation of drug-induced liver disease. Though there is insufficient data regarding the true incidence in the United Kingdom, Danish literatures suggests that cholestatic injury accounts for 17% of all hepatic adverse drug reactions (Friis and Andreasen, 1992). A broad clinical-pathologic spectrum of acute injury is produced that includes simple jaundice, pure cholestasis, cholestatic hepatitis and bile duct injury mimicking extrahepatic biliary obstruction (Lewis and Zimmerman, 1999).

1.2.1 Pure Cholestasis

Often referred to as simple, bland, or canalicular cholestasis, this form of drug-induced cholestatic liver injury is rare. Early symptoms include nausea and malaise followed by the development of jaundice pruritus (itching of the skin). Typical biochemical aberrations include a relatively small increase in serum alkaline phosphatase (associated with significant hyperbilirubinemia) and mildly abnormal liver transaminase levels. Histologically, pure cholestasis is quite distinct from the more common cholestatic hepatitis (Figure 1.1). Bland cholestasis shows no sign of inflammatory infiltrate (particularly eosinophils) or necrosis, features quite apparent in cholestatic hepatitis (Levy and Lindor, 2003). Dilated canaliculi filled with bile casts (or plugs) can also be seen, particular in the centrilobular area of the liver (Lewis and Zimmerman, 1999).

International consensus criteria of drug-induced liver disorders defines the biochemical classification of cholestasis by “An increase of more than twice the upper

limit of normal range in alkaline phosphatase alone or a ratio to alanine transaminase $R < 5$ " (Benichou, 1990).

1.2.2 Genetic Susceptibility to Cholestatic Liver Disease

Mutated genes, primarily encoding for transporter proteins, have been identified as key components of several hereditary types of cholestatic disease (Bull, 2002).

Benign recurrent intrahepatic cholestasis (BRIC) is an autosomal recessive inherent condition where sufferers experience recurrent bouts of intrahepatic cholestasis that resolve spontaneously with no lasting liver damage. Progressive familial intrahepatic cholestasis is a more severe autosomal recessive disorder which manifests as cholestasis in infancy, malnutrition and often end-stage liver disease before adulthood. Both BRIC (Houwen *et al.*, 1994) and a form of PFIC, termed PFIC1 or Bylers' Disease (Carlton *et al.*, 1995), have been localised to chromosome 18q21-22. Further studies identified the gene mutated in both disorders as ATP8B1, a member of the ATP-dependant membrane transporter super-family (Bull *et al.*, 1998).

A second form of PFIC, termed PFIC2 (Bylers' Syndrome), was mapped to chromosome 2q24 (Strautnieks *et al.*, 1997). The gene mutated in PFIC2 is ABCB11 (also termed bile salt export protein (BSEP) and sister of p-glycoprotein), an ATP-binding cassette transporter. ABCB11 is expressed in the hepatocanalicular membrane and functions as a transporter of bile acids from hepatocytes to the canaliculus (Gerloff *et al.*, 1998). The presence of mutations in the ABCB11 gene and lack of ABCB11 expression have been demonstrated in PFIC sufferers (Jansen *et al.*, 1999).

PFIC3 differs from types 1 and 2 in that sufferers present with high serum levels of γ -glutamyl transpeptidase (GGT) and is sometimes termed high GGT-PFIC. Studies

have indicated that some cases of PFIC3 are caused by mutations of the ABCB4 gene (also known as MDR3 in humans and MDR2 in mouse) (de Vree *et al.*, 1998).

ABCB4 is also expressed in the hepatocanicular membrane and functions as a transporter of phosphatidylcholine (Deleuze *et al.*, 1996; Smit *et al.*, 1993).

Phosphatidylcholine is present in bile in large quantities and probably helps protect the liver from bile acid-induced damage (Bull, 2002). ABCB4 mutations have also been implicated in cholesterol gallstone disease (Rosmorduc *et al.*, 2000) and intrahepatic cholestasis of pregnancy (Jacquemin *et al.*, 1999), (Dixon *et al.*, 2000).

Bile is formed in the liver by a secretory unit comprised of hepatocytes and cholangiocytes. Deficiency of specific membrane transport proteins has been shown in many instances to result in cholestasis. Recent data has also shown that many members of the nuclear hormone receptor (NR) super-family transcriptionally regulate such proteins, as well as enzymes associated with bile acid synthesis. As such this would make them good candidates for investigation into their potential role in mechanisms of drug-induced cholestasis.

Among the most important NR's within this area are the Pregnane X Receptor (PXR) and the Farnesoid X Receptor (FXR). Indeed, the argument for role of the former in drug-induced cholestasis is further added to by observations that some drugs associated with cholestatic effects are in fact efficacious ligands and potent activators of PXR. Examples include the anti-convulsant carbamazepine (Aithal and Day, 1999) and the macrolide antibiotic rifampicin (Hartleb *et al.*, 2002). Interestingly, rifampicin is the therapy of choice for treatment of the most common extrahepatic manifestation of cholestasis, pruritus (Hofmann, 2002; Mela *et al.*, 2003).

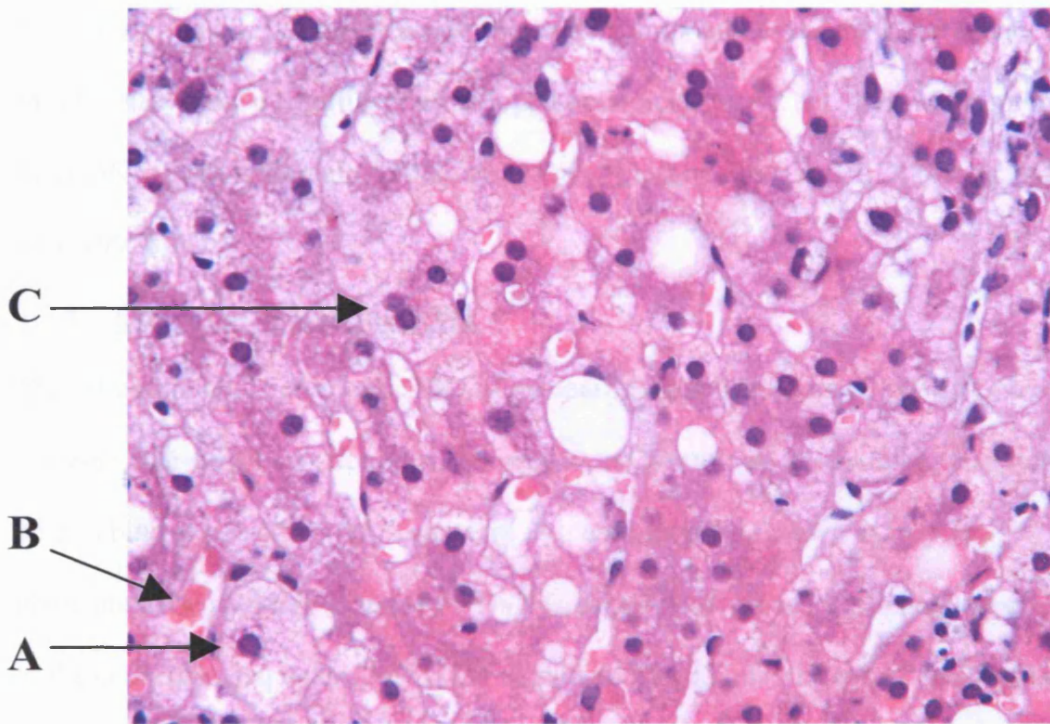


Figure 1.1. Bland Cholestasis in a 5 μ m liver core needle biopsy section. Common features consistent with bland cholestasis can be seen. **A** indicates a hepatocytes swollen with intracytoplasmic bile. **B** shows a dilated canaliculus obstructed by a bile plug. **C** is a normal bi-nucleated hepatocyte. No inflammatory cells are visible. (Haematoxylin-eosin stained, 200x magnification).

1.3 Nuclear Hormone Receptor Super Family.

Both FXR and PXR are members of the nuclear hormone receptor super family.

Nuclear hormone receptors (NR) are ligand-activated transcription factors that transform extracellular and intracellular signals into cellular responses by triggering the transcription of NR target genes. Since they are members of the same super-family, NRs show a significant homology to classical steroid and thyroid receptors in their DNA-binding domain (DBD) and Ligand-binding domain (LBD) (Mangelsdorf, *et al* 1995b).

1.3.1 Response element and DBD.

The 70-amino-acid conserved DBD of nuclear receptors consists of two cysteine-cysteine zinc-finger sub-domains followed by a C-terminal. The nuclear receptor is able to bind to specific DNA sequences in the target gene, known as response elements. The response element of a NR is usually composed of two half sites related to the consensus sequence, AGGTCA separated by a number of spacer nucleotides. The half sites are arranged as either direct repeats (DR), inverted repeats, (IR) or everted repeats (ER) (Honkakoski, *et al* 2000). For example the sequence AGGTCANNAGGTCA is the sequence of the DR3 response element. Organisation of the response element determines the nature of receptor binding. Nuclear receptors can bind as monomers or homodimers to the response element or heterodimers in association with other receptors. In the case of many of the orphan nuclear receptors, this occurs by heterodimerisation with the retinoid X receptor (RXR).

1.3.2 Ligand-Binding and Activation

The LBD consists of approximately 250 C-terminal residues. Though the LBD is structurally similar in all NRs (a three-layered helix fold) (Honkokoski, *et al*, 2000),

the ligand-binding pocket shows a great deal of variation amongst the NR super-family. This variability is mainly observed within the NR ligand-specificity due to differences in LBD size and the amino acid sequence.

Within the LBD is also a region for ligand-dependant activation commonly referred to as AF-2 (activation function 2). Ligand binding induces structural change causing the repositioning of AF-2 to form a hydrophobic patch that is accessible to common co-activators and co-integrators (e.g. p300/CBP). Danielian, *et al.* (1992) demonstrated the need for the AF-2 region, by showing how introducing point mutations into the AF-2 region can inhibit transcriptional activation. Co-activators either possess intrinsic histone acetyltransferase or recruit further histone acetyltransferases which modify the suppressive effects of chromatin and thus activate transcription of the target gene.

1.4 Pregnane X Receptor (PXR).

First cloned from a mouse liver cDNA library (Bertilsson *et al.*, 1998; Kliewer *et al.*, 1998), the Mouse Pregnane X Receptor (PXR), a ligand-activated orphan nuclear receptor, was initially demonstrated to bind, as a heterodimer with the Retinoid X receptor (RXR), to response elements within the upstream promoter region of the CYP3A gene and modulate its transcription. Mouse PXR is activated by the glucocorticoid receptor (GR) antagonist pregnenolone 16 α -carbonitrile (PCN) and GR agonist dexamethasone, both of which had previously been demonstrated as inducers of CYP3A expression in mouse hepatic tissue.

The human homologue of PXR (hPXR), sometimes termed the steroid and xenobiotic receptor (SXR) (Blumberg *et al.*, 1998), was first cloned and characterised later the same year (Lehmann *et al.*, 1998).

hPXR showed close homology to mPXR within the DNA binding domain (DBD) (96%) but less so within the ligand binding domain (76%) (Jones *et al.*, 2000). This explains the difference in the range of activating compounds between the two homologues. hPXR is efficaciously activated by the macrolide antibiotic rifampicin but not by PCN (Lehmann *et al.*, 1998) but the opposite is true of mPXR.

1.4.1 Activation of hPXR by a diverse range of xenobiotics

hPXR has been shown to have a wide and diverse spectrum of both endogenous and exogenous ligands of wide ranging potency (Ekins and Erickson, 2002). Among the xenobiotics that have been demonstrated as hPXR ligands are: calcium-channel modulators, such as nifedipine (Drocourt *et al.*, 2001); the endocrine disrupter, RU486 (Moore *et al.*, 2000b); the breast cancer therapeutic agent, tamoxifen (Desai *et al.*, 2002); and the herbal anti-depressant St John's Wort (Moore *et al.*, 2000a).

The reasons for such ligand promiscuity can be explained by analysing the crystal structure of the hPXR ligand-binding domain (Watkins *et al.*, 2001). The hPXR-LBD has a small number of polar residues paced throughout the smooth, hydrophobic ligand-binding pocket. This composition allows the binding, not only of a diverse set of chemicals, but also means that a single ligand (the cholesterol-lowering agent SR12813) can dock in multiple orientations (Watkins *et al.*, 2001). Induced mutations in only a few of the polar residues can, potentially, have a detrimental effect on the docking of compounds (e.g. Hyperforin) to the hPXR-LBD and hence the responsiveness of hPXR (Watkins *et al.*, 2003). Specific residue differences between the human and murine PXR-LBD are the reason for inter-species variations in ligand activation spectra such as those described previously.

1.4.2 Genomic organization of hPXR

In recent years, the genomic structure of the hPXR gene (Figure 1.2) has been determined and has been shown to span a 35kb region mapped to chromosome 13q11-13 (Zhang *et al.*, 2001) and with this has come the functional characterization of allelic variants (Ghaheri *et al.*, 2001) and the identification of single nucleotide polymorphisms, both functional and non-functional (Zhang *et al.*, 2001).

A large multi-center (Zhang *et al.*, 2001) identified 38 SNPs including 5 in the coding

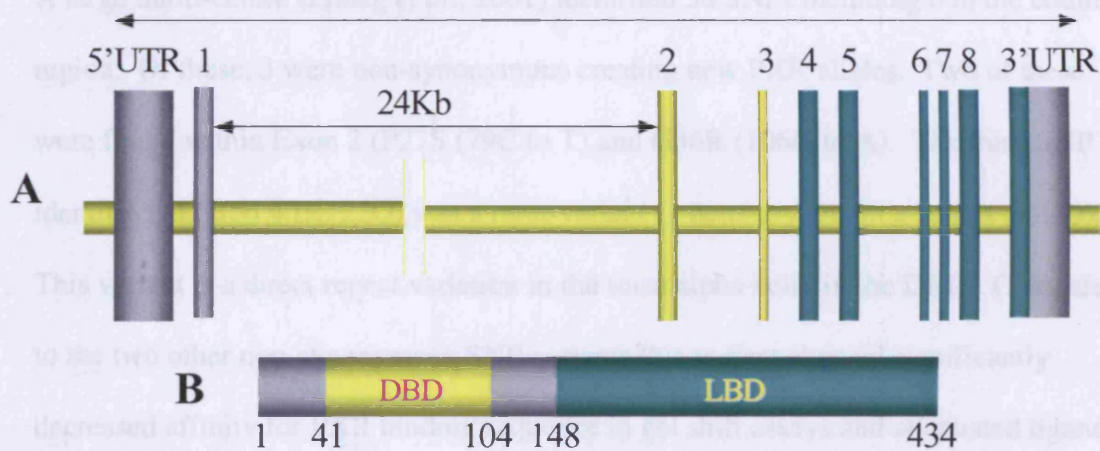


Figure 1.2. The genomic organization, and schematic protein structure, of the hPXR gene. **A** demonstrates the genomic structure of the hPXR gene locus. Yellow vertical bars represent the exons coding the DBD, and green bars the exons encoding the LBD. Grey bars are the 5' and 3' untranslated regions (UTRs) (drawn from data by (Zhang *et al.*, 2001)). **B** schematically represents the wild type translated protein structure of hPXR with the distinct DBD (Yellow) and LBD (Green). Numbers below indicate amino acid residues (redrawn from Moore and Kliewer, (2000)).

Another source of functional sequence variations of the human PXR gene may be within the upstream proximal promoter region. Zhang *et al.* (2001) identified a number of SNPs arising proximal to the promoter in a region 50 to 1.1kb upstream of the transcription start site. Among the consensus response elements altered were

1.4.2 Genetic variation of hPXR

In recent years, the genomic structure of the hPXR gene (Figure 1.2) has been determined and has been shown to span a 35kb region mapped to chromosome 13q11-13 (Zhang *et al.*, 2001) and with this has come the functional characterization of allelic variants (Hustert *et al.*, 2001) and the identification of single nucleotide polymorphisms, both functional and non-functional (Zhang *et al.*, 2001).

A large multi-centre (Zhang *et al.*, 2001) identified 38 SNPs including 6 in the coding region. Of these, 3 were non-synonymous creating new PXR alleles. Two of these were found within Exon 2 (P27S (79C to T) and G36R (106G to A). The third SNP identified in Exon 4 (R122Q) was a rarer variant (1 heterozygote in a cohort of 150). This variant is a direct repeat variation in the third alpha helix in the DBD. Compared to the two other non-synonymous SNP variants this variant showed significantly decreased affinity for PXR binding sequence in gel shift assays and attenuated ligand activation of the CYP3A reporter plasmid in transient transfection assays. The same study also demonstrated the potential relevance of the 38 SNPs identified in the cohort of individuals to those patients demonstrating atypical CYP3A metabolising states. Another study by a group from Epidauros Biotechnologie (Hustert *et al.*, 2001) identified a further three protein variants (V140M, D163G and A370T) all of which exhibited altered basal and/or induced transactivation of CYP3A promoter reporter genes.

Another source of functional sequence variations of the human PXR gene may well be within the upstream proximal promoter region. Zhang *et al.* (2001) identified a number of SNPs altering proposed response elements in a region up to 1.1kb upstream of the transcription start site. Among the consensus response elements altered were

those for hepatocyte nuclear factor 1A (HNF1A) and progesterone receptor. It is possible that such variant response elements may induce a functional effect on the regulation of PXR expression. Indeed, C to T and G to A variants at positions -24385 and -24113 from the translation start site were associated with an increase in breath ¹⁴C from the erythromycin breath test after rifampicin administration. Another study (Uno, *et al.* 2003) characterised a six-base pair deletion within another putative HNF1 site 1.5kb upstream of the PXR transcription start site. The HNF1 response element was observed to have an essential role in the transcriptional activity of PXR and that the six base-pair deletion diminished this activity. This deletion was however was not found to have an association with the pathology under study, aspirin-induced asthma (AIA). Other pathologies however may well be associated with such a dysfunctional variant.

Sequence variations introducing amino acid residue changes may be the most obvious and, in many cases, the most dramatic source of gene dysfunction. Studies have suggested that synonymous SNPs may actually introduce a functional change by affecting mRNA stability (Capon *et al.* 2004) and even pre-mRNA splicing (Cartegni *et al.* 2002). Given the number of such “silent” SNPs in the PXR protein coding region (Zhang *et al.* 2001 and Koyano *et al.* 2004) and the large number of potential splice variants (Fukuen *et al.*, 2002), an association between a sequence variation and a functional protein truncation extension is not unfeasible.

Non-protein-coding region genotypes can also demonstrate an association with an altered function phenotype. Zhang, *et al.*, (2001) identified a number of UTR and intronic SNPs within the PXR gene with an association to altered downstream transcription target phenotype. 3'UTR genotypes were associated with increased intestinal MDR1 mRNA expression (11156 and 11193 from the translation start site).

In both cases expression appears to be abolished in heterozygous individuals. Two SNPs were also identified in introns 5 and 6 (A7625Q and C78055T) and demonstrated an association with increased rifampicin-induced intestinal CYP3A expression.

1.4.3 Transcriptional variation of hPXR

As well as inter-individual sequence variations, a number of splicing variations of the

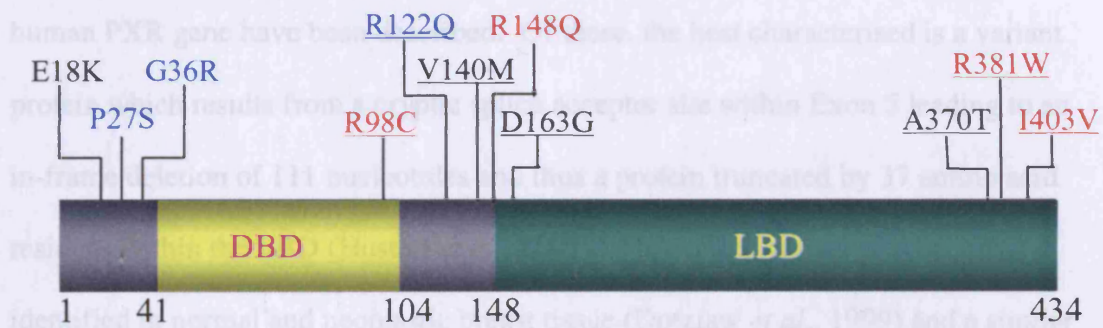


Figure 1.3. Reported non-synonymous human PXR mutations. The diagram demonstrates the variants described by (Hustert *et al.*, 2001) (Black), (Zhang *et al.*, 2001) (Blue), (Koyano *et al.*, 2004) (Red) as encoding protein variants in relation to the PXR protein.

Seven other splice variants have been identified from human liver cDNA by Fukue *et al.* (2002) (Figure 1.4). These protein variants vary in size from 393 to 306 amino acids in size. The functional significance of these variants has yet to be determined, but being such non-conservative changes many are likely to affect the properties of the receptor.

In both cases expression appears to be abolished in heterozygous individuals. Two SNPs were also identified in introns 5 and 6 (A7635G and C8055T) and demonstrated an association with increased rifampicin-induced intestinal CYP3A expression.

1.4.3 Transcriptional variation of hPXR.

As well as inter-individual sequence variations, a number of splicing variations of the human PXR gene have been described. Of these, the best characterised is a variant protein which results from a cryptic splice acceptor site within Exon 5 leading to an in-frame deletion of 111 nucleotides and thus a protein truncated by 37 amino acid residues within the LBD (Hustert *et al.*, 2001). This splice variant was originally identified in normal and neoplastic breast tissue (Dotzlaw *et al.*, 1999) and a similar splice variant was previously described in mPXR (Kliwer *et al.*, 1998). The variant protein demonstrated altered (reduced) induction properties due to direct alteration of ligand binding ability.

Bertilsson *et al.* (1998) also noted a transcriptional variation of hPXR, which possesses a different, alternatively spliced first exon (exon 1B) and is 39 amino acid residues longer than the wild-type protein.

Seven other splice variants have been identified from human liver cDNA by Fukuen *et al.* (2002) (Figure 1.4). These protein variants vary in size from 393 to 106 amino acids in size. The functional significance of these variants has yet to be determined, but being such non-conservative changes many are likely to affect the properties of the receptor.

It is also unclear as to the prevalence of PXR splice variants with the hepatic tissue of individuals. It has been shown that there is significant inter-individual variability of FXR expression in the human liver (Chang *et al.*, 2003; Hesse and Coust, 2003).

However, PXR splice variant expression variability in individuals has not been studied. It has been shown that the PXR gene is highly polymorphic (A4 and p-

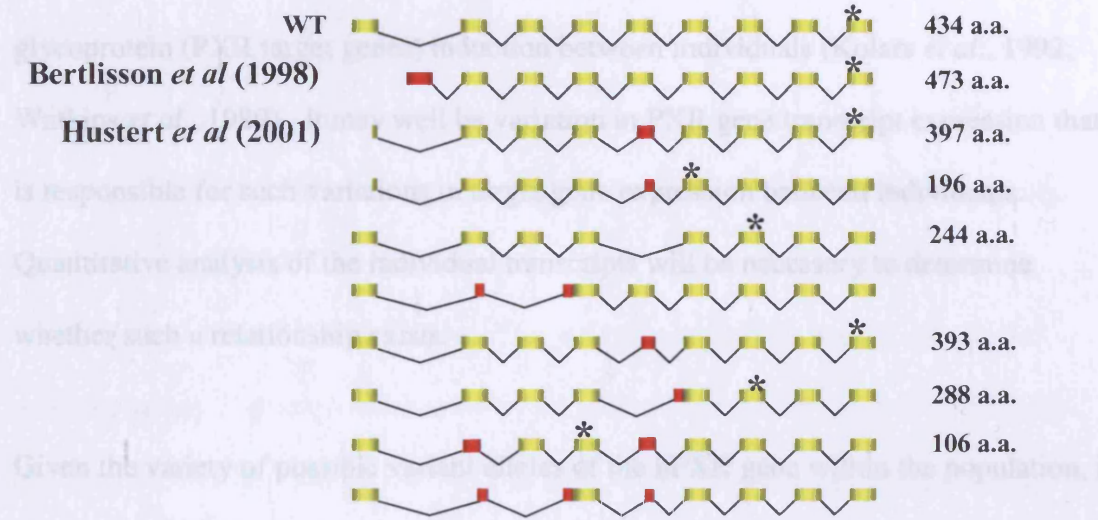


Figure 1.4. Splice variation of human PXR gene transcripts. The 9 published splice variations are shown aligned to the wild type mRNA (WT). The numbers 1-9 indicate the PXR exon reference. Red exons denote truncation of the wt sequence. * indicates the termination codon of the open reading frame. Translated protein length is shown on the right. All variants are as described by (Fukuen *et al.*, 2002) with the exception of those indicated.

number of hepatic phase I xenobiotic metabolizing enzymes such as CYP3A4 (metabolizes 50% of all prescribed pharmaceuticals which undergo metabolism by a P450) (Goodwin *et al.*, 2002), and CYP2B6 (Goodwin *et al.*, 2001). PXR is also involved in the regulation of a number of phase II xenobiotic conjugation clearance enzymes including glutathione S-transferase (GST) (Falkner *et al.*, 2001) and Uridine diphosphate-glucosyltransferase (UGT) (Chen *et al.*, 2003; Maglich *et al.*, 2002).

It is also unclear as to the prevalence of PXR splice variants with the hepatic tissue of individuals. It has been shown that there is significant inter-individual variability of PXR expression in the human liver (Chang *et al.*, 2003; Hesse and Court, 2003).

However, PXR splice variant expression variability between individuals has not been studied. It has been shown that there is noticeable variation in CYP3A4 and p-glycoprotein (PXR target genes) induction between individuals (Kolars *et al.*, 1992; Watkins *et al.*, 1989). It may well be variation in PXR gene transcript expression that is responsible for such variations in target gene expression between individuals.

Quantitative analysis of the individual transcripts will be necessary to determine whether such a relationship exists.

Given the variety of possible variant alleles of the hPXR gene within the population, it is possible that an association to inter-individual variation in the regulation of PXR target genes could be made. The potential for novel mutations within PXR and their association with disease states, such as cholestasis, and ADRs in general, is not entirely unfounded.

1.4.4 Regulation of Hepatic Detoxification pathways by hPXR

It is well known that hPXR has a role in the transcriptional regulation of a number of important phase I xenobiotic metabolising enzymes such as CYP3A4 (metabolises >60% of all prescribed pharmaceuticals which undergo metabolism by a P450) (Goodwin *et al.*, 2002), and CYP2B6 (Goodwin *et al.*, 2001). PXR is also involved in the regulation of a number of phase II xenobiotic solubilisation clearance enzymes including glutathione-S-transferase (GST) (Falkner *et al.*, 2001) and Uridine diphosphate-glucuronosyltransferase (UGT) (Chen *et al.*, 2003; Maglich *et al.*, 2002).

Coupled with the phase III transporter genes, this coordinated clearance system plays a role in controlling levels of lithocholic acid (LCA) which is a substrate for many of the processes controlled by PXR. LCA is also a potent agonist of PXR (Staudinger *et al.*, 2001b) and as such may regulate its own clearance and feedback inhibition (Gillam, 2002).

Further support to the theory of bile acid regulation is added by the identification of PXR as a mediator of the xenobiotic sulphonation cascade (Sonoda *et al.*, 2002).

Activation of PXR increases the activity and expression of dehydroepiandrosterone sulfotransferase (STD) (Echchgadda *et al.*, 2004), a phase II conjugating enzyme known to facilitate LCA elimination. The enzyme responsible for generating the donor cofactor (3'-phosphoadenosine 5'-phosphosulfate synthetase 2 (PAPSS2)) for this reaction was also found to be regulated by PXR. Bile acid precursors (Goodwin *et al.*, 2003) and sterols (Dussault *et al.*, 2003) have also been demonstrated to be potent PXR ligands.

This concept of PXR as a "xenosensor" for endogenous toxic bile acids has led to the belief that PXR, in fact, acts as a second line of defence against bile acid toxicity to another more characterized nuclear receptor-modulated bile acid receptor pathway, the Farnesoid X Receptor (FXR). (Xie *et al.*, 2001 and reviewed by Goodwin and Kliewer, 2002).

1.5 Farnesoid X Receptor (FXR).

Like PXR, the Farnesoid X Receptor (FXR, NR1H4) is a member of the nuclear receptor super family and shares the same modular architecture consisting of a highly conserved DBD and carboxy-terminal LBD. It also, like PXR binds to target gene

response elements as a heterodimer with RXR (Mangelsdorf and Evans, 1995). FXR was originally proposed as a receptor for farnesol metabolites (Forman *et al.*, 1995). However it was shown that farnesol does not bind to FXR and indeed supra-physiological concentrations were required to activate the receptor. However, in 1999, 3 independent groups proposed FXR as a nuclear receptor for bile acids (BA) (Makishima *et al.*, 1999; Parks *et al.*, 1999; Wang *et al.*, 1999). FXR is implicated as a key regulator against cholestatic disease states by knock out animal models which developed impaired bile acid homeostasis (Sinal *et al.*, 2000).

1.6 Role of PXR and FXR in Bile Acid Homeostasis.

Under cholestatic conditions, high concentrations of toxic bile acids accumulate within hepatic tissue and may overwhelm the protective capacity of the FXR system. It is at this point that PXR is believed to represent the second line of defence. Working in this manner, FXR and PXR co-ordinately mediate bile acid homeostasis in two profound ways: a) Regulation of hepatobiliary transporter gene expression and b) Modulation of the expression genes involved in the cholesterol catabolism. This has led to theories that FXR and PXR ligands could be developed as anticholestatic therapies (Willson *et al.*, 2001)

1.6.1 Regulation of Hepatobiliary Transport by PXR and FXR.

As shown in Figure 1.5, FXR and PXR transcriptionally regulate two distinct sets of hepatobiliary transporters, both of which play important roles in bile acid homeostasis.

Bile acid-bound and activated FXR inversely regulates hepatic uptake and secretion of bile acids by down regulating the major basolateral uptake system for conjugated bile acids sodium taurocholate co-transporting protein (NTCP/SLC10A1). Hepatic steady state mRNA levels of NTCP are inversely related to serum bile acid levels in human with various cholestatic disorders (Zollner *et al.*, 2001). Indeed individuals showing an inability to down-regulate NTCP in the presence of toxic levels of bile acids show abnormal responses to hypercholanemia (Shneider *et al.*, 1997). Regulation of NTCP by FXR involves an inhibitory intermediate gene Short Heterodimer Partner 1 (SHP-1) (Denson *et al.*, 2001). SHP-1 is an atypical orphan nuclear receptor in that it lacks the highly conserved DBD typical of other members of this family. FXR binds, as a heterodimer with RXR, to an IR-1 response element in the upstream promoter region of SHP-1 resulting in transcription. SHP-1 in turn inhibits NTCP transcription by binding to a DR2 response element in the promoter region of NTCP as a heterodimer with RXR and preventing competitive activator binding (Jansen *et al.*, 2001).

The Bile Salt Export Pump (BSEP/ABCB11) formally known as sister of p-glycoprotein (sPGP), is transactivated by FXR (Ananthanarayanan *et al.*, 2001).

BSEP is critical for ATP-dependant transport of bile acids across the hepatocytes canalicular membrane.

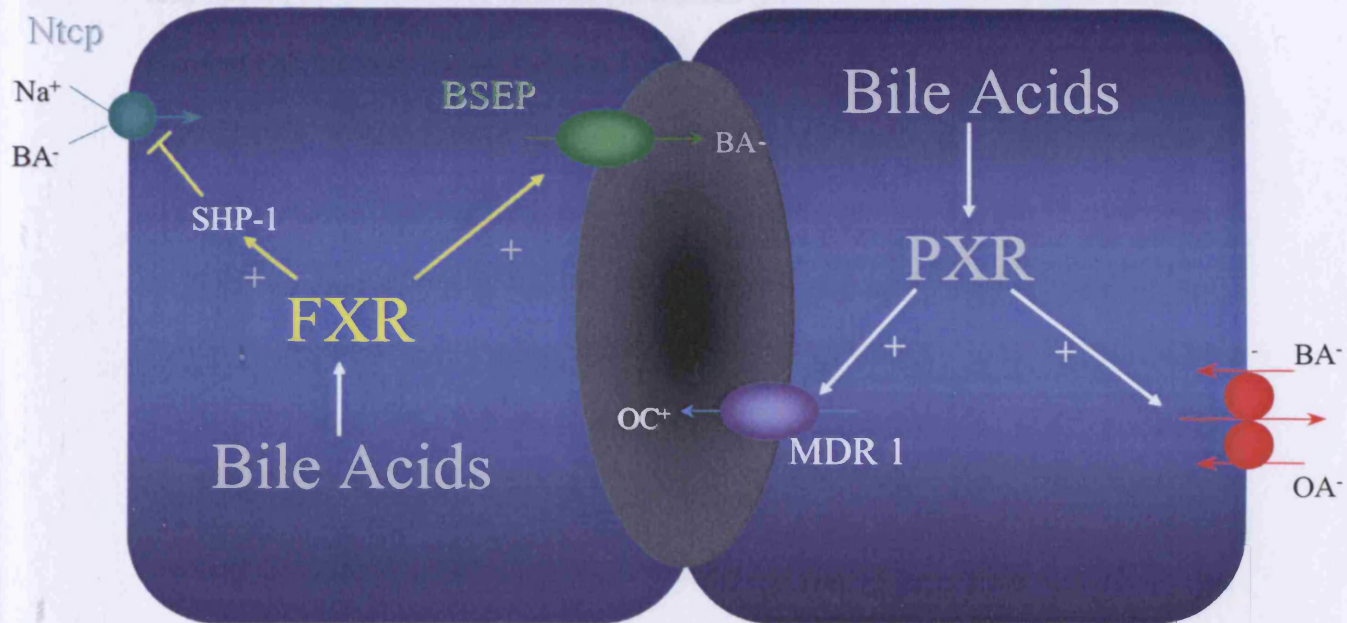


Figure 1.5. PXR and FXR mediate bile acid-activated transcription of genes involved in hepatic bile acid clearance. The schematic diagram represents two neighbouring hepatocytes sharing a common canaliculus. The two nuclear receptors, upon activation by bile acids (BA⁻), regulate the transporter proteins whose primary roles are the flux of BA⁻ and organic anions (OA⁻) across the basolateral membrane and BA⁻ and organic cations (OA⁺) across the hepatocanalicular membrane. NTCP (Sodium Taurocholate Co-transporting Peptide), BSEP (Bile salt Export Pump), SHP-1 (Short Heterodimer Partner 1). Redrawn from Zollner *et al.*, (2001) with additional data from Jansen *et al.*, (2001).

The function of BSEP is critical in bile acid homeostasis. Indeed, animal models have demonstrated inhibition of BSEP can lead to induction of drug-induced cholestasis (Stieger *et al.*, 2000) and, in one example, BSEP was shown to be directly inhibited by troglitazone to subsequently induce cholestasis (Funk *et al.*, 2001a; Funk *et al.*, 2001b). As well as this, mutations of the gene encoding BSEP are recognised to be responsible for progressive familial cholestasis (PFIC-2), an inherited cholestatic disorder (Thompson and Strautnieks, 2001).

The Multi Drug Resistance 1 gene (MDR1/ABCB1) codes for a product, known as p-glycoprotein, which is highly expressed in the canalicular membrane of hepatocytes. Its main role is as a drug efflux transporting xenobiotics out of the hepatocytes. Earlier studies had recognised that MDR1 and CYP3A4 seemed to be co-induced by a number of compounds (Schuetz *et al.*, 1996). One such compound, which stood out was rifampicin (Greiner *et al.*, 1999), the classic hPXR mediated transcription inducer. This eventually led to the discovery of a DR4 nuclear receptor response element within the MDR1 response element by which rifampicin-bound PXR binds and activates p-glycoprotein transcription (Geick *et al.*, 2001). In cholestatic animal models, produced by ligation of the common bile duct, MDR1 expression was markedly increased (Schrenk *et al.*, 1993). This event could be attributed to activation of PXR by bile acids, though has not been investigated. The potential ability of p-glycoprotein to transport bile acid metabolites from hepatocytes could explain the therapeutic benefit of increased MDR1 expression in cholestasis but this too is not known.

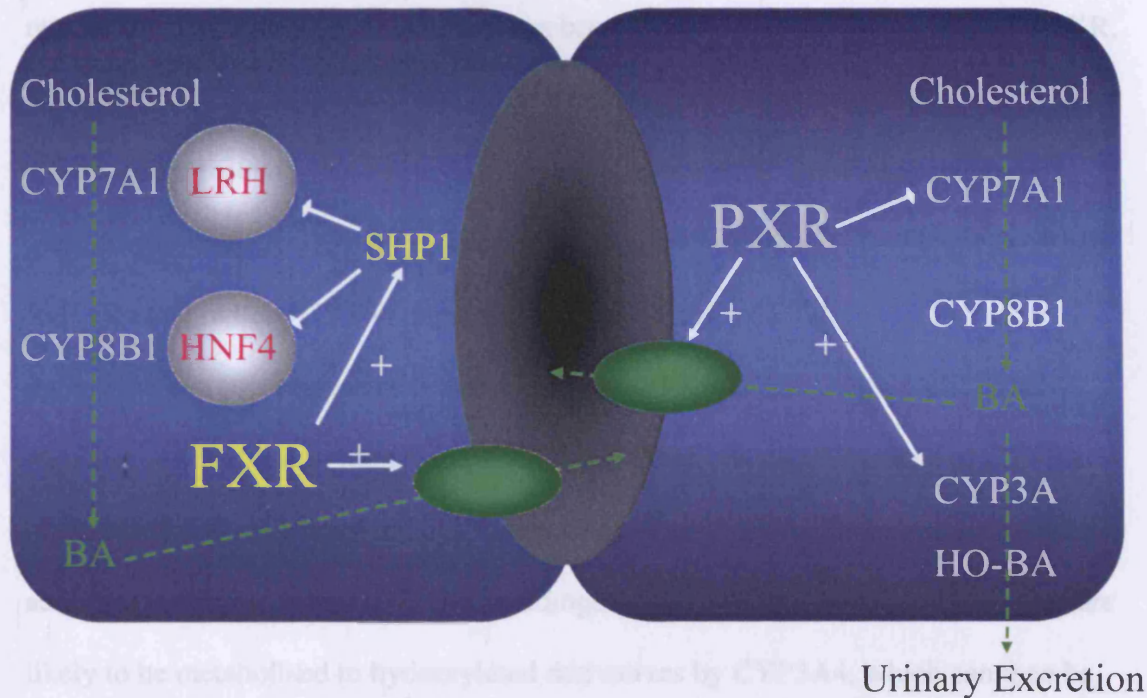
Organic anion transporting polypeptide 2 (OATP2/Slc1a5) is a sodium dependant hepatocyte basolateral organic anion transporter whose expression in mouse hepatic tissue is regulated by PXR and induced by PCN (Staudinger *et al.*, 2001a). Though

often referred to as human OATP2 (Jansen *et al.*, 2001), the correct nomenclature protocol of ABC transporters dictates that Slc21a5, the human homologue of mouse OATP2 be termed OATPC (Kullak-Ublick *et al.*, 2002). However, functionally, mouse OATP2 is more similar to human OATP-A than -C. It is yet to be determined whether PXR transcriptionally regulates OATP-A expression in human hepatic tissue. Since the substrate-specificity of mouse OATPs extends to bile salts, it is reasonable to assume this to be the case in humans. The role of OATPs combined with the possibility of regulation, in human hepatocytes, by PXR suggests a potential role in bile acid homeostasis for members of the OATP family. Interestingly rifampicin has been shown to inhibit OATP function in the human liver (Vavricka *et al.*, 2002). This could potentially be an inhibition of bile acid transport and lead to a cholestatic state and, given that rifampicin has been implicated in drug-induced cholestasis, is a possibility. However there is no evidence to support this at present.

1.6.2 Regulation of Cholesterol Catabolism by PXR and FXR.

As was demonstrated with FXR and PXR regulation of bile acid transporter within the hepatocyte-canalculus system, the two nuclear receptors also regulate two distinct pathways of cholesterol catabolism (Figure 1.6). Bile acid-bound FXR up regulates SHP-1 expression by binding, as a heterodimer with RXR, to an IR-1 response element. SHP-1 interacts with a number of other nuclear receptors, most notably hepatocytes nuclear factor 4 α (HNF4 α) (Lee *et al.*, 2000) and liver receptor homologue 1 (LRH-1) (Lee and Moore, 2002). It is through the interaction with LRH-1 that SHP-1 is able to repress LRH-1 dependant transcription of cholesterol-7-alpha-hydroxylase CYP7A1 (Goodwin *et al.*, 2000). CYP7A1 regulates the pathways through which cholesterol is catabolised to bile acids and as such plays an important

role in regulating bile acid homeostasis. Induction of SHP expression also results in inhibition of LRH-1 and HNF4 α -mediated activation of sterol-12- α -hydroxylase (CYP8B1) (deCastillo-Olivares and Fajal, 2001; Zhang and Chiang, 2001). CYP8B1 is an enzyme within the cholesterol catabolism pathway and so is important in



eliminated from the body (Figure 1.6).

Figure 1.6. Regulation of Bile acid homeostasis and cholesterol catabolism by FXR and PXR. The diagram represents two neighbouring hepatocytes sharing a common canalculus. Primary bile acid sensor FXR indirectly inhibits expression of CYP7A1 and CYP8B1 cholesterol metabolism. Secondary sensor PXR directly inhibits CYP7A1 as well as upregulating CYP3A expression and thus increasing bile acid hydroxylation, aiding bile clearance. Green membrane transporters represent generic hepatocanalicular transporters regulated by FXR and PXR. Redrawn from Goodwin and Kliewer, (2002).

and liver androgenic hormone models may provide clues to the effect that FXR dysfunction may have with androgens. Initial PXR-null studies demonstrated mice with lack of ability to induce hepatic CYP3A when treated with classic FXR agonists such as PCN (Xie *et al.*, 2000). In later experiments PXR-null mice were co-administered LCA with PCN. PCN has long been known to have a protective effect

role in regulating bile acid homeostasis. Induction of SHP expression also results in inhibition of LRH-1 and HNF4 α –mediated activation of sterol-12-alpha-hydroxylase (CYP8B1) (del Castillo-Olivares and Gil, 2001; Zhang and Chiang, 2001) CYP8B1 too is an enzyme within the cholesterol catabolising pathway and so is important in regulation of bile acid homeostasis. It has been known for some time that rodent PXR, activated by PCN, suppressed transcription of the CYP7A1 gene (Chiang *et al.*, 1990). More recently this has been demonstrated as a PXR-dependant occurrence (Staudinger *et al.*, 2001b). In rodents, PCN does not stimulate SHP-1 expression and so PXR must repress CYP7A1 expression independently of FXR.

As well as this suppression of bile acid synthesis, PXR is also the transcriptional regulator of CYP3A4 in human hepatic tissue. Often chemicals capable of CYP3A induction (PXR activators) are also substrates and so it is feasible that since toxic bile acids are potent activators of PXR (Staudinger *et al.*, 2001b; Xie *et al.*, 2001) they are likely to be metabolised to hydroxylated derivatives by CYP3A4, which can then be eliminated from the body (Figure 1.6).

Somewhat paradoxically, SHP-1 has been shown to interact with PXR to repress transcription of CYP3A (Ourlin *et al.*, 2003). This seems to be counter to the perceived role of SHP-1 in the inhibition of bile acid accumulation. The answer is believed to lie in the theory that SHP-1 is in fact preventing the accumulation of toxic bile acid derivatives via CYP3A hydroxylation (Ourlin *et al.*, 2003).

PXR-null and transgenic murine models may provide clues to the effect that PXR dysfunction may have with man. Initial PXR-null studies demonstrated mice with lack of ability to induce hepatic CYP3A when treated with classic PXR activators such as PCN (Xie *et al.*, 2000). In later experiments PXR-null mice were co-administered LCA with PCN. PCN has long been known to have a protective effect

against LCA-induced cholestasis and liver injury. However, in null mice, the PCN protection was attenuated and compared to wild-type PXR mice, severe LCA-induced injury was observed as characterised by massively elevated serum ALT levels and increased incidence of necrotic foci within the hepatic morphology (Staudinger *et al.*, 2001). These studies do suggest PXR has a key role in hepatoprotection, both from xenobiotics and endogenous bile acid, though relating animal model data to a possible human clinical aetiology should be with some scepticism. It is clear that both FXR and PXR play important roles on two fronts in regulating bile acid homeostasis within hepatic tissues. As the intermediary factor in FXR's regulatory pathways, SHP-1 too would appear to have an important central role in bile acid homeostasis. Functional mutations in any of these three genes could therefore be a contributing factor to predisposing an individual to drug-induced cholestasis.

1.7 Aims and Objectives.

The aim of this project is to identify novel gene mutations or SNPs, within the human pregnane X receptor in individuals demonstrating histopathological or biochemical evidence of drug-induced hepatic injury.

Having identified novel SNPs it would be important to undertake functional characterisation. In order to do this, a cohort of biopsy samples from the hepatic tissue of individuals suspected of having drug-induced injury need to be identified from an original archive of nearly 2000 liver biopsy specimens dating back to 1990 from the Leicester University Hospitals NHS Trust.

By utilising a tissue archive, a retrospective cohort of Hepatic ADRs can be compiled that prospectively would take several years to gather from a single study centre.

Isolating ADRs from a larger population of hepatic biopsies could serve as means of

enriching the population to increase the potential frequency of rare PXR variant which may have an ADR predisposing functionality.

The tissue archive, available for the purposes of this study, consists of hepatic biopsies, which have been formalin-fixed and paraffin-embedded. The nucleic acids extracted from these samples therefore carry a number of issues regarding quantity and quality. In order to overcome these obstacles, methodologies for nucleic acid extraction and amplification need to be developed in order to overcome the limitations imposed by the tissue specimens.

The primary objective is to develop a methodology to allow genotyping of the protein-coding region of hPXR gene from archival biopsies identified as suspicious of ADR. In parallel with this a gene expression study is intended to determine possible correlations between the disease-state, abnormal expression of hPXR transcription targets (bile acid transporters/drug-metabolising enzymes) and mutations within the functional domain of hPXR.

Chapter 2: Materials & Methods

2.1 Materials

2.1.1 Chemicals and kits

10bp ladder	Invitrogen
100bp ladder	Invitrogen
Accuprime Pfx Reaction Buffer (10x)	Invitrogen
Acrylamide (19:1)	Flowgen
Acrylamide (29:1)	Biorad
Ammonium Persulphate	Sigma
Ammonium Sulphate	Fisher
AMV Buffer (10x)	Promega
β -Mercaptoethanol	Sigma
Biodyne B membrane	Pall
Biotinalated alkaline phosphatase	Dako
Boric Acid	Fisher
Bovine Serum Albumin	Roche
CDP Star Reagent	Amersham Biosciences
Chloroform	Fisher
Cobalt Chloride	Sigma
dATP	Invitrogen
dNTPs	Invitrogen
Dexamethasone	Sigma
Dextran-coated charcoal	Sigma
Dimethyl Sulphoxide	Sigma
Dithiotheritol (DTT)	Sigma
Dulbecco's Modified Eagle's Media	Invitrogen
DynaBeads	Dynal
Ethylenediamine tetraacetic acid (EDTA)	Fisher
Enhanced Chemiluminescence System	Amersham Biosciences
Ethanol	BDH
Ethidium Bromide	BDH
Expand High Fidelity Taq Buffer	Roche Diagnostics
FireLite Luminescence Detection Assay Kit	Packard Biosciences

Foetal Bovine Serum	Invitrogen
Formaldehyde	Fisher
Gene Juice	Novagen
Glacial Acetic Acid	Fisher
Glycogen	Invitrogen
HEPES	Sigma
Hyperfilm™	Amersham Biosciences
Hyperforin	Calbiochem
Isopropanol	Sigma
Lambda DNA	Invitrogen
Lithocholic Acid	Sigma
Magnesium Chloride	Roche Diagnostics
Maleic Acid	Sigma
Maxi Plasmid Purification Kit	Qiagen
MegaBACE™ loading buffer	Amersham Biosciences
Microspin G-50 Columns	Amersham Biosciences
NEB Restriction Buffer 1,3 & 4	New England BioLabs
Nitrocellulose Membrane	Biorad
Non-essential Amino Acids	Invitrogen
NP-40	Sigma
Nusieve GTG Agarose	Cambrex
Oligonucleotides	All Sigma Genosys
Penicillin/Streptomycin	Invitrogen
PicoGreen™	Molecular Probes
Ponceau S	Sigma
Pregnenolone 16 α - Carbonitrile	Sigma
Proteinase K	Sigma
QiaQuick PCR Clean-Up Kit	Qiagen
Quikchange Site-Directed Mutagenesis Kit	Stratagene
Rifampicin	Sigma
RNAsin	Promega
Seakem LE Agarose	BioWhittaker
Silver Nitrate	Sigma

Sodium Cacodylate	Fisher
Sodium Carbonate	Sigma
Sodium Citrate	Sigma
Sodium Dodecyl Sulphate (SDS)	Fisher
Sodium Hydroxide	Fisher
Streptavidin	Dako
T4 Kinase	Promega
TdT Buffer (5x)	Roche Diagnostics
Tetramethylethylenediamine (TEMED)	Sigma
TriReagent™	Sigma
Tris	Fisher
Ultima Gold F Scintillation Fluid	Perkin Elmer
Xylene	Genta Medical

2.1.2 Enzymes

Accuprime Pfx DNA Polymerase	Invitrogen
AMV Reverse Transcriptase	Promega
Bcc I	New England BioLabs
Btg I	New England BioLabs
DYEnamic ET Terminator reagent premix	Amersham Biosciences
ExoSAP-IT™ (Shrimp Alkaline Phosphatase)	USB Corporation
Expand High Fidelity Taq Polymerase	Roche Diagnostics
Mwo I	New England BioLabs
Recombinant Terminal Deoxynucleotidyl Transferase (rTDT)	Roche Diagnostics
Taq Polymerase	Promega

2.1.3 Plasmids

pBSIISK-	Stratagene
pcDNA3.1	Invitrogen
pcDNA.ratPXR	AstraZeneca, UK
pcDNA.hPAR1	AstraZeneca, Sweden
pGLuc.(ER6) ₂	AstraZeneca, UK
pGLuc.(DR3) ₂	AstraZeneca, UK

pcDNA.hPAR1 consists of the pcDNA3.1 expression plasmid containing the 1608bp nucleotide sequence for the PXR (NR1I2) transcript variant which encodes for the 434 amino acid protein designated hPAR1 (Bertilsson, *et al.*, 1998). Similarly pcDNA.ratPXR is pcDNA3.1 containing the nucleotide sequence translating to the 431 amino acid rat PXR protein product designated PXR.1 by Kliewer, *et al.*, (1998). pGLuc.ER6 and DR3 are the luciferase reporter plasmid, pGLuc (Stratagene), containing 2 copies of the CYP3A4 proximal promoter, nuclear receptor response elements ER6 and DR3.

2.1.4 Buffers, Solutions and other agents

2.1.4.1 4% Upper Stacking Gel

375mM Tris-HCl/SDS (pH6.8)
4% Acrylamide-Bisacrylamide (29:1)
0.05% Ammonium Persulphate
0.1% TEMED

2.1.4.2. 4% Non-denaturing Acrylamide Gel

4% Acrylamide-Bisacrylamide (19:1)
0.1% Ammonium Persulphate
0.04% TEMED
in 0.6x TBE

- 2.1.4.3 7% Non-denaturing Acrylamide Gel
 7% Acrylamide-Bisacrylamide (19:1)
 0.1% Ammonium Persulphate
 0.04% TEMED
 in 0.6x TBE
- 2.1.4.4 12% Lower Resolving Gel
 125mM Tris-HCl/SDS (pH8.8)
 12% Acrylamide-Bisacrylamide (29:1)
 0.05% Ammonium Persulphate
 0.1% TEMED
- 2.1.4.5 Alec Jeffries (AJ) Buffer (10x)
 45mM Tris.HCl (pH8.8)
 11mM Ammonium Sulphate
 6.7mM β -Mercaptoethanol
 4.5mM MgCl₂
 1mM dNTPs
 4.4 μ M EDTA (pH8.0)
 110 μ g/ μ l BSA
- 2.1.4.6 Blocking Solution
 5% Milk powder
 in TBS-t (2.1.4.17)
- 2.1.4.7 Charcoal Stripping Buffer
 250mM Sucrose
 1.5mM MgCl₂
 10mM HEPES (pH7.9)
- 2.1.4.8 Electrode Buffer
 0.1% SDS
 in 1x Tris/Glycine (2.1.4.23)
- 2.1.4.9 EMSA Binding Buffer
 10mM Tris.HCl (pH8.0)
 40mM KCl
 0.05% NP-40
 6% Glycerol
 1M DTT

- 2.1.4.10 HeLa/Cos-7 Growth Media
Dulbecco's Modified Eagle's Medium
10% Foetal Bovine Serum
1% Non-essential Amino Acids
100U/ml Penicillin/Streptomycin
- 2.1.4.11 Lysis Buffer (Protein Extraction)
20mM Tris-HCl9 (pH7.4)
135mM NaCl
1.5mM MgCl₂
1% Triton X-100
10% Glycerol
- 2.1.4.12 Lysis Buffer (Luciferase Assay)
0.25M HEPES (pH7.9)
1% Triton X-100
500μM MgCl₂
500μM CaCl₂
50% Phosphate-Buffered Saline (PBS)
- 2.1.4.13 Maleic Acid Buffer (pH7.5)
100mM Maleic Acid
150mm NaCl
- 2.1.4.14 Proteinase K Digestion Buffer (1x)
10mM Tris.HCl pH8.8
100μM EDTA
2% SDS
0.5mg/ml Proteinase K
- 2.1.4.15 Rapid Extraction Buffer
50mM KCl
10mM Tris pH8.3
250μM MgCl₂
0.45% Tween 20
0.45%NP40

- 2.1.4.16 Sample Buffer
- 0.5M Tris.HCl pH6.8
60% Glycerol
8% SDS
0.2% Bromophenol Blue
5% β -mercaptoethanol
- 2.1.4.17 TBS-t
- 0.1% Tween 20
in Tris-Buffered Saline (TBS)
- 2.1.4.18 T4 Kinase Buffer
- 0.5M Tris HCl pH7.6
0.1M MgCl₂
50mM DTT
1mM Spermidine
1mM EDTA pH8.0
- 2.1.4.19 Transfection Lysis Buffer
- 250mM HEPES (pH7.9)
1% Triton-X-100
0.5mM MgCl₂
0.5mM CaCl₂
50% PBS
- 2.1.4.20 Transfer Buffer
- 5% Methanol
in 1x Tris/Glycine (2.1.4.23)
- 2.1.4.21 Tris Acetate EDTA (TAE) gel running buffer (50x) (pH8.5)
- 2M Tris.HCl
50mM EDTA
5.7% Glacial Acetic Acid
- 2.1.4.22 Tris Borate EDTA (TBE) gel running buffer (10x) (pH8.3)
- 1M Tris.HCl
0.88M Boric Acid
20mM EDTA

2.1.4.23	<u>Tris/Glycine</u>	3g/L Tris 14.4g/L Glycine
21.4.24	<u>Tris-HCl/SDS (0.5M)</u>	6% Tris.HCl (pH6.8) 0.4% SDS
2.1.4.25	<u>Tdt Buffer (1x)</u>	30mm Tris.HCl (pH7.2) 140mM Sodium Cacodylate 1mM Cobalt Chloride
2.1.4.26	<u>Wash solution</u>	0.3% Tween in Maleic Acid buffer (2.1.4.13)

2.1.5 Control Liver DNA

200 formalin-fixed, paraffin-embedded liver biopsy specimens were identified from the University Hospitals of Leicester NHS Trust. These consisted of 100 biopsies coded as histologically normal and 100 coded as metastatic. These were identified as appropriate controls for genotypic screening. A panel of normal control DNAs was provided by AstraZeneca Pharmaceuticals. This consisted of 53 Caucasians, 47 Hispanics and 8 Chinese individuals. The total 308 DNAs were used for PCR amplification and restriction nuclease-based screening only.

2.2 Methods

2.2.1 Nucleic Acid Extraction.

Sections of formalin-fixed and paraffin-embedded liver biopsy tissue 5µm thick were dewaxed in xylene (2x5mins) and rehydrated in 99% ethanol (2x2mins) and 95% ethanol (2mins). The tissue was then incubated overnight at 60°C in 200µl Proteinase

K digestion buffer (2.1.4.14). From the same tissue section both DNA and RNA were isolated. To the digestion buffer, 1ml TriReagent™ was added and stood for 5mins at room temperature. Simultaneous RNA and DNA extractions were carried out using the TriReagent™ manufacturers' protocol.

2.2.1.1 RNA Isolation.

RNA extraction was undertaken according the manufacturers instructions with the following alterations to the protocol: The aqueous phase was removed and the process repeated using 500µl TriReagent™ and 100µl chloroform. RNA was precipitated twice in 500µl isopropanol with 20µg Glycogen as carrier. RNA was resuspended in 100µl sterile ultra pure (UP) H₂O.

2.2.1.2 DNA Isolation.

The remaining aqueous phase was removed and isolation of DNA from the interphase was carried out using TriReagent according to the manufacturer's instructions. To aid precipitation, 20µg Glycogen was added at the ethanol precipitation step and all subsequent steps. DNA was resuspended in 20-50µl Sterile UP H₂O dependant on the surface area of the initial tissue section.

2.2.1.3 "Rapid" DNA Isolation

Paraffin-embedded sections were dewaxed and rehydrated as stated above. Tissue was vacuum dried for 10mins. 100µl of rapid extraction buffer (2.1.4.15) containing 0.5mg/ml Proteinase K was added and incubated overnight at 58°C. Proteinase K was deactivated at 95°C for 15mins and microcentrifuged at 13000rpm for 5mins before use. 8µl/ reaction was used for subsequent PCR (polymerase chain reaction) amplification.

2.2.1.4 DNA Quantification by PicoGreen™ Fluorescence Assay.

Both DNA extracted from formalin-fixed and that amplified by WGA were quantified using the PicoGreen™ DNA fluorescence detection assay according to the manufacturers protocol. This quantification method has been demonstrated to be accurate for use on small amounts of formalin-fixed DNA (Serth et al., 2000). A standard curve was constructed using Lambda DNA ranging in concentration from 2ng/μl to 10pg/μl. Samples were analysed by a Cary Eclipse fluorescence spectrophotometer microplate reader (Varian Inc, Palo Alto, CA) in a 300μl reaction volume.

2.2.2 Whole Genome Amplification (WGA).

2.2.2.1 Global Polyadenylation (GPA) PCR

Polyadenylation was undertaken incubating 10μl DNA (1-30ng) at 95°C for 5mins and transferring to wet ice. 10μl TdT buffer containing 4mM CoCl₂, 1mM dATP (source of poly A) and 10U rTdT was added. The reaction was incubated at 37°C for 15mins and terminated at 60°C for 10mins.

The resulting polyadenylated genomic DNA was PCR globally amplified using a GeneAmp 9700 thermocycler (Perkin-Elmer, Foster City, CA). The reaction was set up by adding 20μl TdT reaction to a GPA-PCR mix to give a 50μl reaction consisting of: 0.4μM GA-Tag-24dT oligonucleotide (CAG GGT TTT CCC AGT CAC GAC-24dT); 4μM GA-Tag oligonucleotide; 3.5U Expand High Fidelity Taq in 1x Alec Jeffries Buffer). Forty Amplification Cycles were performed consisting of a 30sec denaturation at 94°C followed by 10 cycles GA-Tag incorporation (30secs at 47°C,

30secs at 94°C); 30 cycles GA-Tag priming (30secs at 64°C, 30secs at 94°C) and a final extension at 72°C for 7mins.

2.2.2.2 Improved Primer Extension Preamplification (IPEP).

IPEP PCR (Dietmaier *et al*, 1999) was performed on 1-25ng Genomic DNA by a GeneAmp 9700 thermocycler in a final reaction volume of 50µl consisting of: 16nM degenerate 15mer oligonucleotide, 0.1mM dNTPs, 5U Expand High Fidelity Taq, 1mM MgCl₂ in 1x Expand Buffer 3. Fifty amplification cycles were undertaken consisting of a denaturation step of 30secs at 94°C; 2mins at 37°C; a ramping step of 0.05°C/sec; 5mins at 52°C, and a 30sec elongation step at 68°C.

2.2.2.3 Specific Target PCR amplification of WGA products

24 pairs of oligonucleotides were designed to PCR amplify the entire functional domain of the hPXR. All primers had an optimal annealing temperature of 58°C. Forward primers upstream of the target nucleotide sequence were designed at least 75bp upstream (within intronic regions) so as to allow for the inability to detect these bases. In this way all exonic sequence could be amplified in a single amplicons/exon. In the 3'UTR, 5'UTR and upstream promoter region, where the sequencing target region is greater than the size parameters of the amplicons, overlapping amplicons were designed, taking into account the 75bp upstream exclusion rule as described. To allow for generic sequencing reactions a set of all forward primers were M13-tagged (ACT GTA AAA CGA CGG CCA GT) at the 5' terminus and reverse primers likewise (CAG GAA ACA GCT ATG ACC).

Specific target PCR was carried out on 1/50th WGA reactions in a 25µl reaction mixture containing: 0.1mM dNTPs, 0.7U Expand High Fidelity Taq, 3.5mM MgCl₂, 0.4µM Forward Primer, 0.4µM Reverse Primer in 1x Expand Buffer 3.

Thermocycling, consisting of an initial 94°C for 2mins followed by 40 cycles of 94°C for 30secs, 58°C for 30secs, 72°C for 30secs, and a final extension of 72°C for 7mins was carried out by a GeneAmp 9700 thermocycler

An alternative Touchdown cycling program was also used consisting of 94°C for 2mins with 5 cycles of 94°C for 30secs, 63°C for 30secs (decreasing by 1°C/cycle), 72°C for 30secs, followed by 35 cycles of 94°C for 30secs, 58°C for 30secs, 72°C for 30secs, and a final extension of 72°C for 7mins.

2.2.3 Multiplex Nested PCR Amplification

A further set of 24 primers, which flanked the previous set of PXR functional domain primers, was designed (Figure 2.1). These primers were divided into two alternating sets so as no overlapping amplicons could be amplified in either set of 12. DNA extracted from formalin-fixed liver tissue was amplified in 2 multiplex reactions using the two different primer pair sets. Each 50µl reaction consisted of 0.16µM of each primer (24 primers per reaction), 0.1mM dNTPs, 5U Expand High Fidelity Taq, 1mM MgCl₂ in 1x Expand Buffer 3. Amplification was performed, using a GeneAmp 9700, consisting of an initial 94°C for 2mins followed by 40 cycles of 94°C for 30secs, 58°C for 30sec, 72°C for 30secs and a final 7mins extension at 72°C. Specific amplification was undertaken as previously detailed using M13-tagged primers corresponding to the flanking primers used within the multiplex reaction.

2.2.3.1 Modified Multiplex Nested PCR Amplification

18 primer pairs were designed so as 2 pairs were able to cover an entire exon (Figure 2.1). Each pair per exon was placed into one of two primers mixes A or B. In addition A contained two primers designed to flank the FGA STR locus specific primers (Applied Biosciences).

Each 50 μ l reaction contained either 0.2 μ M primer (A) or 0.2 μ M primer (B) in 1x Accuprime pfx reaction buffer as well as 2.5U Accuprime pfx DNA polymerase and ¼ of the DNA extracted from a given sample. Thermocycling was carried out using a GeneAmp 9700 with the following parameters: 94°C, 2mins denaturation with 40 cycles of 94°C, 30secs, 58°C, 30secs and 68°C, 30secs; concluding with 7mins extension at 68°C

The 50 μ l reaction was then cleaned of all free primer by Qiaquick PCR clean-up columns according to the manufacturers' protocol, and eluted with 50 μ l Sterile UP H₂O.

Specific target PCR amplification was carried out using the same thermocycling conditions with a 25 μ l reaction, in 1x Accuprime pfx reaction buffer, containing 0.4 μ M F M13-tagged and 0.4 μ M R M13-tagged primers (designed internal of those in the multiplex reaction), 1U Accuprime pfx, and 1/50th multiplex reaction product.

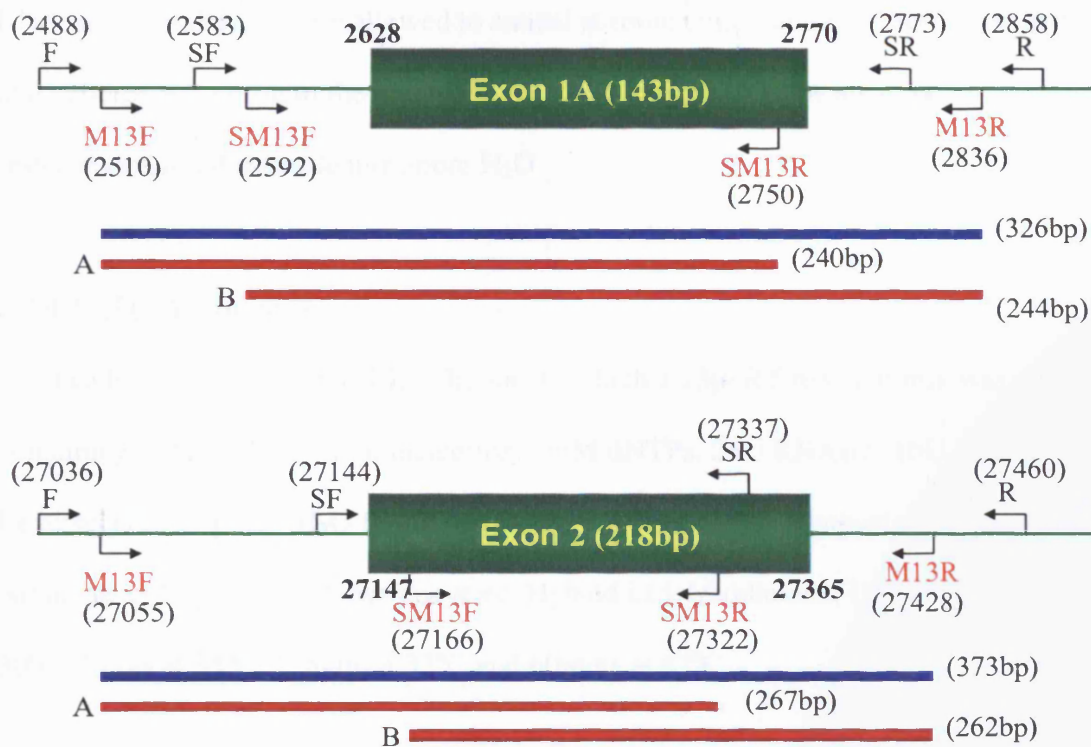


Figure 2.1. Primer design strategy for multiplex nested PCR amplification of the human PXR gene exonic regions. The diagram represents a schematic illustration of the name and position of the primers (arrows) for both the first round and subsequent amplification reaction (red). All numbers illustrate the position with reference to the chromosome 13q11 contig (accession no. NT_005594). The blue bars represent the secondary PCR product obtained using the outer M13-tagged primers and the red bar, the 2 products obtained with the inner M13-tagged primers (with size in bp indicated).

2.2.4 Reverse Transcriptase PCR

RNA extracted from Formalin-fixed tissue was resuspended in 100µl and added to 20µl of conditioned DynaBeads[®] (according to the manufacturer's protocol). The RNA and DynaBeads were allowed to anneal at room temperature for 5mins washed and pelleted according to the manufacturer's instructions. The beads were resuspended in 20µl sterile ultra-pure H₂O.

2.2.4.1 cDNA Synthesis.

The beads were divided into 10µl aliquots to which a 15µl RT reaction mix was added containing: 0.6µM 24dT oligonucleotide, 1mM dNTPs, 25U RNAsin, 10U AMV Reverse Transcriptase/ H₂O Blank in 1X AMV Buffer cDNA synthesis was carried out using an OmniGene[™] thermocycler (Hybaid Ltd, Middlessex, UK) for 2mins at 30°C, 2mins at 35°C, 15mins at 37°C and 60mins at 42°C.

2.2.4.2 PCR amplification of cDNA

1/20th of the cDNA reaction was amplified by PCR in a 50µl reaction mixture consisting of: 0.4µM Forward Primer, 0.4µM Reverse Primer, and 1U Taq Polymerase in 1x AJ buffer. A GeneAmp 9700 thermocycler was used for amplification with the following program: 98°C for 3mins, 60°C hold to add Taq, 72°C, 30secs followed by 39 cycles of 94°C for 30secs, 60°C, 30secs and 72°C, 30secs with a final extension of 72°C for 7mins.

2.2.4.3 Primer Design for cDNA amplification

Primers for cDNA amplification were designed to yield amplicons of approximately 100bp, which were located no more than 200bp upstream of the polyadenylation-

signalling motif (AATAAA). The location of this motif within the 3'UTR of target genes was determined by examination of cDNA sequence data.

2.2.5 Restriction Endonuclease Digestion of PCR Products

2.2.5.1 BccI Restriction Endonuclease

A 20 μ l digestion reaction containing 10U BccI Restriction Endonuclease, 1x BSA and 4 μ l of PCR reaction product in 1x NEB Restriction Buffer (1) was incubated at 37°C for 12 hours and inactivated at 65°C for 20mins.

2.2.5.2 MwoI Restriction Endonuclease

A 20 μ l digestion reaction containing 5U MwoI Restriction Endonuclease, 1x BSA and 4 μ l of PCR reaction product in 1x NEB Restriction Buffer (3) was incubated at 60°C for 4 hours.

PCR products incorporated an additional MwoI site and the product is truncated in the presence of the MwoI enzyme thus acting a control for restriction endonuclease.

2.2.6 Gel Electrophoresis (GE)

2.2.6.1 Agarose Gel Electrophoresis

WGA products were analysed by GE using a gel consisting of 1% Seakem LE

Agarose and 0.5 μ g/ml Ethidium Bromide in 1x TAE solution

Specific Target PCR products were analysed by GE using a gel consisting of 3%

Seakem LE Agarose and 1% NuSieve™ GTG Agarose with 0.5 μ g/ml Ethidium

Bromide in 1x TBE.

2.2.6.2 Polyacrylamide Gel Electrophoresis And Silver Staining

PCR and restriction digestion products were run on a 7% non-denaturing polyacrylamide gel (2.1.4.3) in 0.6xTBE buffer for 3 hours at 300v. Gels were fixed by incubation in 10% Ethanol/ 0.5% Glacial Acetic acid solution for 3mins and stained in 0.1% silver nitrate for 10mins. After 2 rinses in H₂O, gels were developed in 1.5% NaOH/0.16% Formaldehyde for 20minutes prior to neutralization in 0.75% Na₂CO₃.

2.2.7 DNA Sequencing

15µl M13-tagged PCR amplicons were cleaned of primers by incubation with 1µl ExoSAP-IT™ shrimp alkaline phosphatase solution at 37°C for 45mins with deactivation at 80°C for 15mins.

Sequencing was undertaken in a 96-well format, by R&D Genetics, AstraZeneca Pharmaceuticals PLC, using the MegaBACE™ DNA Analysis System (Amersham Biosciences). 1µl of cleaned-up PCR amplicon was added to a sequencing 19µl reaction containing 8µl DYEnamic™ ET reagent premix and 4.8pmols M13 primer. Each amplicon was sequenced in both directions using the Forward M13 (ACT GTA AAA CGA CGG CCA GT) and Reverse M13 (CAG GAA ACA GCT ATG ACC) primers. Thermocycling was carried out using a Biometra™ Thermocycler (Whatman) consisting of 30 cycles of 25secs at 95°C, 10secs at 50°C and 2mins at 60°C.

134µl Am-Ac/Ethanol (80% ethanol/ 0.2M ammonium acetate) solution was added to each reaction before centrifugation at 3000rpm for 45mins before the supernatant was decanted. A subsequent centrifugation at 600rpm for 1min was undertaken and the pellet air-dried.

The samples were loaded, with 10 μ l MegaBACE™ loading buffer, and analysed on the MegaBACE™ DNA Analysis System according to the following parameters: injection conditions, 3kV: 25secs and run conditions, 9kV: 120mins.

2.2.8 *In vitro mutagenesis*

The C301R variant clone was created from pcDNA3-hPAR1 using the QuikChange™ site-directed in vitro mutagenesis kit according to the manufacturer's protocol with 16 PCR cycles. Complementary oligonucleotides incorporating the codon change were used (Accession number: AF061056), CT GGA ACC TGG GAG **AGA** GGC CGG CTG TCC (1190-1218) and GGA CAG CCG GCC **TCT** CTC CCA GGT TCC AG (1218-1190). The altered codon is shown in bold with reference sequence position also denoted.

XL-1 Blue super-competent *E. coli* cells (as supplied within the QuikChange™ kit) were transformed according the manufacturers' protocol and 250 μ l of transformed *E. coli* cells were transferred onto LB agar plates containing 50 μ g/ml kanamycin.

The variant plasmid was extracted from the chemically competent *E. coli* cells (in 250ml L-broth overnight culture) using the Maxi plasmid purification kit according to the manufacturers protocol.

2.2.9 *Western Blotting*

2.2.9.1 *In vitro coupled transcription/ translation*

Human PXR (hPAR1 and C301R) proteins were synthesised from 1 μ g of the relevant pcDNA3 expression plasmid using the TNT quick-coupled transcription/translation Kit according to the manufacturer's protocol. 1 μ g of empty vector (pcDNA3.1) was used as a negative control.

2.2.9.2 Preparation and quantification of HeLa cell protein lysates

Transfected HeLa cells (2.2.10) were lysed by applying 50µl of protein extraction lysis buffer (2.1.4.11)/well. Lysates from six repeat wells were combined (final volume of 300µl).

1µl lysate was added to 1ml Bradford Reagent (1:5 dilution) and incubated for 10mins at room temperature. Absorbance at 595nm was determined by spectrophotometry and protein concentration calculated by way of a standard curve of bovine serum albumin (BSA) at 10, 5, 1, 0.5, 0.1µg/µl final concentration. 25µg protein lysate was added to 4x sample buffer (1:4 dilution) and heated to 95°C for 5mins prior to SDS-PAGE.

2.2.9.3 Sodium Dodecyl Sulphate-Polyacrylamide Gel Electrophoresis (SDS-PAGE)

A denaturing SDS gel was poured consisting of a 12% lower resolving gel (7ml) (2.1.4.4) and a 4% upper stacking gel (2.1.4.1). Prior to sample loading, wells were rinsed with electrode buffer (2.1.4.8)

Gels were assembled into electrophoresis apparatus containing electrode buffer. 2µl of translated hPXR protein reactions or 25µg lysate with 1x sample buffer (2.1.4.16) were loaded alongside 10µl Precision Protein Standard Broad Range ladder. Gels were run at 100V for 15mins in order for samples to pass through the upper stacking gel and run at 120V for a further 90mins.

2.2.9.4 Transfer and Blocking

Proteins were transferred overnight in transfer buffer (2.1.4.20) at 30V onto a nitrocellulose membrane. The membrane was rinsed twice and washed for 5mins in sterile ultra-pure H₂O. The presence of total protein was detected by staining with

Ponceau S (5mins); rinsing with sterile ultra-pure H₂O and destaining with 0.1M NaOH for 30secs. A further 2 rinses and a 5mins wash in sterile ultra-pure H₂O were undertaken followed by 5mins in TBS-t (2.1.4.17) and an overnight incubation in blocking solution (2.1.4.6) at 4°C.

2.2.9.5 Antibody Labelling

The membrane was rinsed in TBS-t followed by 2x15mins and 2x5mins washes in TBS-t. The primary goat anti-human PXR antibody (Santa Cruz Biotechnology) was added at 1:100 dilution in 10% blocking solution and incubated for 90mins at room temperature.

A further rinse plus 2x5mins and 2x15mins washes in TBS-t preceded the application of the secondary rabbit anti-goat IgG peroxidase conjugate (Sigma) at 1:10000 dilution in TBS-t with a 90mins incubation at room temperature.

The membrane was rinsed twice in TBS-t followed by 2x10mins and 2x5mins TBS-t washes.

Development was by the Enhanced Chemiluminescence System according to the manufacturers' protocol with detection on Hyperfilm™ with a 5secs exposure.

2.2.10 Reporter gene co-transfection assay

HeLa (human cervical carcinoma) and Cos-7 (African green monkey kidney fibroblast) cell-lines were seeded in 48-well tissue culture plates (NUNC) at a density of $4 \times 10^4 / \text{cm}^2$ in 400µl growth media (2.1.4.10) and incubated for 24hours.

For each well, 1µl Gene Juice was added to 100µl serum-free media (2.1.4.10 without 10% FBS) and incubated for 5mins at room temperature. To this, 500ng of plasmid DNA was added. This consisted of 400ng pBSIISK-, 50ng pCMV.Renilla; 25ng

pGLuc containing either 2 repeats of the DR3 or 2.5 repeats of the ER6 response element; and 5ng pcDNA3 or pcDNA3 containing the cDNA sequence corresponding to the protein-coding region of the rat or human wild type (hPAR1) and human C301R variant PXR gene. After 20mins incubation at room temperature, 300µl of growth media with charcoal-stripped serum (2.2.10.1) was added to each mixture. 400µl/well was then applied to the cells (pre-washed with 200µl 37°C PBS with Ca²⁺ Mg²⁺). Cells were incubated for a further 24hours at 37°C. Cells were then rinsed with 200µl 37°C PBS (with Ca²⁺ Mg²⁺). 400µl/well of serum-free media was applied containing the appropriate treatment compound at the specific concentration. All compounds were diluted in DMSO and so negative control wells were treated with an equivalent volume of DMSO only. After 24hours incubation, cells were rinsed twice in 200µl PBS and lysed with 100µl transfection lysis buffer (2.1.4.19). Lysates were shaken for 20mins and 50µl/well transferred to a white 96-well Optiplate™ (NUNC). Luminescence was assayed using the FireLite™ luminescence detection kit according to the manufacturer's protocol on the Top Count plate luminometer (Packard Biosciences). Renilla readings allowed for normalisation against transfection variability.

2.2.10.1 Preparation of HeLa cell lysates for mRNA analysis.

2 sets of 6 replicate wells of cells transfected and treated with 0.1% DMSO (2.2.10) were lysed by the addition of 100µl TriReagent/ well. Each set of 6 replicates was combined and total RNA isolated according to the protocol (2.2.1.1). mRNA isolation and cDNA synthesis were undertaken as described in 2.2.4.

2.2.11 Electrophoretic mobility shift assay

2.2.11.1 γ ³²P Radio-labelling of Double-Stranded Oligonucleotide

Wild type double stranded oligonucleotides representing the CYP3A4 PXR DNA binding element with an everted repeat separated by six base pairs (ER6) (GAT CAA TAT GAA CTC AAA GGA GGT CAG TG) and with a direct repeat separated by three base pairs (DR3) (CTA GTG CTC GGG TAG AGG TCA AGG AGG TCA CTC GAC) were synthesised along with mutated ER6 (GAT CAA TAT **TAA** CTC **AAT** GGA **ATA** CAG TG) and DR3 oligonucleotides (CTA GTG CTC GGG TAG **AGA** **ACA** AGG **AGA** **ACA** CTC GAC) with disrupted nuclear receptor half-sites (mutated bases bold/underlined). These were created by heating equal amounts of sense and complimentary antisense single-stranded oligonucleotides to 95°C for 15mins and allowing the to cool slowly to room temperature.

A 20 μ l radio-labelling reaction consisted of 100ng double stranded ER6/mutated ER6 oligo, 2 μ l 5x T4 kinase buffer (2.1.4.18), 30 μ Ci γ -³²P-dATP and 5U T4 polynucleotide kinase. The reaction was incubated for 37°C for 45mins and inactivated at 65°C for 10mins.

Unincorporated radiolabel was removed by use of G-50 Microspin™ columns according to the manufacturer's protocol. Purified probes were diluted to a volume of 500 μ l and 5 μ l added to 5ml of Ultima Gold F scintillation fluid. ³²P activity was determined using a LS6500 scintillation counter (Beckman Coulter).

2.2.11.2 EMSA DNA/Protein Complex Binding Reaction

2.5 μ l of transcribed and translated PXR and 2.5 μ l mRXR (2.3.10.1) proteins were incubated with 8 μ l EMSA binding buffer (2.1.4.9), 2 μ g poly dI-dC. Reactions were in the presence or absence of 50, 100 or 500 molar excess of unlabelled ER6 or 500x mutated ER6 and were incubated on ice for 10mins. 2 μ l radio-labelled probe at

25,000cpm/ μ l or 10ng Biotin-labelled probe was added and the reaction incubated on ice for a further 10mins.

Radio-labelled complexes were resolved by electrophoresis through a 4% non-denaturing gel at 150V for 2.5hrs. Gels were dried using a vacuum drier at 65°C for 90mins. Complex formation was detected on x-ray film with an overnight exposure at -70°C exposure.

2.2.11.3 Biotinylated EMSA complex detection.

Biotin-labelled EMSA complexes were transferred to Biodyne B membrane for 30mins at 300mA in 0.5xTBE. The membrane was baked for 30mins at 85°C and placed in blocking solution for 30mins. Streptavidin solution (diluted 1:1000 in blocking solution) was applied for 10mins, the membrane washed again in wash solution and a biotinylated alkaline phosphatase (BAP) solution applied (1:500 dilution in blocking solution) for 10mins. The membrane was washed again in wash solution for 10mins and the streptavidin, BAP application repeated. Two further 15mins washes were undertaken followed by 5mins in substrate buffer. 0.4% CDP Star solution was applied to the membrane for 5mins. Biotin-labelled complex formation was detected on Hyperfilm™ with a 5mins exposure.

2.2.12 Other protocols.

2.2.12.1 Preparation of charcoal-stripped foetal calf serum.

To strip 250ml of foetal calf serum (FCS), 0.625g dextran-coated charcoal was prepared by incubating in 250ml charcoal stripping buffer (2.1.4.7) overnight at 4°C. 50ml of charcoal/buffer spun down briefly at 3000rpm and the supernatant discarded. 50ml FCS was added to the retained charcoal and incubated overnight at 4°C. The

FCS was spun down briefly at 3000rpm and filter sterilised using a 4.5µm Acrodisc™ prior to addition to growth media.

2.2.13 *Statistical Analysis.*

Statistical significance in reporter gene assays was determined by way of a pair-wise, one-way ANOVA. A step-down analysis was applied whereby, firstly, statistical between the highest concentration of compound and the no treatment control is determined and working backwards until significant difference is not observed. This maintains type 1 error and allows for comparison of the drug response between different receptors without the need for a two-way analysis which, given the obvious differences in response was not deemed necessary. No post-hoc correction was applied, since n=3 may make such corrections too rigorous for a sample of this size. Data represented in figure 5.11 was analysed by one-way ANOVA but without a step-down approach.

Allele frequency significance between cohorts was determined by a Fishers' Exact Test. All statistical analysis was undertaken using the SPSS 12.0.1 software package.

**Chapter 3: Identification and
characterisation of a Hepatic ADR cohort
from the clinical tissue archive.**

3. Identification and characterisation of a Hepatic ADR cohort from the clinical tissue archive.

3.1 Adverse Drug Reaction Cohort Identification.

The University Hospitals of Leicester NHS Trust possesses a vast archive of formalin-fixed, paraffin embedded biopsy tissue. Utilizing tissue taken for biopsy from the 3 trust satellite hospitals (Leicester Royal Infirmary, Leicester General Hospital and Glenfield Hospital) between 1992 and 2001, access to 1893 liver biopsies was possible.

Ethical approval for this study was granted on the understanding that patient information was anonymised and limited only to that available from analysis of clinical pathology and biochemistry archive records. There was therefore no possibility of prospective sample collection and patient recall, for example.

In order to determine to identify, within the collection, those hepatic biopsies exhibiting morphological features consistent with adverse drug reactions, two distinct selection procedures were undertaken as summarized in Figure 3.1. In the first instance, biopsies were categorised on the basis of the codes within the database which represent a single phrase description of the aetiology as determined by the histopathologist.

Given that the hypothesis of the study is that PXR is potentially dysfunctional in cases of hepatic ADR, it was felt necessary to discriminate for biopsies showing morphological evidence that specifically relate to disrupted detoxification and/ or bile acid homeostasis. In essence the intention was to isolate cases of drug-induced cholestasis.

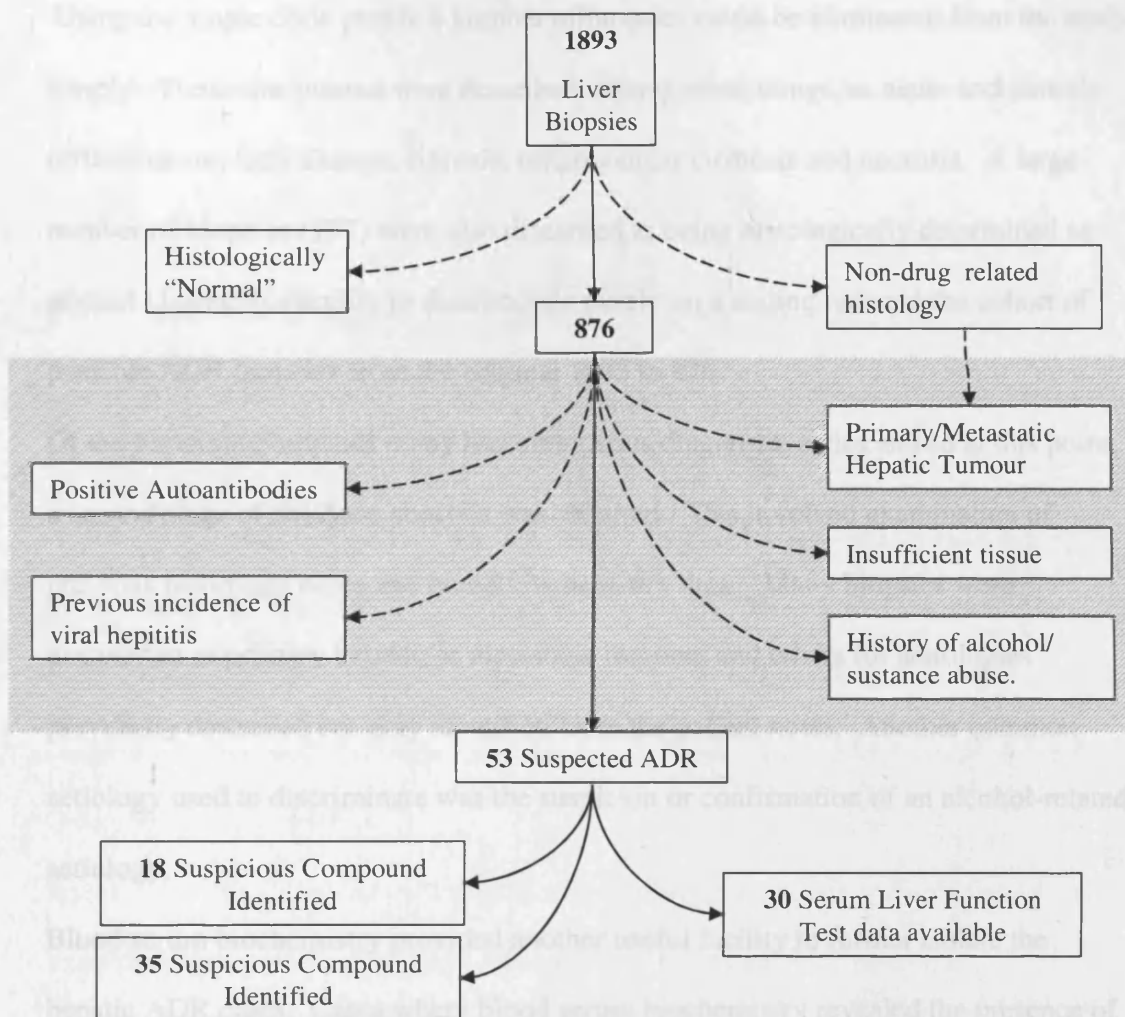


Figure 3.1. Identification of a Hepatic ADR cohort from a clinical archive of core needle liver biopsies. The schematic diagram summarizes the process by which cases were discriminated against in the process of isolating those cases which demonstrated morphological evidence of ADR. The cross-hatched area shows decisions taken based on information dissected from within the pathology notes and blood biochemistry. Initial decisions were made based purely on the single code description of the histopathologist respectively.

Using the single code phrase a number of biopsies could be eliminated from the study simply. Those discounted were described, among other things, as acute and chronic inflammation, fatty change, fibrosis, micronodular cirrhosis and necrosis. A large number of biopsies (137) were also discarded as being histologically determined as normal. Using this ability to discriminate purely on a coding reduced the cohort of possible ADR biopsies from the original 1893 to 876.

Of the remaining biopsies many had ambiguous diagnostic codes and so at this point, a second stage of database analysis was required. This involved examination of previous pathology notes and blood biochemistry data. Many biopsies were discounted as primary hepatic or metastatic tumours and others for aetiologies previously described but only identified from the patient notes. Another common aetiology used to discriminate was the suspicion or confirmation of an alcohol-related aetiology.

Blood serum biochemistry provided another useful facility to further isolate the hepatic ADR cases. Cases where blood serum biochemistry revealed the presence of autoantibodies and/or previous incidence of viral hepatitis were discounted.

Discrimination against the presence of autoantibodies provides the opportunity to eliminate cases where other cholestatic liver diseases of autoimmune origin, such as primary biliary cirrhosis (PBC) and primary sclerosing cholangitis may be the cause. Using the process as described, a set of 53 patient biopsies was determined as being suspicious of drug aetiology with all other reasonable alternative aetiologies seemingly discounted.

Of the cohort of 53 patients identified, reference to the notes revealed that in the case of 18 of these ADRs, a drug therapy administered was named as suspicious of being the aetiology of the ADR. These included methotrexate, simvastatin, flucloxacillin, azathiopine diclofenac, vancomycin, cephalaxone, metranidazole and norethisterone as

well as recognised human PXR ligands carbamazepine, nifedipine and tamoxifen.

The gender of the cohort was observed as 62% male and 38% female with a mean age of 56.4years \pm 17.6SD and 52.2years \pm 18.6SD

3.2 Blood Serum Liver Function Test Data for ADR cohort

Liver function tests provide additional diagnostic information in the determination of aetiology in hepatic injury. In many instances serum blood levels of alanine transaminase (ALT), alkaline phosphatase (ALP) and bilirubin are measured prior to undertaking a hepatic core needle biopsy. Due to the retrospective nature of the collection of such data for the 53 ADR cases, as well as inter-patient variation in diagnostic procedure, pre-biopsy data for only 30 (ALT), 29 (ALP) and 28 patients (bilirubin) were available.

Assessment of ALT levels in the ADR cohort showed that 22/30 (73.3%) had levels exceeding the upper normal limit (Figure 3.2). The mean ALT level was 297.1% \pm 45.0 of the upper normal, equivalent to 152.9 \pm 23.9iU/L. Of the 29 patients where data was available regarding ALP levels, 25 (86.2%) showed pre-biopsy levels above the upper normal limit (Figure 3.2). Mean ALP levels were lower than those of ALT with a mean of 206.9% \pm 130.0 of the upper normal limit. This is equivalent to 268.9 \pm 45.3iU/L.

In the case of the bilirubin levels for the 28 ADR patients available, 22 (75.6%) of individuals displayed levels above the upper normal limit with mean of 679.2% \pm 170.2 (Figure 3.2). This is equivalent to 115 μ mol/L \pm 28.9 compared to a normal range of 3-17 μ mol/L. The data is suggestive of significant raised levels above the normal range for all 3 markers, with levels of bilirubin particularly high.

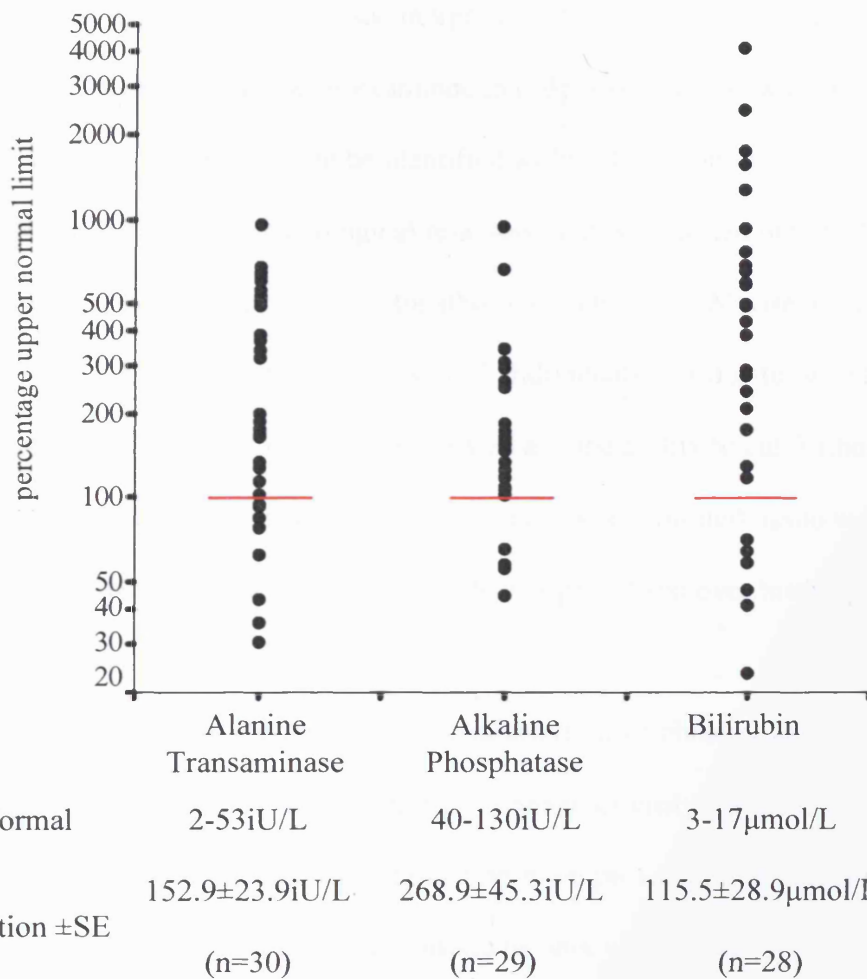


Figure 3.2. Blood serum liver function test levels in the ADR patient cohort. Data represents the log percentage of the upper limit of the clinical normal range (represented by the red line) and is plotted on a log scale. Mean concentration \pm SE in clinically relevant units of concentration are also shown.

3.3 Morphological assessment and classification.

Despite having isolated the 53 cases of suspected ADRs using the notes compiled by the pathologist, it was felt that the tissue morphology from which the original aetiology was concluded could be re-examined in order to determine whether any patterns of common histology could be identified within the cohort.

Of the 53 ADR liver biopsies, histological re-assessment was carried out on 40 H&E specimens (Table 3.1) by a specialist histopathologist (Dr Angus McGregor, Leicester Royal Infirmary). The absence of sections of 13 individuals was due to two reasons. Firstly, no archived H&E section could be located and the ability to cut further sections was negated by the size of remaining tissue. Where limited tissue was available, the process of extracting nucleic acids was prioritised over histological assessment.

Of the 40 cases assessed 30 showed features characteristic of cholestasis. Of these 17 were classed as mild with some bile plugging of canaliculi visible (Figure 3.4A). 5 cases were identified as moderate cholestasis with more prevalent bile plugging visible and in some cases the presence of mitotic hepatocytes (Figure 3.4B) suggesting quite severe injury. 8 cholestatic hepatic tissues out the 30 were deemed as severe cholestasis with massively swollen bile retentive hepatocytes visible and considerable degree of necrotic tissue evident (Figure 3.4C).

Aside from cholestasis, fatty change was next most frequently observed morphology with the 40 representative specimens from the ADR cohort with 8 incidents. Of these, 5 were classified as mild, 1 as moderate and 2 as severe (Figure 3.5). Bile duct injury (Figure 3.6) characterised by large inflammatory infiltrate of ductal regions and truncated ducts was observed in 7 individuals.

	<u>Sex</u>	<u>Age</u>	<u>Cholestasis</u>	<u>Bile Duct Injury</u>	<u>Steatohepatitis</u>	<u>Fatty Change</u>	<u>ALT</u> (iu/L)	<u>ALP</u> (iu/L)	<u>Bilirubin</u> (umol/L)	<u>Putative Associated Compound</u>
1	M	75	NA							Nifedipine
2	M	79	+				16	384	7	
3	M	31	+++							
4	M	38		++	++		206	399	99	
5	F	47	+++				23	175	301	Tamoxifen
6	F	18	+							Unknown Oral Contraceptive
7	M	28	+				41	216	706	
8	F	65	++				510	1226	420	Vancomycin
9	F	46	+							
10	F	58		++						
11	F	26	+			++	282	335	73	
12	F	30	+				195	153	30	Diclofenac/Co-proxamol
13	M	46	+							Methotrexate
14	F	66			+++		99	163	217	
15	M	66	NA				89	206	85	
16	F	85	+				61	213	47	
17	M	67	+++				318	326	36	
18	M	32	++	++			357	344	49	Amoxicillin
19	F	73	+	++						
20	M	65				+++	179	85	41	
21	M	49				+	49	133	10	
22	M	53				+++	169	75	20	
23	F	56	NA							
24	F	54	+++				87	240	83	
25	M	84	+							
26	F	66	+++				267	164	66	
27	F	62	NA							Methotrexate
28	M	42	NA							Methotrexate
29	F	43	NA				94	140	22	
30	M	52	NA				298	139		Carbamazepine
31	M	28	NA				340	142		
32	F	76	NA							
33	M	34	NA				50	133	8	
34	M	37	NA							Methotrexate
35	M	71	NA				19	58	4	Methotrexate
36	F	53	NA				260	449	130	Norethisterone
37	F	26	+				45	341	111	
38	M	39	+	++			332		101	
39	F	30	+++							Unknown Oral Contraceptive
40	M	76	+++	++						
41	M	55	+				33	869	268	
42	M	78	+++	++						
43	M	61	+	++						Azathiopine
44	M	31				+	107	72	12	
45	M	71	+							
46	M	62	++				71	201	159	
47	M	66	+				323	193	117	Simvastatin
48	M	78				+				
49	M	55				+	68			
50	F	64	+							Flucloxacillin
51	M	76	++							
52	M	62	++							Cephalexon/Metranidazole
53	M	74				+	54	225	11	

Table 3.1. Classification of the morphology of hepatic biopsy sections from the ADR patient cohort. The four observed pathologies were scored as mild (+), moderate (++) and severe (+++). NA denotes specimens where no morphology data was available due to the absence of, and inability to cut further sections of, the biopsy tissue. Data in red represents liver function test data at 2x ULN.

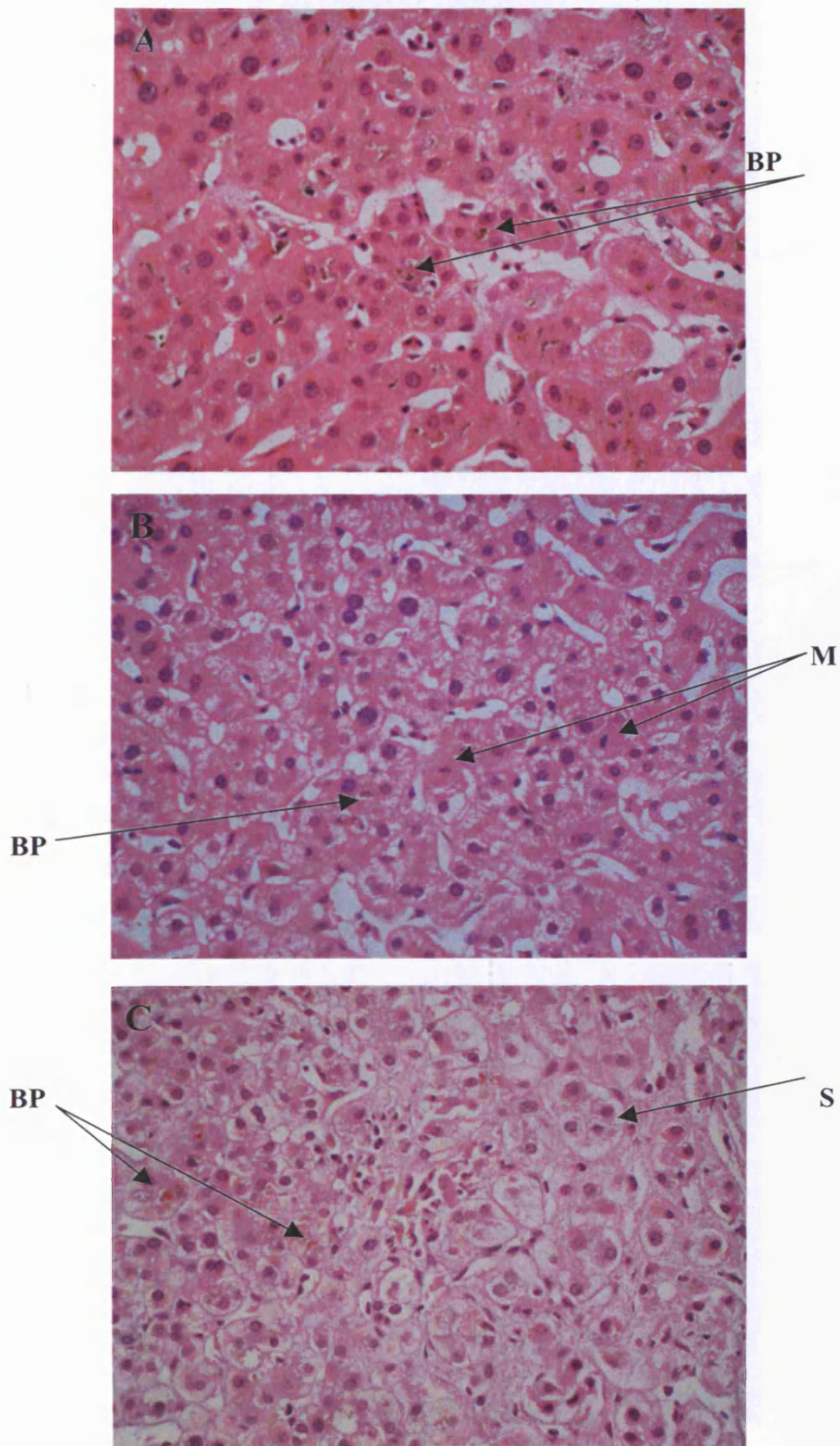


Figure 3.4. Representative (H&E) stained liver histology from ADR patients exhibiting cholestatic injury. Represented is mild (A), moderate (B) and severe (C) injury. Examples of canalicular bile plugging (BP), mitotic (M) and swollen bile-retaining hepatocytes (S) are indicated. Images are high power (400x) magnification.

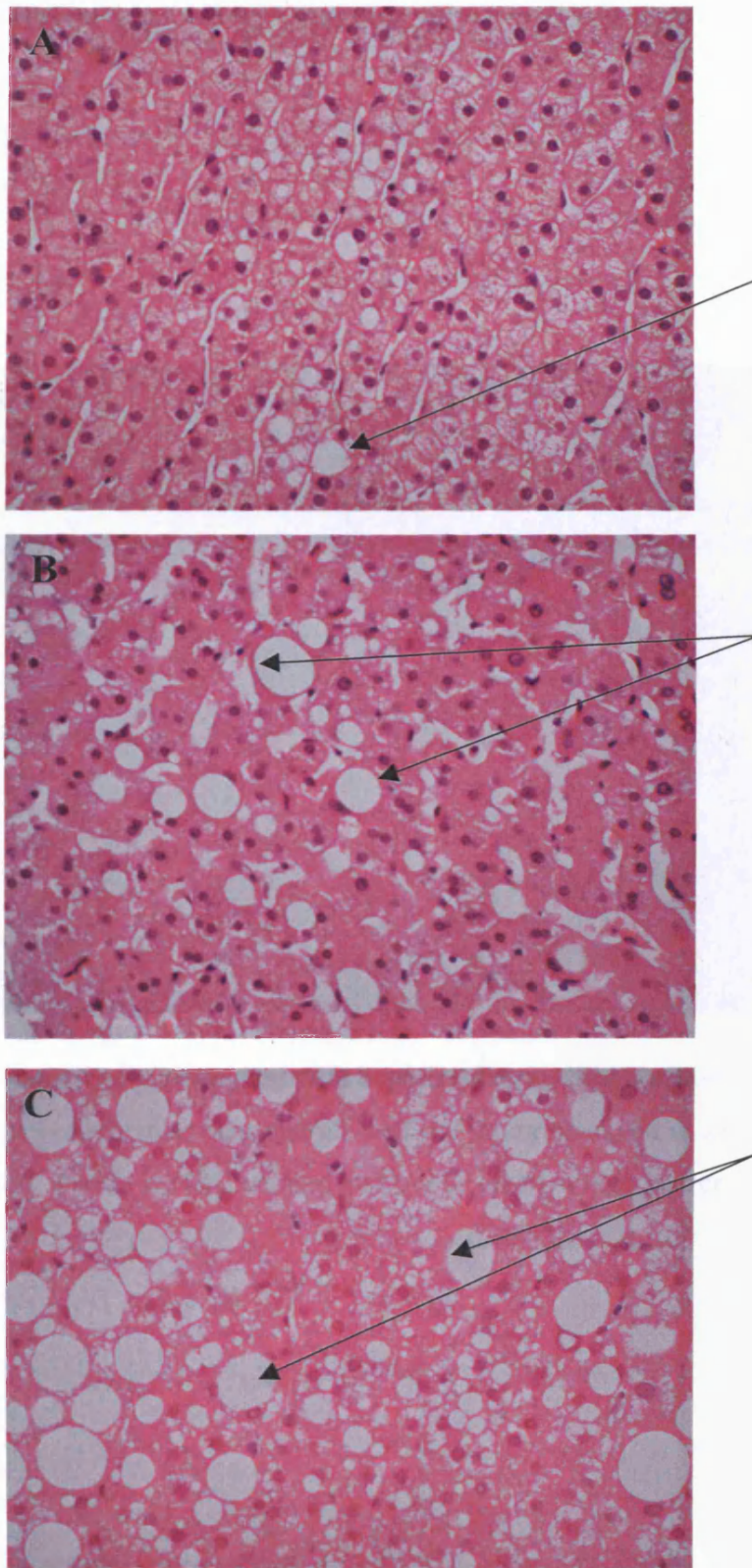


Figure 3.5. Representative (H&E) stained liver histology from ADR patients exhibiting fatty change (steatosis). Represented is mild (A), moderate (B) and severe (C) injury. Examples of fat accumulation are indicated by arrows. Images are high power (400x) magnification.

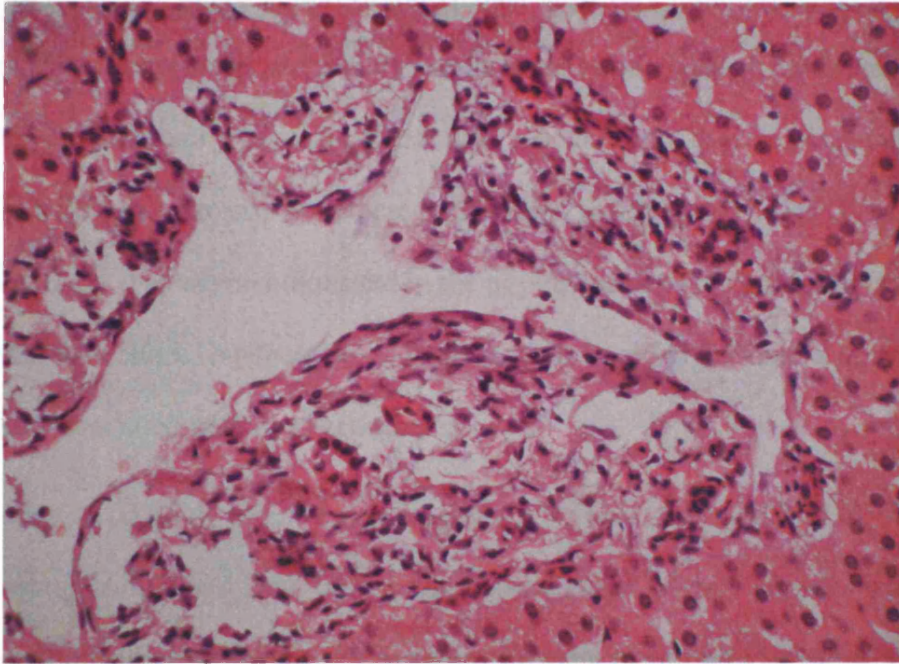


Figure 3.6. Bile duct injury associated with hepatic adverse drug reactions. The image shows a representative bile duct demonstrative of the injury observed in a number of others of the ADR cohort. Tissue is H&E stained and image taken at high power (400x).

3.4 Discussion

3.4.1 *Selection of hepatic ADRs from the archival collection.*

In evaluating the process by which the 53 ADR cases were isolated, from the 1893 liver biopsies available, it is important to emphasise the aim of the exercise. Rather than identify a homogenous cohort of individuals showing similar presentation, biochemistry and pathology, the cohort was intended to be a genetic enrichment of the population, demonstrating hepatic adverse drug reactions of a diverse spectrum. By enriching in this way, the aim is to increase the observed frequency of PXR variants from, potentially, 1 in several thousand in the population as whole, to a detectable level within the cohort. Attenuation of PXR function could give rise to a number of pathologies associated with drug aetiologies.

Identification of 53 ADR patients over a period of 9 years (1992-2001) is similar to the findings of (Aithal and Day, 1999). Their investigation of liver biopsies over an 18-year period from a Newcastle, UK teaching hospital identified 110 patients with hepatic biopsies coded as drug-induced or hepatitis/cholestasis of unknown aetiology.

(Aithal and Day, 1999) subsequently reduced their cohort to 44 by review of comprehensive biochemistry and pathology records. They did however include cases of drug-induced hepatitis within the cohort. Though this process may have been possible with the cohort identified within this project, the concept of genetic enrichment for ADR predisposition means that thorough review is not necessary as increased frequency of ADR-associated genetic polymorphism could be observed from the 53 regardless of any possible heterogeneity of the drug-induced aetiology.

3.4.2 Evaluation of LFT data from ADR cohort selection.

Pre-biopsy blood serum biochemistry data would seem to confirm liver injury in the majority of the 30 cases where data is available. ALT levels, observed at a mean of 2.88-fold above ULN are indicative of hepatic cells damaged but not necessarily undergoing cell death (Limdi and Hyde, 2003)

A 6.79-fold over the ULN for serum bilirubin levels, with some cases exhibiting >30-fold increases, were observed. Only 6/28 observed serum bilirubin levels were within the clinically normal levels. This would suggest a consensus pattern of hepatic biliary obstruction within the ADR cohort.

The raised serum ALP levels observed in 26/29 individuals, at a mean of 2.1-fold above ULN, would seem to correlate with the idea of predominantly hyperbilirubinaemic injury. Hepatic ALP is localized on the canalicular and luminal domain of bile ducts (Limdi and Hyde, 2003) and such raised levels are usually representative of impaired bile acid homeostasis at a hepatocanalicular level. It would appear that the predominant injury to the liver of the individuals is cholestatic in nature; however, the localisation of the bile flow obstruction is not determinable from blood biochemistry alone.

Clearly, given the method of cohort selection and it's heterogeneity it would be unwise to suggest that the whole cohort exhibit the same aetiology and pathology. However does appear that impairment of bile flow is an important feature of the hepatic injury displayed by a large number of the cohort.

3.4.3 Relationship of serum LFT data with reassessed histology

The evaluation of the cohort by observation of the pre-biopsy serum LFT data is supported by the histological reassessment. Of the 41 cases assessed, 30 were classified as cholestasis of a hepatocanalicular nature, with 6 of these individuals also exhibiting bile duct injury. Given the raised serum bilirubin and alkaline phosphatase levels, this would seem to concur.

Raised ALT levels could be a result of any one of the observed pathologies including steatosis (8 cases) and the necrosis and inflammatory infiltration observed in some livers.

3.4.4 Could altered PXR functionality be a predisposing factor in the drug-induced aetiology of the ADR cases?

Given the number of cases with histology suggestive of hepatocanalicular-derived cholestasis, it is reasonable to presume that the predisposing factors possessed by these individuals may be genetic dysfunction of one, or more of the genes regulating hepatic bile acid homeostasis. Given the central regulatory and sensory role, PXR plays within this system, it may well be that one specific genetic predisposition in some of these cases may well be within the PXR gene.

Of the cases within the cohort not showing cholestatic injury, there is still the likelihood that PXR dysfunction could be a predisposing factor to the drug-induced injury. This however is more likely to be manifest as a result of PXR regulation of drug metabolizing enzymes and transporters. Altered PXR function could affect the pharmacokinetics of the suspect therapy leading to toxic insult in predisposed individuals.

3.4.5 Conclusions

The isolation of the 53 cases as described would seem to have identified a cohort of individuals suitable for the purposes of this study. Whilst there is no direct evidence of ADR (in terms of confirmed therapy with an identified suspect compound), all of these cases possess properties, both histological and biochemical, suggestive of a hepatic ADR. It is therefore reasonable to presume that this cohort represents a suitable enrichment for hepatic ADR predisposition from the population as a whole.

**Chapter4. Whole Genome Amplification
and Nested PCR Pre-Amplification for
Analysis of DNA from low yield formalin-
fixed tissue**

4. Whole Genome Amplification and Nested PCR Pre-amplification for Analysis of DNA from low yield formalin-fixed tissue

4.1 Introduction

Given the age of the archival specimens and the nature of the tissue processing techniques and previous diagnostic analysis, a number of limitations need to be considered when nucleic acid analysis is proposed.

4.1.1 Formalin Fixation

The archival hepatic tissues are Formalin-fixed and paraffin-embedded. Such samples are the most widely available material for retrospective studies and provide an invaluable resource for molecular genetic studies. However, the extraction of high quality DNA and RNA has always been problematic. Studies have shown extraction protocols even, when highly optimised can yield PCR amplifiable genomic DNA in 61% samples and RNA was PCR detectable in 83.7% of samples (Coombs et al., 1999).

Formalin-fixation has also been shown to give rise to chemical modifications in both DNA and RNA. In both cases these modifications result in lowered PCR efficiency. Formalin-fixation causes DNA base mutation artefacts at a frequency as high as 1 per 500 bases. In order to prevent such artefacts from influencing PCR amplification and subsequent sequencing a sample containing >300 cells has been demonstrated to be sufficient (Williams et al., 1999). Despite these limitations, genotypic analysis of formalin-fixed human hepatic tissue has been previously achieved. An example of this is the mutation analysis of the human hemochromatosis (HFE) gene in hereditary hemochromatosis (Przygodzki et al., 2001).

In the case of RNA, formalin causes the addition to the bases of mono-methylol groups (Masuda et al., 1999). This is simply overcome by elevating the sample temperature in formalin-free buffer to 70°C.

The specimens in question range in size from a true-cut biopsy with a cross-sectional surface area of 1cm² to a core needle biopsy with a surface area of >10mm². An example of a typical core biopsy is illustrated in Figure 4.1. Because of the small size of some core needle biopsy tissue specimens, the amount of DNA and RNA, which is present, and extractable, is extremely limited. Whilst in the case of larger true cut biopsy sections, adequate amounts of DNA for genotyping are present; in smaller specimens this is not the case. In order to include all the specimens in the cohort within this study, a strategy whereby the amount of representative genomic DNA was significantly increased needed to be considered.

4.1.2 Whole Genome Amplification

Several strategies, termed whole genome amplification, have been developed to pre-amplify the entire genome from minimal amounts of DNA for subsequent molecular genetic analysis (Dietmaier et al., 1999; Stoecklein et al., 2002; Zhang et al., 1992).

However many such methods have found global amplification of formalin-fixed DNA limited (Dietmaier et al., 1999; Zhang et al., 1992).

Many of these strategies use degenerate priming methods. Degenerate oligonucleotide-primed PCR uses a degenerate hexamer with defined flanking sequences at initial low stringency followed by higher stringency PCR. However, using cells from formalin-fixed tissue, an efficiency of only 30-70% of target amplicons was achieved from <500 cells (Dietmaier et al., 1999). A modified protocol for longer length fragment amplification (long-length DOP-PCR) was also



Figure 4.1. An Hepatic Core Needle Biopsy. The photograph illustrates a typical 5µm section of morphologically normal human liver core biopsy. The tissue is stained with Haematoxylin and Eosin and measured approximately 8mm in length

limiting in its ability to pre-amplify degraded DNA from formalin fixed tissue (Kittler et al., 2002).

Another method, termed primer extension pre-amplification (PEP) PCR (Zhang et al., 1992) uses a totally degenerate 15mer primer with 50 cycles of very low stringency PCR. Like DOP-PCR, this too had a very low efficiency (50-66% of amplicons) with specific target PCR. A modified version of PEP, improved PEP (IPEP) PCR was later demonstrated to have an efficiency of 100% of subsequent PCR target amplicons in samples <30cells (Dietmaier et al., 1999). This differs from PEP by using a taq polymerase incorporating a proof reading subunit and an additional cyclical 68°C extension. Further optimisation of IPEP has shown an optimal amplification with a minimal input DNA of 25ng. TaqMan™ PCR has also been used to demonstrate IPEP DNA concordance with raw genomic DNA (Powell, H. (AstraZeneca Pharmaceuticals), personal communication, 2002).

Other methods of note for whole genomic amplification of formalin-fixed DNA have also been demonstrated. These include single cell comparative genomic hybridisation (SCOMP) (Stoecklein et al., 2002), which uses restriction digestion and subsequent primer ligation within a PCR method. Polyadenylation and PCR using dT24 primers of degraded DNA fragments, found in formalin-fixed samples in a manner similar to that demonstrated for global cDNA amplification (Al-Taher et al., 2000) is also a consideration of this study (self-termed Global Polyadenylation (GPA) PCR).

This study aims to investigate the use of appropriate DNA pre-amplification techniques in order to use their products for genotyping the tissue specimen whose raw DNA yield is too low for such investigation.

4.2 DNA Pre-amplification

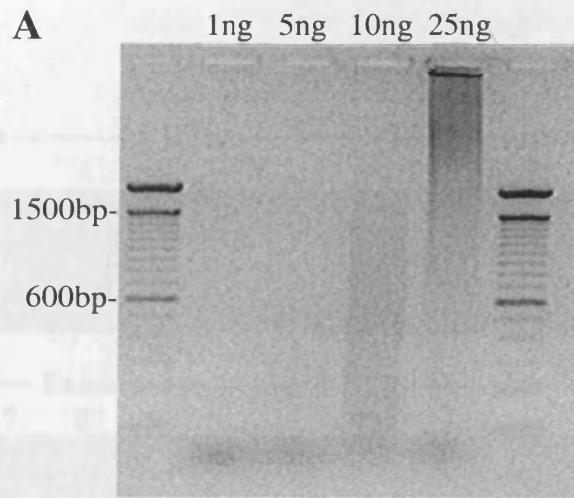
The aim of the pre-amplification step was to provide a suitable amount of DNA template for a second PCR reaction in order to produce PXR exon-targeted amplicons for sequencing analysis. M13-tagged amplicons were created allowing for the utilisation of generic sequencing primers and hence high throughput protocols.

4.2.1 Whole Genome Amplification

The strategies investigated for whole genomic amplification of DNA from fixed liver DNA samples showed considerable variation in sensitivity and efficiency both in the initial WGA pre-amplification and in the subsequent specific target PCR amplification.

4.2.1.1 Global-polyadenylation PCR

Initial investigation centred on the use of the GPA PCR protocol for pre-amplification of DNA from the formalin-fixed biopsy tissue. As Figure 4.2 demonstrates there is a marked difference in the GPA PCR products yielded when the amount of input formalin-fixed DNA is altered. Though the magnitude of GPA products is similar (25ng DNA yields 2.8 μ g DNA, while 1ng yields 0.9 μ g), there appears to be inversely proportional amplification of DNA (1ng of DNA is amplified 935.45-fold while 25ng is amplified just 114.17-fold). Not only does the amount of the yield vary but also the nature of the fragments amplified. Amplification of 25ng input DNA yields a product consisting of fragments, the majority of, which appear to be >2000bp in length. 10ng of input DNA gave rise to amplified fragments between approximately 2000bp and 100bp in size; 5ng to fragments 600-100bp.



B

<u>Input Genomic DNA (ng)</u>	<u>Genome amplification DNA (ng)</u>	<u>Fold Amplification</u>
1	935	933x
5	958	192x
10	1667	167x
25	2854	114x

Figure 4.2. Global Polyadenylation-PCR DNA yield from varying amounts of input formalin-fixed liver DNA. **A.** GPA-PCR products from amplification reactions containing 1, 5, 10 and 25ng of DNA extracted from a 5 μ m formalin-fixed true-cut liver biopsy section. Molecular weight markers are shown (100bp ladder). Each lane contains 10 μ l of GPA-PCR reaction mixture. **B.** Quantification of the same GPA-PCR products by PicoGreen fluorescence DNA detection. Fold amplification is calculated as input DNA (ng)/ Yield GPA DNA (ng).

Curiously despite detection by FluoGreen no product was observed by gel electrophoresis for GPA-PCR amplification of IgG input DNA.

Amplification of specific targets within the functional domain of the hPXR gene demonstrated an adverse effect on the number of initial DNA input into the GPA-PCR. Addition of 25ng of GPA-PCR product to subsequent PCR reactions

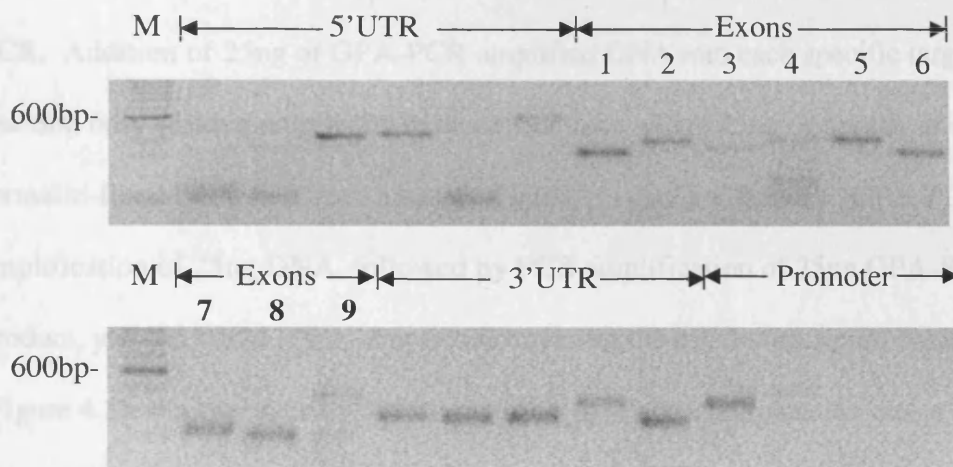


Figure 4.3. PCR amplification of the hPXR functional domain from the product of DNA globally pre-amplified by GPA-PCR. GPA-PCR was undertaken on 25ng of DNA extracted from a 5µm formalin-fixed true-cut liver section. 25ng of the GPA product per reaction was PCR amplified using an M13-tagged F Primer and standard reverse primer. Labels denote the location of the amplicons within the functional domain, while numbers are the hPXR exons which specific amplicons span. M= Molecular Weight Marker (100bp). 10µl of the PCR was loaded into the lane.

Curiously despite detection by PicoGreen no product was observed by gel electrophoresis for GPA-PCR amplification of 1ng input DNA.

Amplification of specific targets within the functional domain of the hPXR gene demonstrated an adverse efficiency the smaller the initial DNA input into the GPA-PCR. Addition of 25ng of GPA-PCR amplified DNA into each specific target reaction only yielded amplicons in those reactions where 25ng or greater of extracted formalin-fixed DNA had been amplified initially (data not shown). GPA-PCR amplification of 25ng DNA, followed by PCR amplification of 25ng GPA-PCR product, yielded 19/24 (79%) amplicons covering the hPXR functional domain (Figure 4.3). Further repeats of this gave rise to fewer amplicons but also a different range of those amplicons (data not shown) suggesting that the missing amplicons are not a specific effect but a random event.

4.2.1.2 Improved Primer Extension PCR

Initial IPEP-PCR pre-amplification was undertaken on 25ng of extracted formalin fixed tissue. This amount had previously observed as optimal for subsequent PCR analysis of the product (Powell, H. (AstraZeneca Pharmaceuticals), personal communication, 2002). 25ng of input DNA from a 5µm true cut archival liver section yielded a mean of $1.502\mu\text{g}\pm 0.37$ of IPEP-DNA (n=3).

Amplification of the hPXR functional domain using 1/50th (approximately 30ng) of an IPEP reaction from an initial 25ng DNA in each subsequent PCR reaction gave rise to 22/24 (91.7%) of the hPXR amplicons set (Figure 4.4). Despite yielding the majority of the hPXR target amplicons, a number of the reactions gave rise to smaller unspecific amplicons. For this reason, a touchdown PCR thermocycling program was subsequently used for amplification from IPEP reactions.

Using the same IPEP reaction as previously (25ng input DNA), and standard PCR

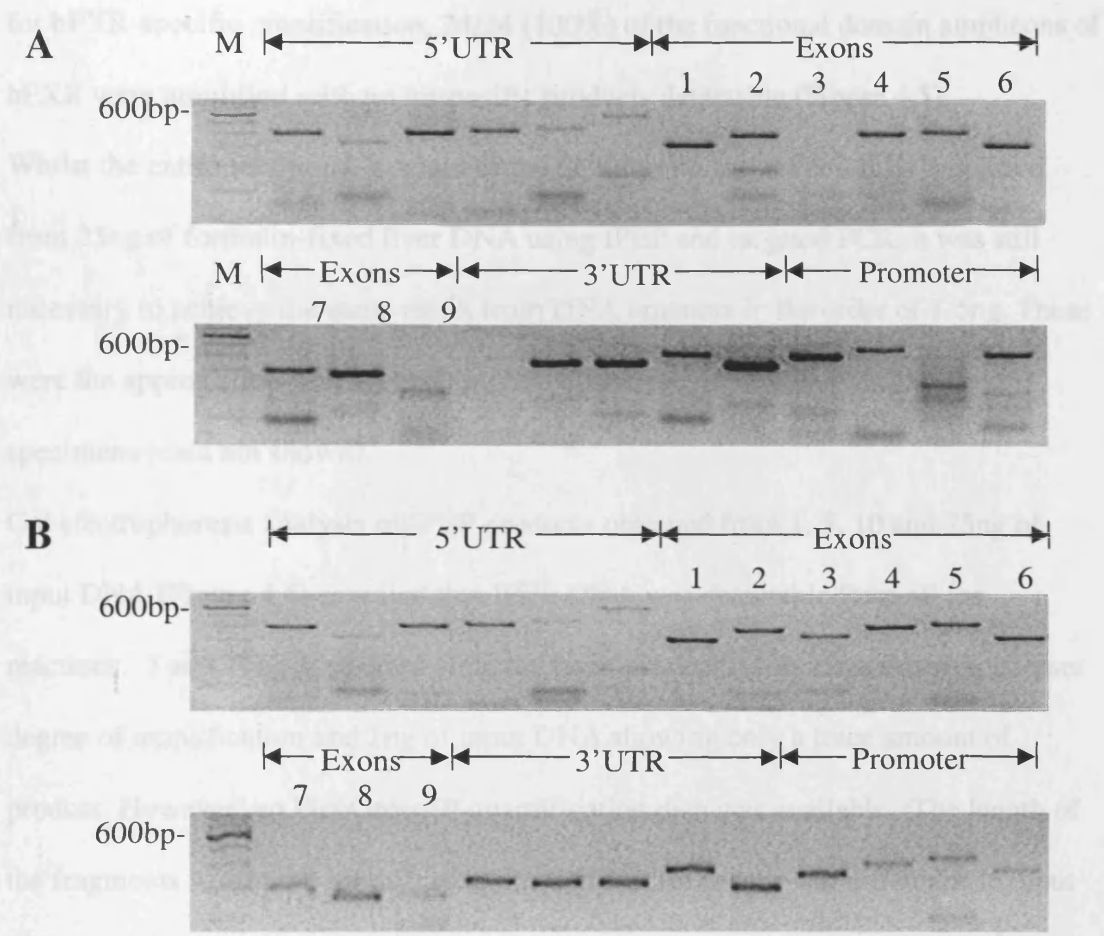


Figure 4.4. PCR amplification of the hPXR functional domain from the IPEP-PCR product of 25ng formalin-fixed DNA extracted from a 5µm true cut liver biopsy section. PCR was carried out using M13-labelled F and R primers. **A** denotes PCR using a standard 3-step cycling and **B**, PCR using a touchdown cycling program. Labels denote the location of the amplicons within the functional domain while numbers are the hPXR exons which specific amplicons span. M= Molecular Weight Marker (100bp). 20ul of the PCR was loaded into each lane.

Using the same IPEP reaction as previously (25ng input DNA), and touchdown PCR for hPXR-specific amplification, 24/24 (100%) of the functional domain amplicons of hPXR were amplified with no unspecific products detectable (Figure 4.5).

Whilst the entire functional domain of the hPXR gene was successfully amplified from 25ng of formalin-fixed liver DNA using IPEP and targeted PCR, it was still necessary to achieve the same result from DNA amounts in the order of 1-5ng. These were the approximate yields from single sections of core needle liver biopsy specimens (data not shown).

Gel electrophoresis analysis of IPEP products obtained from 1, 5, 10 and 25ng of input DNA (Figure 4.6) revealed that IPEP DNA was detectable from all the reactions. 5 and 10ng seemed to yield the most products with 25ng showing a lesser degree of amplification and 1ng of input DNA showing only a trace amount of product. However, no PicoGreen™ quantification data was available. The length of the fragments within the product reaction was similar despite the difference in input DNA. All IPEP reactions yielded very long fragments ranging from a considerable length >2000bp to no less than 1500bp.

Amplification of 5 amplicons spanning the 5'UTR of hPXR from the IPEP reactions containing 1, 5, 10 and 25ng input DNA gave rise to adverse amplicon detection efficiency as input DNA was reduced (Figure 4.7). Touchdown PCR cycling conditions was used for amplification. Using 1/50th of an IPEP reaction containing 25ng initial input DNA, 3/5 amplicons were present. With 10ng DNA in the IPEP, 2/5 amplicons were amplifiable albeit at lower detection level. 3/5 amplicons were attained from IPEP product with 5ng input DNA. The signal of detection for 5ng input was further reduced. At 1ng input DNA, amplification of the IPEP product yielded no detectable amplicon products.

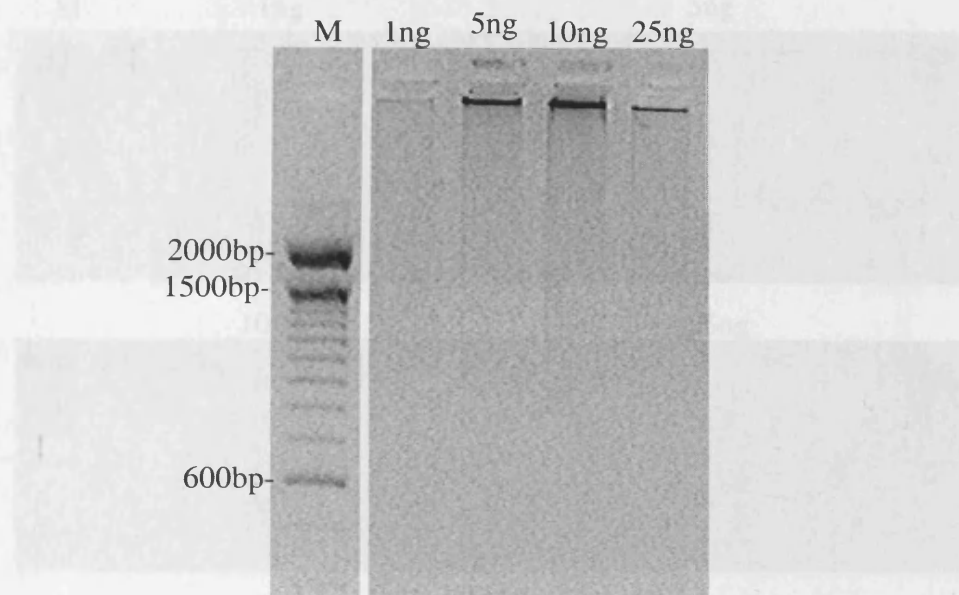


Figure 4.5. Improved Primer Extension Pre-amplification-PCR DNA yields from varying amounts of input formalin-fixed liver DNA. IPEP-PCR products from amplification reactions containing: 1, 5, 10 and 25ng of genomic DNA extracted from a 5 μ m formalin-fixed true-cut liver biopsy section are shown. M= Molecular weight markers (100bp ladder). Each lane contains 10 μ l of IPEP-PCR reaction mixture. Products resolved on a 4%, ethidium bromide stained agarose gel.

Further amplification of IPEP products from input DNA <math>< 25\text{ng}</math> yielded no detectable products (data not shown). Therefore it was necessary to investigate other techniques by which the hPXR gene could be amplified and analysed from formalin-fixed DNA amounts less than 25ng.

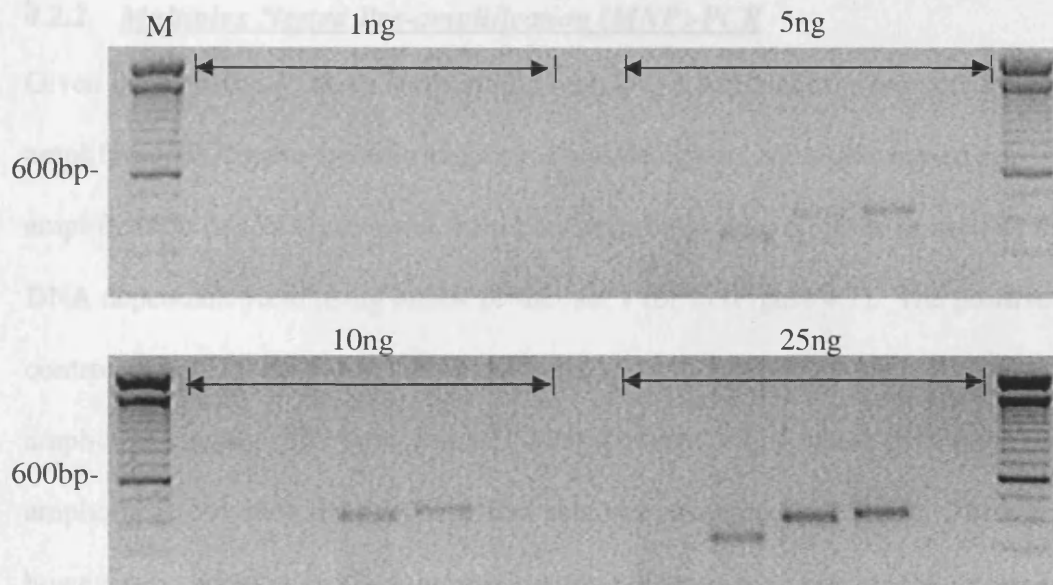


Figure 4.6. PCR amplification of amplicons spanning the hPXR 5'UTR from IPEP-PCR products pre-amplified from varying amounts of input DNA. IPEP was undertaken on 1, 5, 10 and 25ng of DNA extracted from a single 5 μm true cut liver biopsy section (as labelled). PCR was carried out using standard F and R Primers. 10 μl of PCR reaction was run per lane. M= molecular weight ladder (100bp).

Further amplification of IPEP products from input DNA <25ng yielded no detectable products (data not shown). Therefore it was necessary to investigate other techniques by which the hPXR gene could be amplified and analysed from formalin-fixed DNA amounts less than 25ng.

4.2.2 Multiplex Nested Pre-amplification (MNP)-PCR

Given the sensitivity issues surrounding both WGA techniques, a protocol for pre-amplifying PXR gene-specific sequences was designed. Multiplex nested pre-amplification of DNA extracted from Formalin-fixed liver biopsies showed an input DNA dependant yield using hPXR primer set 1 (of 2) (Figure 4.7). The positive control sample (fresh blood DNA) gave rise to a product containing 4 distinct amplicons ranging from approximate 550bp down to 350bp which fit into the range of amplicon sizes which the twelve primer sets were designed to amplify. There was however one smaller product (approximately 200bp in size) which was present in the positive control, as well reactions containing 5, 10 and 25ng of input DNA. The yield of this amplicon was consistent in all samples regardless of input DNA amounts except 1ng. The detectable signal of the 4 larger amplicons was inversely proportional to the input DNA. No products were detected for 1ng starting template DNA. The 10 bands expected from the 10 primer sets were not observed though in the positive control, the band density would suggest that more than one product is present, possibly two or three overlying. However distinction of all ten given the similarity in size is not realistic.

Subsequent PCR amplification of Multiplex Nested PCR products using primers internal to those within the multiplex mixture gave rise to 5/5 amplicons, spread across the hPXR functional domain regardless of the amount of DNA template within the pre-amplification reaction (Figure 4.8). There was no DNA dependant variation

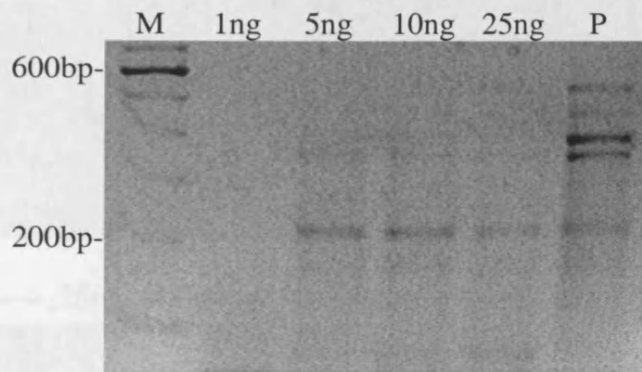


Figure 4.7. Multiplex Nested PCR pre-amplification yield from varying amounts of input formalin-fixed liver DNA from a single 5 μ m true cut biopsy section. Products from amplification reactions containing 1, 5, 10 and 25ng of genomic DNA, amplified using hPXR multiplex primer set 1 (of 2) are shown P represents a positive control, the product of amplifying DNA from a fresh blood sample. Each lane contains 10 μ l of multiplex nested pre-amplification reaction mixture. M= Molecular weight markers (100bp).

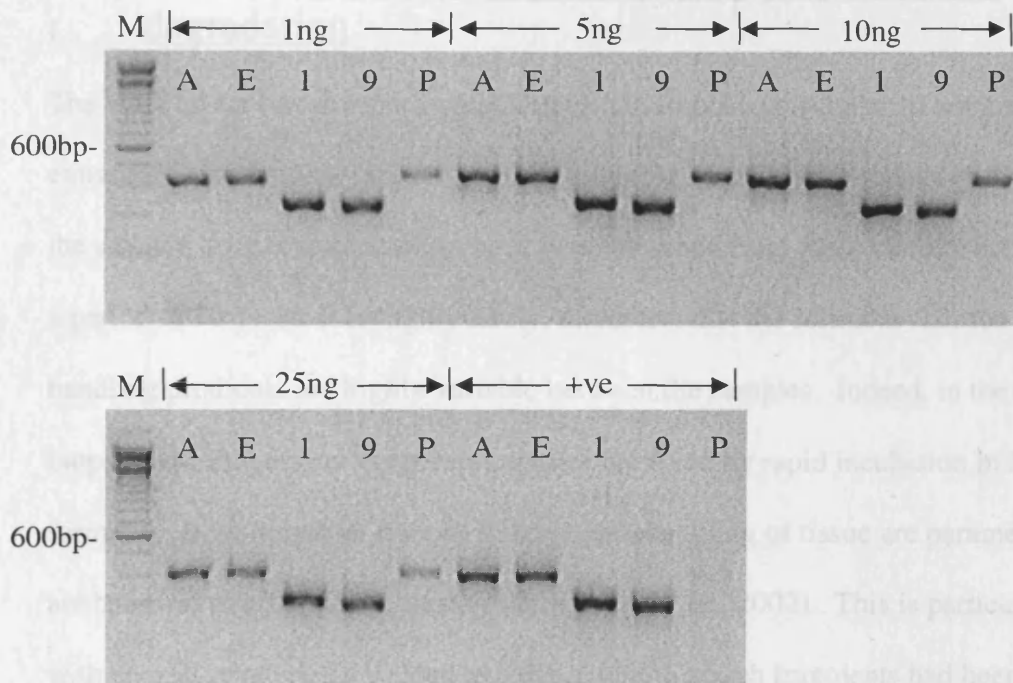


Figure 4.8. PCR amplification of amplicons within the hPXR functional domain from the product of multiplex nested-PCR pre-amplification. Products varying amounts of formalin-fixed true-cut liver DNA (1, 5, 10 and 25ng) as well as fresh blood DNA (+ve control) are represented. A and E represent the 1st and 5th amplicons from within the 5'UTR; 1 and 9 are amplicons respectively, spanning exons 1 and 9 and P represents the first amplicon within the upstream promoter region. PCR was carried out using M13-tagged F primers and standard R primers. M= Molecular weight Marker (100bp). 10 μ l of PCR reaction was loaded into each lane.

in yield as all 5 multiplex pre-amplifications amplified to give 5 amplicons of the same strong detectable signal even down to 1ng of starting template DNA.

4.3 Inter-sample variability of formalin-induced DNA degradation

The work so far has involved obtaining hPXR amplicons from small amounts of DNA extracted from a single large liver biopsy sample. The patient biopsies gathered within the adverse drug reaction cohort have been obtained from three satellite hospitals over a period of 10 years. It is highly likely, therefore, that the formalin-fixation and tissue handling protocols are highly variable between the samples. Indeed, in the event of a biopsy requiring urgent diagnosis samples are fixed by rapid incubation in heated formalin. Both length of time in fixative and handling of tissue are parameters which are believed to affect DNA quality (Srinivasan et al., 2002). This is particularly true with respect to amounts yielded and the extent to which fragments had been degraded. For this reason, it was necessary to optimise the multiplex nested PCR protocol in order for it to be robust enough to amplify hPXR products from biopsies where the DNA is considerably more degraded than the tissue sample previously used.

The initial round of multiplex PCR amplification was carried out using 9 primer sets specific to the 9 PXR exons with a further 9 pairs of primer nested internally to these. This amplification reaction contained half of the DNA extracted from any given tissue sample from the ADR cohort. However it was noted that in many cases, amplification of some of the larger products was not occurring, indeed amplicons where the first round product was greater than approximately 370bp were not amplified (Figure 4.9A). This would appear to be as a result of degradation by the fixation process in particular samples reducing the copy number of templates of such length to below

detectable levels. It was therefore decided that to alleviate this problem of degradation, the multiplex PCR products needed to be considerably smaller. By amplifying each exon in two overlapping products (containing $\frac{1}{4}$ of the initial DNA extraction) in two separate multiplex reactions (18 amplicons per sample), the requirement for representation of larger products was lowered. Indeed, the largest product was now 290bp. Amplification of hPXR exons in 18 smaller products gave a greater yield of products in comparison to the larger products of the 9-amplicon strategy (Figure 4.9B&C). This therefore provided a protocol, which was more sensitive and yielded PCR products in samples where previously DNA degradation was too great to allow robust amplification of multiple hPXR products.

Thus far amplifications were carried out using Expand High Fidelity Taq Polymerase. Equivalent comparison of amplification of formalin-fixed sample DNA with another DNA polymerase, Accuprime pfx, demonstrated a greater sensitivity in amplifying previously weak and undetectable products (using manufacturers recommended cycling parameters) than with Expand Taq polymerase (data not shown). For this reason subsequent multiplex nested PCR was carried out on the cohort samples using Accuprime pfx Taq polymerase.

Given that 18 different primer pairs within a PCR reaction was quite a complex undertaking, the decision was made at this point that the focus of the pre-amplification and subsequent amplification and sequence should be limited to the 9 exons encoding for the hPXR protein.

4.4 Inter-sample contamination controls

Given the small amount of the tissue samples from which DNA is being extracted and

number of cycles of PCR amplification, it is possible that the DNA of other

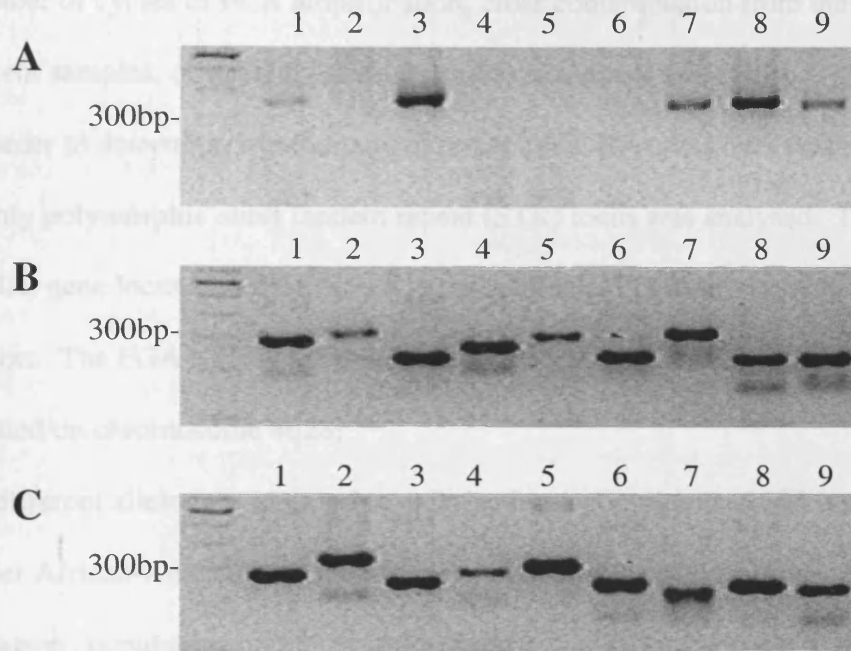


Figure 4.9. Multiplex nested PCR amplification of hPXR exons from DNA extracted from hepatic core-needle biopsy tissue (patient 26 of the ADR cohort). Numbers represent the relevant hPXR exon to which the amplicon is targeted. **A** shows products amplified by the 9-amplicon protocol using $\frac{1}{2}$ the DNA extracted. **B** and **C** show the products from the 18-amplicon protocol where two distinct multiplex reactions are carried out, each containing $\frac{1}{4}$ of the extracted DNA.

4.4 Inter-sample contamination controls

Given the small nature of the tissue samples from which DNA is being extracted and number of cycles of PCR amplification, cross contamination from the DNA of other patient samples, or indeed, external sources is a strong possibility.

In order to determine whether any inter-sample DNA cross over was occurring, a highly polymorphic short tandem repeat (STR) locus was analysed. The Fibrinogen A (FGA) gene locus was determined to be a suitable STR to investigate within the ADR cohort. The FGA STR is a tetranucleotide repeat polymorphism (Mills et al., 1992) located on chromosome 4q28.

18 different alleles are reported to exist within a population of 395 individuals of either African-American or US Caucasian ethnicity (Applied-Biosystems, 2001). However, population studies of more diverse populations suggest as many as 22 variant alleles of the FGA STR locus may exist (Fregeau et al., 1998).

The FGA locus is one of ten STR loci routinely used for DNA “fingerprinting” by the British Forensic Science Service as part of the AmpF/STR SGM Plus Kit by Applied Biosystems. Probability of identity values, based on the STR kit, demonstrate a p value (probability of two randomly selected individuals having identical FGA alleles) of 0.035 in African Americans and 0.036 in US Caucasians (Applied-Biosystems, 2001). By incorporating this discriminatory capability into the pre-amplification reactions of the hPXR in the patient samples, FGA STR analysis could give a good indication that the DNA amplified gives an accurate representation of the individual from whom it is extracted.

Comparison of the allele frequency of an SNP previously characterised within the human PXR gene locus, with the frequency within the sample cohort, can be used as a determination of cross-contamination. This could also provide the opportunity to

demonstrate the robustness of sequence analysis within the amplified products. A SNP was identified which was located 17 bases upstream of the intron 6/exon 7 boundary of the hPXR gene (Accession number: ss20421435). The Entrez SNP database allele frequency is recorded at C=0.802, T=0.188 from a sample size of N=96 (192 chromosomes). The estimated heterozygosity is calculated at 0.321. The ability to amplify DNA from these samples is an important step towards elucidating any role for PXR polymorphisms within the ADR patient samples. However it is vital that integrity and validity of the DNA sequence is controlled for. Such control amplification techniques could be applied generically to the genotypic analysis of genes in many disease states where small amounts of formalin-fixed tissue is the sole material available.

4.4.1 Sample discrimination by use of the fibrinogen A short tandem repeat (STR) locus.

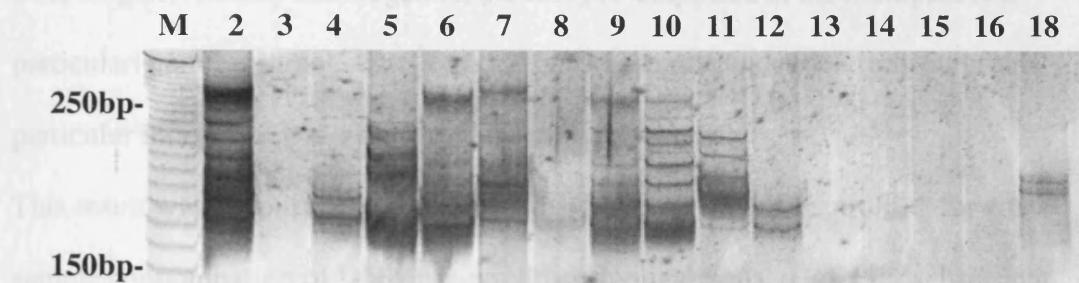
In addition to the 18 primer sets within the described multiplex PCR, primers flanking the FGA STR locus were included in the pre-amplification reaction.

Subsequent PCR Amplification of the FGA locus, using nested primers, of individuals from the ADR cohort gave rise to inter-individual variability in the clarity of the products (Figure 4.10). Of the 16 individuals analysed, 3 gave rise to the anticipated 2 allelic products (numbers 4, 12 and 18).

Whilst a further 6 samples showed no visible products, the remaining 7 individuals yielded products with a significant number of bands of varying size. The primers used for the secondary amplification are as used in the Amp/F STR SGM Plus Kit and as such are highly optimised for this purpose.

It is likely that rather than being non-specific products of the amplification, these bands are representative of "noise" of the target sequence and as such could be alleviated by reducing the number of cycles in which the secondary PCR amplification is undertaken.

At this point, a full 10 loci STR profile of the ADR cases, using the AmpF STR SGM plus kit, was undertaken on 1/50th of the PCR multiplex. An example of this is demonstrated in Figure 4.11. A number of STR loci can be genotyped according to STR length. Notably fibromycin A, the locus not amplified in the multiplex, is a



analysis of a further 25 of the ADR multiplex reactions by STR profiling gave no

Figure 4.10. Multiplex nested PCR amplification of the FGA STR locus from DNA extracted from hepatic tissue samples of the ADR cohort. 5 μ l PCR product was loaded alongside 6 μ l 10bp ladder on a 7% polyacrylamide gel and detected by silver staining. Numbers represent the reference number of the individual within the cohort.

It is likely that rather than being non-specific products of the amplification, these bands are representative of “stutter” of the target sequence and as such could be alleviated by reducing the number of cycles at which the secondary PCR amplification is undertaken.

At this point, a full 10 loci STR profile of the ADR cases, using the Amp/F STR SGM plus kit, was undertaken on 1/50th of the PXR multiplex. An example of this is demonstrated in Figure 4.11. A number of STR loci can be genotyped according to STR length. Notably fibrinogen A, the loci pre-amplified in the multiplex is a particularly strong signal. The X and Y chromosome gender determinant of this particular individual was also clearly identifiable as male.

This result was encouraging as a highly discriminate way of controlling for cross-sample contamination of DNA pre-amplification reactions. However subsequent analysis of a further 25 of the ADR multiplex reactions by STR profiling gave no clear result and so this particular method could not be used to analyse the whole cohort. It was felt that at this stage, analysis of cross-contamination should be focused on the frequency of a published SNP within the ADR cohort multiplex reactions and a control population of patient formalin-fixed liver biopsy sections.

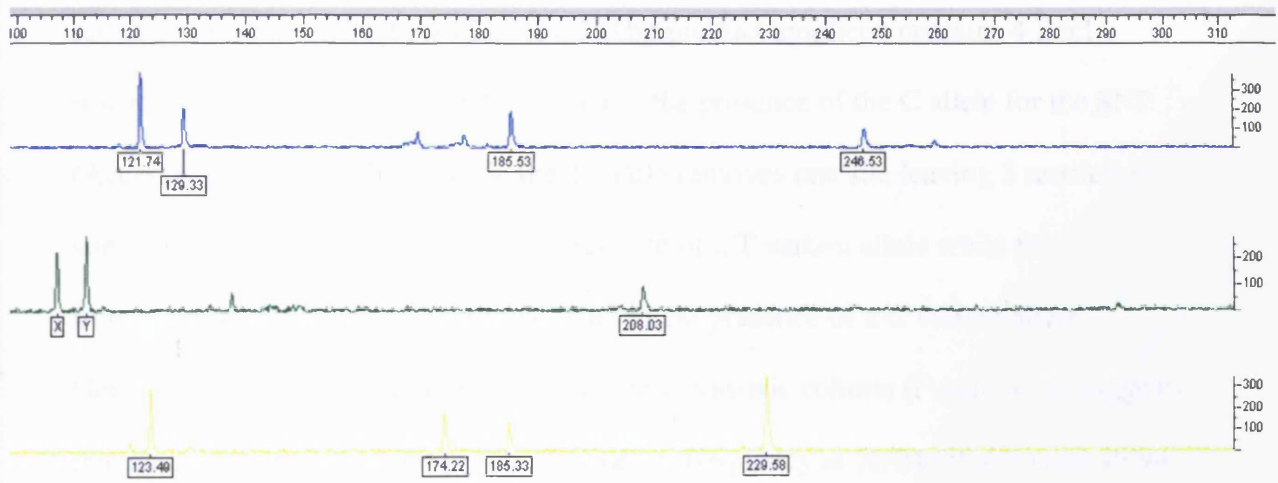


Figure 4.11. STR profile of a multiplex nested pre-amplification of formalin-fixed DNA from an ADR cohort liver biopsy. STR loci were amplified from 1/50 multiplex reaction using the AmpF/STR SGM Plus kit. Products were analysed on an ABI 377 sequencer and images compiled using Genotype v3.7 software. 5-FAM™, JOE™ and NED™ fluorescent-labelled PCR products are detected as blue, green and yellow respectively. Product size ladder shown.

4.4.2 Allele frequency comparison with a published SNP

Multiplex nested PCR of DNA from the 53 ADR cases yielded exon 7 products from 41 of the patients. “Rapid” DNA extraction and PCR of 100 normal and 100 metastatic formalin-fixed liver biopsies yielded the same exon 7 product in 94 patients from each cohort.

Products generated from hPXR Exon 7 product were digested using the BccI restriction enzyme (Figure 4.12). The 311bp product amplicon contains 4 BccI restriction motifs (5'...CCATC(N)₄...3') in the presence of the C allele for the SNP (Accession no: rs2276708), while the T-allele removes one site leaving 3 restriction sites. A 98bp fragment confirms the presence of a T variant allele while the truncation of this fragment to 87bp occurs in the presence of a C variant allele.

Genotyping for rs2276708 in the normal and metastatic cohorts (Figure 4.13) suggests that a homozygous C genotype has the highest frequency at 56/94 (59.6%) and 49/94 (52.1%) respectively. This was true of the ADR cohort (68.3%). Homozygous T was observed in only 3/94 (normal), 2/94 (metastatic) and 2/41 (ADR).

Statistical analysis of the frequency of patients in all 3 cohorts displaying a non-homozygous C genotype was undertaken (Table 4.1). Comparison of the normal with the metastatic cases suggests that the frequency of CT and TT genotypes is not significant with a Fisher's exact test ($p=0.378$). An odds ratio of 1.058 seems to support this. The ADR cohort frequency of non-homozygous C was compared with that of the normal cohort and gave rise to $p=0.440$ from a Fisher's exact test and an odds ratio of 0.936. These results appear to support the notion that the frequency distribution of rs2276708 genotypes in the ADR and normal cohorts is not significantly different.

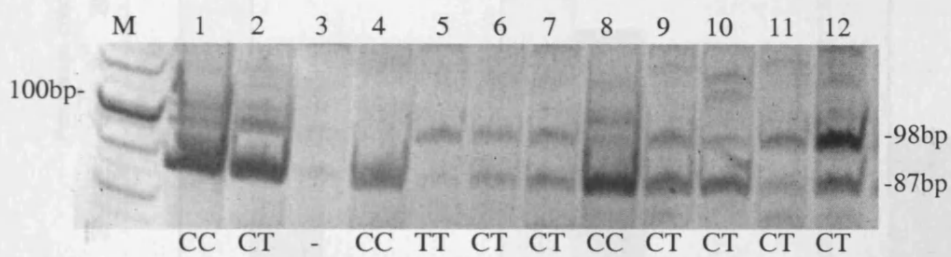


Figure 4.12. BccI restriction digestion of Exon 7, product A, for determination of rs227678 SNP in 12 hepatic tissue samples from the ADR cohort. 20 μ l of digested PCR product was loaded into each lane alongside 6 μ l 10bp ladder (M) on a 7% polyacrylamide Gel and detected by silver staining. The presence of a T variant allele removes a BccI restriction site and so the 98bp fragment is uncut.

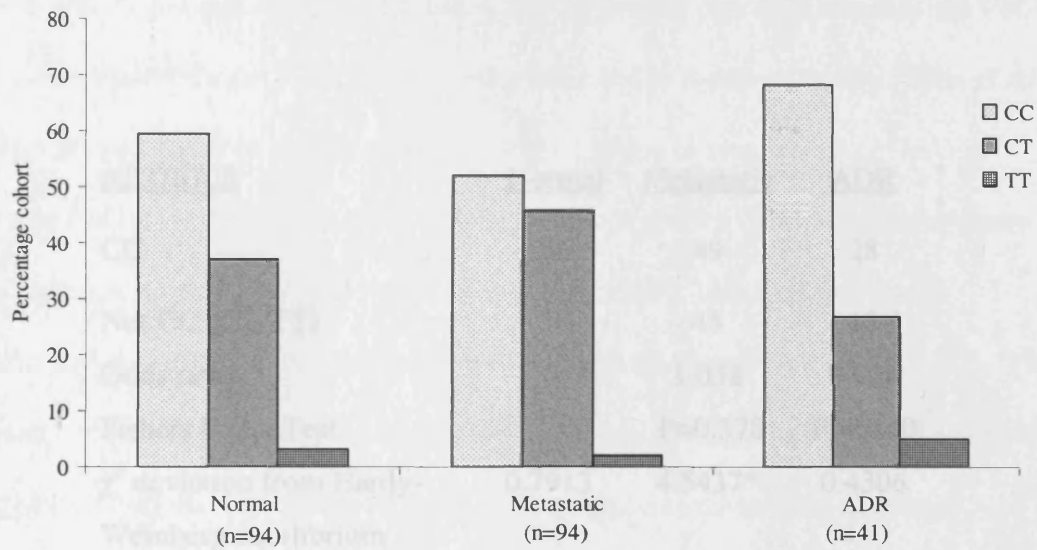


Figure 4.13. Percentage frequency of variant alleles for the rs2276708 SNP in the normal, metastatic and ADR cohorts. Genotype is as determined by the BclI restriction endonuclease screen (Figure 4.12) (n as stated).

<u>rs2276708</u>	<u>Normal</u>	<u>Metastatic</u>	<u>ADR</u>
CC	56	49	28
Not CC (CT/TT)	38	45	13
Odds ratio	-	1.058	0.936
Fishers Exact Test		P=0.378	P=0.440
χ^2 deviation from Hardy-Weinberg equilibrium	0.7913	4.5437*	0.4306

Table 4.1. Statistical analysis of rs2276708 SNP genotype within normal, metastatic and ADR liver biopsy cohorts. * denotes allelic distribution out of Hardy-Weinberg equilibrium.

4.5 mRNA expression analysis from formalin-fixed liver biopsies.

Within the remit of the project, analysis of hepatic gene expression, at the mRNA level was intended for the 53 ADR patients. mRNA was extracted simultaneously from a single, histologically, normal 5µm needle biopsy section and downstream PXR target gene expression assessed (Figure 4.14). Given the degraded nature of the RNA due to formalin fixation, PCR primers were designed to sequence within 100bp of the mRNA polyadenylation motif and for products <120bp in length.

Reverse transcriptase PCR of mRNA from the single section of a core needle biopsy was undertaken and expression levels of CYP3A, MDR1 and PXR itself were determined as well as that of a housekeeping gene, beta-2-microglobulin (B2M). The products of RT-PCR for all for targets can be clearly identified in Figure 4.14 with no genomic contamination evident in the cDNA synthesis reaction void of reverse transcriptase.

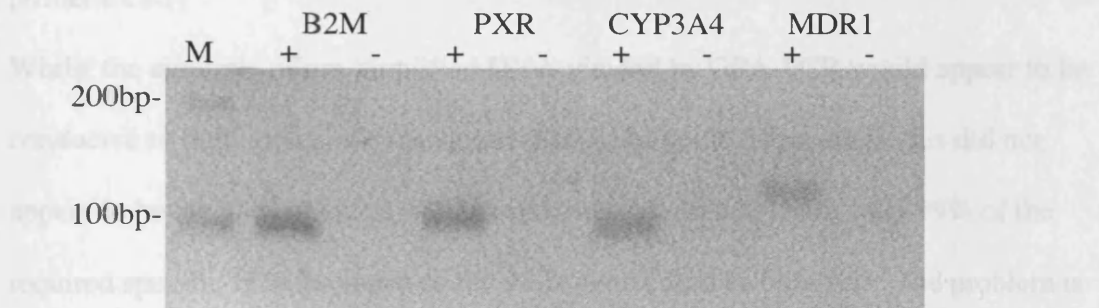
Given appropriate time and resource, the future intention for utilising simultaneous DNA and RNA extraction was to analyse down-stream PXR target gene expression within the liver biopsy. In particular, it may be of interest to determine whether there is any significant variability in putative PXR dysfunctional individuals.

4.5 Discussion

4.5.1 Pre-amplification of DNA from Formalin Fixed tissue

The initial attempt for formalin-fixed DNA pre-amplification, GPA-PCR, seemed to be the best protocol with which to utilize the fragmented and degraded nature of the extracted DNA. By genetic labelling the entire "genome" of the sample DNA, it was possible, in theory, to amplify a whole genome using a specific (M13) sequence primer (PCR).

primers (PCR).



most likely to be with the genetic M13 labelling. Electrophoresis of GPA-PCR pre-amplified DNA showed the product with a 25ng starting material (Figure 4.14) to be of similar efficiency to specific PCR was very achievable and despite the requirement of their primer, for a sensitivity of amplification of 1-5ng, GPA-PCR was discounted. As with GPA-PCR, IPEP pre-amplification yielded high molecular weight DNA complexes in excess of 2kb (Figure 4.15). This again is likely to be the result of cross-linking of PCR products as result of extreme sequence homology, brought about by the degenerate primers. Using of starting material, albeit formalin-fixed, was again optimal for subsequent specific PCR as previously suggested by Powell. B (AstraZeneca Pharmaceuticals) personal communication, (2012). However, the fact that IPEP could be used to pre-amplify DNA with partial success for subsequent

Figure 4.14. mRNA expression analysis PXR and downstream target genes from a single 5 μ M hepatic core needle biopsy section. B2M, PXR, CYP3A4 and MDR1 expression was detected by PCR of cDNA synthesised in the presence (+) and absence (-) of reverse transcriptase enzyme. 100bp molecular marker (M) is also demonstrated. Products are resolved on an ethidium bromide stained 4% agarose gel.

4.6 Discussion

4.6.1 Pre-amplification of DNA from formalin fixed tissue.

The initial concept for formalin-fixed DNA pre-amplification, GPA-PCR seemed to be the ideal protocol with which to utilize the fragmented and degraded nature of the extracted DNA. By generic labelling the entire “genome” of the sample DNA, it was possible, in theory to amplify a whole genome using a specific (M13) sequence primer PCR.

Whilst the amounts of pre-amplified DNA yielded by GPA-PCR would appear to be conducive to high yields of subsequent specific target PCR products, this did not appear to be the case. Indeed, at 25ng of starting template DNA, only 79% of the required specific PCR products of the PXR gene could be obtained. The problem is most likely to lie with the generic M13 labelling. Electrophoresis of GPA-PCR pre-amplified DNA showed the product from 25ng starting material (Figure 4.2A) to be of a very high molecular weight (>2kb). This is likely to be a result of DNA complex formation brought about by PCR fragments annealing to common sequence created by M13 labelling. It is likely that this may also be the reason why even at 25ng, 100% efficiency of specific PCR was not achievable and given the requirement, of this project, for a sensitivity of amplification of 1-5ng, GPA-PCR was discounted.

As with GPA-PCR, IPEP pre-amplification yielded high molecular weight DNA complexes in excess of 2kb (Figure 4.5). This again is likely to be as result cross-annealing of PCR products as result of common sequence homology, brought about by the degenerate primers. 25ng of starting material, albeit formalin-fixed, was again optimal for subsequent specific PCR as previously suggested by Powell, H (AstraZeneca Pharmaceuticals), personal communication, (2002). However the fact that IPEP could be used to pre-amplify DNA with partial success for subsequent

specific PCR would appear to contradict the findings of (Dietmaier et al., 1999). The problems of specific PCR did appear to be primer-specific and not a result of the IPEP reaction since modification of cycling parameters (Figure 4.4) was able to increase the yield of the range of PXR-targeted products. This, however, was only the case with IPEP DNA synthesised from 25ng DNA. At amounts from 1-10ng, specific PCR from IPEP DNA was less efficient and of lower yield (Figure 4.6).

So, in the case of both WGA techniques investigated by this project, the ability to pre-amplify, and subsequently specific target PCR amplify was not possible within the realms of sensitivity (1-5ng starting DNA) required within the remit of this study. This leaves the only viable option to be a pre-amplification protocol specifically designed for the gene in question, PXR.

4.6.2 Multiplex PCR for pre-amplification of DNA from formalin-fixed tissue.

The concept of gene specific pre-amplification by multiplex PCR would seem to be without precedent. Unlike GPA-PCR and IPEP-PCR, the starting DNA template, between 1 and 25ng, does not seem to be a limiting factor in terms of sensitivity (Figure 4.8). This means that for the purpose of this study multiplex nested PCR is sensitive enough to allow genotypic analysis of the exonic PXR sequence from the <5ng DNA yielded from liver biopsies.

However, one factor that does impact the success rate of this method of pre-amplification and subsequent PCR is the inter-sample variability of the formalin-fixation process. Some samples exhibited greater degrees of DNA degradation than others and so the procedure must be limited to sequence targets <300bp (Figure 4.9) as reported by (Bonin et al., 2003).

Despite this limitation of amplicon size, the ability to amplify and sequence the entire protein-coding region of a gene from as little as 1ng of formalin-fixed DNA would appear to be validated. This has been achieved from a number of liver biopsies of varying DNA yields and quality. A technique such as multiplex nested PCR has the flexibility to be designed specifically for a number of genomic targets for genotypic analysis of patient archival biopsy material of any source.

4.6.3 Internal controls for evaluation of inter-sample contamination of multiplex PCR pre-amplification.

In principal, the idea of incorporating a highly variable STR locus such as FGA was a viable and highly discriminatory way of eliminating concerns over inter-sample contamination within the process of multiplex nested PCR.

However amplification of the FGA locus gave rise to a number of non-specific products and sample variability in terms of reaction efficiency. Figure 4.10 clearly shows 6/16 samples where multiplex nested PCR was unable to yield any visible product. This is more likely to be as a result of formalin-induced DNA fragmentation rather than quantity of yield. Studies ((Bonin et al., 2003)) have suggested that products of 300 bases are the very top end of the sensitivity of PCR of DNA from formalin-fixed tissue regardless of quantity. The range of STR products possible within the population using the FGA primers of the AmpF/STR SGM Plus Kit is in some instances close to and greater than 300bp. Therefore in some individuals the FGA alleles may simply be too long for detection from archival tissue of this nature. The amount of non-specific products was also a concern and is likely to be as a result of considerable stutter within the PCR reaction and possible primer site polymorphisms (Hendrickson et al., 2004). Having observed the inefficiency of yield and the non-specific amplification, incorporating the FGA locus was clearly not a

viable means for determining inter-sample contamination. In hindsight, it may have been possible to use another forensic-based STR locus with shorter PCR products. A full STR profile reaction was undertaken on the multiplex PCR reactions of a number of individuals. As the example of figure 4.11 suggests, a good partial, and certainly discriminatory, STR profile is achievable from then multiplex PCR reaction. This is despite the fact that, ultimately, the genomic DNA profiled has been diluted 250-fold from the extracted concentration. It is this small amount of template for the STR profiling reaction, which is possibly the cause of the failure of the large majority of the cases to yield a profile. Moreover, having been extracted and amplified a considerable amount of time in advance of this facet of the study, it is highly likely that this failure to obtain any profiles is due to the degradation of the sample DNA over time. The fact that an initial profile was demonstrably obtainable suggests that, in the optimal condition, the multiplex reaction mix would yield the highly discriminatory power of an STR profile in order to eliminate inter-sample contamination concerns. Unfortunately, within the realms of this study, demonstration of this was not possible.

Analysis of the reported C/T SNP 17bp upstream of the PXR exon 7 transcription start site (ss20421435) within the multiplex PCR amplified DNA of the ADR cohort provides a good indication of the absence of inter-sample contamination.

Two of the three liver biopsy cohorts analysed (normal and metastatic) were done so by a “rapid “extraction and single PCR amplification method. The genotypic distribution of these two cohorts was statistically determined as not significantly different to the ADR cohort where genotypic analysis had been carried out by the 2-step multiplex amplification method (Figure 4.13). This would suggest that no

apparent cross contamination introduced by nested PCR procedures has influenced the result of typing of this SNP.

Comparison of the allelic frequency observed in the ADR cohort with that published within the Entrez SNP database would seem to suggest that variability of the allelic frequency within the ADR cohort is not influenced by inter sample contamination. The data for the SNP (accession number: ss20421435) has the allelic frequency at C=0.802, T=0.188 within a cohort of 96. The 41 genotyped members of the ADR cohort gave rise to comparable allelic frequencies of C=0.817, T=0.183. The striking similarity between the ADR data and an independent observation of the same SNP would appear to suggest that the multiplex methods employed in the amplification are a true representation of the DNA initially extracted from the liver biopsies.

Use of this allelic frequency comparison as an internal control for inter-sample contamination confirms that for the purpose of PXR exonic sequence analysis, the data generated is a good representation of the sample set and that allelic frequency of other sequence variations can be observed with some confidence.

4.6.4 Simultaneous gene expression and sequence analysis from formalin-fixed tissue.

The results obtained for mRNA expression analysis from a single core needle biopsy where DNA, for sequence analysis, was simultaneously extracted, would seem to suggest that both can be successfully achieved from the same single 5µm section (Figure 4.14). mRNA extractions were performed from the ADR cohort tissue and preliminary RT-PCR analysis was carried out. However comprehensive data for only one individual was available.

The sensitivity of the mRNA detection would appear to be quite low given that the products amplified required 40 PCR cycles. Other studies appear to have achieved

greater yields of similar sized amplicons from micro-dissected (Specht et al., 2001a) and larger formalin-fixed tissue samples (Lewis et al., 2001). However these studies chose to focus attention on DNA extraction and analysis and thus extraction techniques were optimised solely for this purpose.

The nature of the RT-PCR protocol adopted for this study allows for the required sensitivity of the sample but limits the scope of gene expression analysis. Utilizing mRNA poly-A tail bead capture techniques, the sequence available for primer positioning is approximately 150bp upstream of the polyadenylation signal motif. This allows for expression analysis of the total transcript of a gene but not individual isoforms.

(Specht et al., 2001b) have demonstrated the ability to transfer this expression analysis to a TaqMan™ quantitative RT-PCR platform. The size of the products obtained is optimal for TaqMan™ analysis purposes though the necessity for 40 PCR cycles may prove a problem. The possibility of PXR target expression data to correlate to specific functional sequence variability is certainly something that could be very useful in determining the exact mechanisms of adverse drug effect in predisposed individuals.

4.6.5 Conclusions

Despite the low nucleic acid yield demonstrated by the hepatic core needle biopsy tissue and the degradation caused by formalin fixation, a methodology has been developed to allow DNA analysis of the protein coding region of the human PXR gene. Comparison of the frequency of an intronic SNP within the PXR gene with both other cohorts and data within the public domain provides a means of determining whether the nested PCR of the 53 samples is in fact discriminatory. The results of this

within this suggest would suggest that the protocol does allow the analysis of sequence data, which is representative of the cohort.

Simultaneous RNA extraction and subsequent mRNA expression analysis was demonstrated as achievable and could be used to examine PXR downstream target gene expression alongside sequence variation analysis.

The methodologies applied for nucleic acid extraction and analysis have met the objective to develop the means to utilise archival hepatic biopsy tissue for the purpose of a candidate gene sequence analysis with the potential to obtain transcript expression data.

**Chapter 5. Sequence variation of the
hPXR Gene within an Adverse Drug
Reaction Cohort.**

5. Sequence variation of the hPXR Gene within an Adverse Drug Reaction Cohort.

5.1 Identification of a potential novel SNP within the hPXR LBD.

PCR products of the PXR exonic regions from the 53 ADR liver biopsies were obtained by the multiplex nested methodology described previously. None of the reported non-synonymous human PXR SNPs (Hustert *et al.*, 2001; Koyano *et al.*, 2004; Zhang *et al.*, 2001) were identified in any of the 53 ADR cohort patients. In all cases sequencing data for the majority of the 18 exonic products was achieved.

Where sequence analysis was not possible for SNPs of interest, PCR and restriction digest analysis was undertaken. Representative traces of the 18 exonic products are demonstrated in Appendix C.

Sequence alignment of PCR products from the 53 members of the ADR cohort highlighted a potentially significant SNP with the protein-coding region of hPXR. This SNP occurs in codon 301 (exon 6), within the LBD. The wild type sequence (Accession No. AF061056) shows the major allele codon as TGT, which specifies a cysteine amino acid residue. The variant allele codon is CGT and specifies an arginine residue. The variant allele is hence referred to as C301R.

The C301R SNP was, initially, only identified in the sequence analysis of exon 6 in a single individual (Figure 5.1). Initial sequencing suggested that this individual (patient 4 of the 53) was heterozygous for the variant allele in both the forward and reverse sequencing orientations. By returning to the raw source DNA, and amplifying the product again, the same variation in both the forward and reverse sequencing

reactions could be confirmed (Figure 5.1). The presence of the variation in two separate amplifications and in both directions would seem to rule out the presence of any PCR or sequencing artefact.

The variant allele introduces an Mwo I restriction site (5'...GC (N₇) GC...3') and so a restriction digest of the PCR product was used to determine this potential variant by a more rapid method.

5.1.1 In silico prediction of structure and function of C301R variant

In order to determine whether a cysteine to arginine variant at PXR residue 301 was likely to result in altered protein structure and function, the PolyPhen software tool was used (<http://www.bork.embl-heidelberg.de/PolyPhen/>). PolyPhen is a tool which predicts possible impact of an amino acid substitution on the structure and function of a human protein using straightforward physical and comparative considerations (Ramensky *et al.*, 2002). In the case of PXR the prediction was made based on the alignment of a number of reference PXR protein sequences and how conserved the residue was. On the basis of alignment, the calculation concluded, "This variant is predicted to be probably damaging". This gave a good indication that C301R could indeed introduce dysfunctionality to the PXR protein and prompted further functional and frequency studies of the variant.

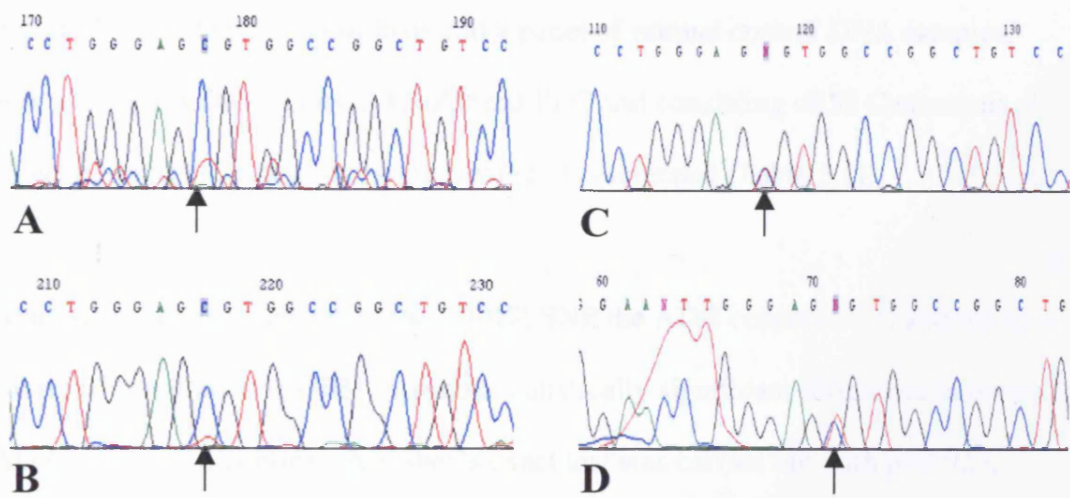


Figure 5.1. Sequence analysis of a potential novel SNP in the hPXR-LBD of an individual within the ADR cohort. Chromatograms show the C301R heterozygote variant as located by arrows in forward (**A**) and reverse (**B**) sequencing directions of the Exon 6B product from ADR patient no.4. C and D represent the forward and reverse sequencing from the same individual but a second independent amplification process. Chromatograms were created by Chromas v1.45.

5.1.2 Determination of C301R allelic frequency

Utilizing the PCR product of Exon 6B of the PXR protein coding region, Mwo I restriction digestion was applied as a means of rapidly screening the cohort of 53 ADR cases. Significantly, the screen gave rise to a second individual displaying the heterozygous C301R variation (Figure 5.2).

As well as the ADR cases, DNA extracted from 100 archival hepatic samples identified as morphologically “normal”; 100 individual cases displaying the morphology of hepatic metastasis and a panel of normal control DNA samples, supplied by R&D Genetics, AstraZeneca PLC and consisting of 53 Caucasians, 47 Hispanics and 8 Chinese individuals were also screened (Table 5.1).

Analysis of the frequencies of the C301R SNP the ADR cohort (2/53) and the total “normal” population (0/308) showed a statistically significant difference between the ADR and normal cohorts. A Fisher’s exact test was carried out with $p=0.023$, suggesting that the C301R is increased in the ADR group significantly at the 95% confidence level.

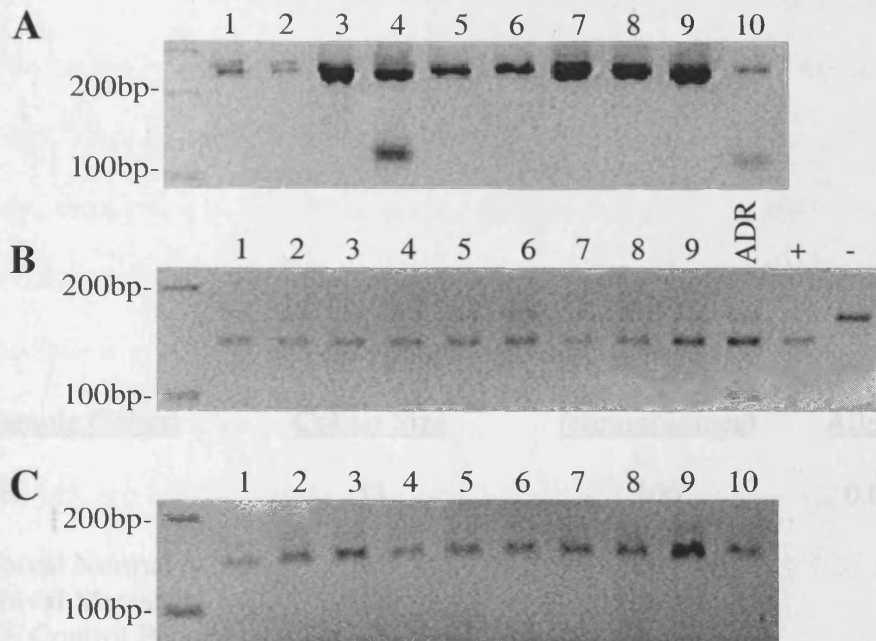


Figure 5.2. Confirmation of 2 members of the ADR cohort possessing the C301R human PXR variant allele. **A** shows gel electrophoresis of PCR products, targeting Exon 6 of the human PXR gene digested using the MwoI restriction endonuclease. The C301R variant allele introduces an MwoI site into the sequence thus the 244bp fragment is cut into two fragments of 130 and 114bp in its presence. **B** and **C** show individuals from the normal and metastatic cohorts respectively. A PCR-introduced MwoI site allows product cleavage from 160 to 137bp. The presence of C301R allows the 137bp product to be cleaved further to 99bp. DNA products were resolved on an ethidium bromide stained 4% agarose gel.

<u>Sample Cohort</u>	<u>Cohort Size</u>	<u>N</u> <u>(chromosomes)</u>	<u>Allelic Frequency</u>
ADR	53	106	0.0189 (2/106)
Archival Normal	100	200	0
Archival Metastatic	100	200	0
DNA Control Panel	<u>108</u>	<u>216</u>	<u>0</u>
	308	616	0

Table 5.1. Frequency of the C301R PXR variant allele in the ADR, normal and metastatic populations as determined by the MwoI restriction digest screen.

5.2 Creation of a C301R variant human PXR cDNA clone.

Having identified the C301R variant allele, it was now necessary to determine the effect it may have on the functionality of the human PXR protein. In order to do this, the cDNA clone referred to as hPAR1 (Bertilsson, *et al*, 1999) consisting of the 1308bp of the protein coding region within the pcDNA3 expression vector was mutated to incorporate the cysteine to arginine variation at residue 301.

In vitro mutagenesis (IVM) was carried out using primers designed to alter the wild type codon 301 sequence from TGT (cysteine) to CGT (arginine) as displayed by the variant allele in the 2 ADR cases. Using these primers IVM reactions appeared to be efficient using 50ng to 5ng of starting plasmid template (Figure 5.3A). However, subsequent transformation of XL-1 blue cells and PCR, targeting PXR cDNA sequence, of colonies formed yielded no colonies possessing a PXR cDNA clone out of 6 screened (Figure 5.3B).

Repeat IVM reactions were undertaken using primers designed to replace codon 301 with a different arginine-translating codon (AGA). Using plasmid template from 5-50ng the IVM reaction appeared marginally more efficient than the CGT incorporating equivalent. Transformation of XL-1 blue using this IVM and a PCR screen of the colonies formed yielded PXR targeted PCR products in 5 out of 5 colonies screened. Therefore it was decided that the C301R variant clone with an AGA at codon 301 should be used. A clone was selected and sequenced to confirm the presence of the mutated codon (Figure 5.4). There was still, however, the question of whether this mutated cDNA clone could yield a PXR protein product. This appears to be confirmed by *in vitro* transcription and translation of both the wild-type and variant receptor clones (Figure 5.5). Both the wild-type and C301R proteins gave rise to the same expected 51kD product at apparently equivalent efficiencies.

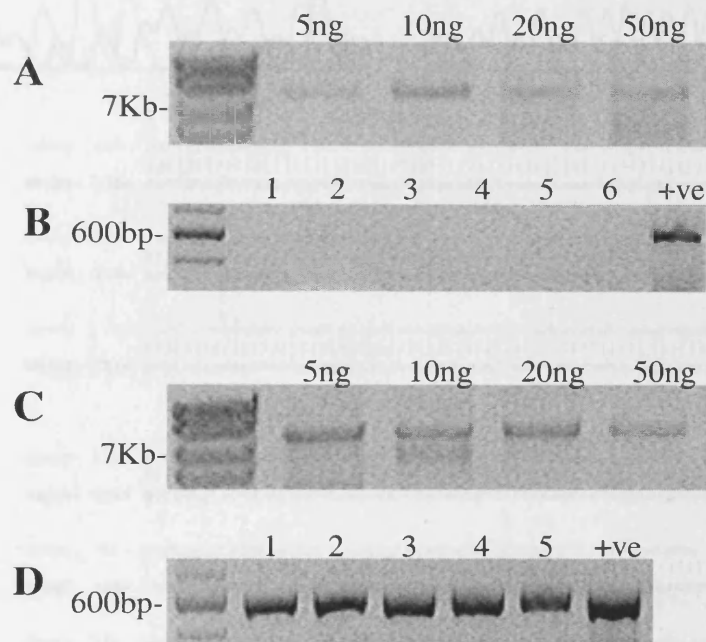


Figure 5.3. *In vitro* mutagenesis of the wild type human PXR cDNA clone. 5-50ng of starting plasmid template was used in IVM reactions introducing an altered codon 301 of CGT (A) and AGA (C). PCR (25 cycles) of a number of transformed XL-blue cell colonies to detect the presence of the mutated PXR clone was carried for both IVM introducing CGT (B) and AGA (D). 50ng PXR cDNA plasmid was used positive PCR controls. All products were resolved on ethidium bromide stained 3% agarose gels with Hyperladder™ (A&C) and 100bp (B&D) molecular weight markers.

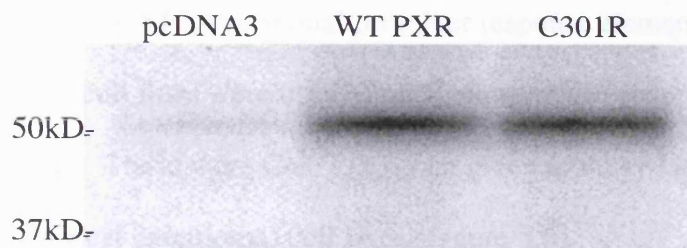


Figure 5.5. *In vitro* transcription and translation of wild-type and C301R human PXR cDNA clones. Proteins are those synthesised from *in vitro* transcription/translation reactions of wild-type, C301R and empty vector control (pcDNA3). 2 μ l of each reaction was resolved by western blotting using a goat anti-human PXR IgG primary antibody. Molecular markers are as stated.

5.3 Reporter gene co-transfection assay of C301R basal and drug-induced activation of downstream proximal promoter response elements.

5.3.1 Selection of a host cell-line for PXR transfection assay.

In order to assess the functional affect of the C301R variant on downstream target gene transcription regulation, reporter gene co-transfection assays were undertaken. Cloned PXR receptors are transfected into cell line along with a luciferase reporter plasmid containing a CYP3A proximal promoter response element.

Two immortalised cell lines were used in preliminary PXR/ reporter gene co-transfection assays. These were Cos-7 (African green monkey kidney fibroblasts) and HeLa (human cervical carcinoma) cell lines (Figure 5.6).

In Cos-7 cells transfected with the wild type PXR, an increase in basal activation of the DR3 luciferase reporter gene of 7.35-fold \pm 2.46 was observed compared to cells containing the empty pcDNA3 vector. Basal activity of the C301R variant PXR in Cos-7 cells appeared to be lower than that observed in cells containing empty vector (0.13-fold \pm 0.01).

In HeLa cells, basal activation of wild type PXR was markedly lower than that observed in Cos-7s (4.39-fold \pm 0.69 compared to 7.35 \pm 2.46). Basal C301R fold activation in HeLa cells was considerably lower than even the empty vector transfected cells (0.14 \pm 0.02).

It was decided that, going forward, HeLas would be the cell line of choice for the PXR reporter gene assays. HeLas demonstrated a far lower basal activity of wild-type PXR in the system and it was thought that, given a lower starting activation, further activation by the addition of a PXR ligand would be more apparent.

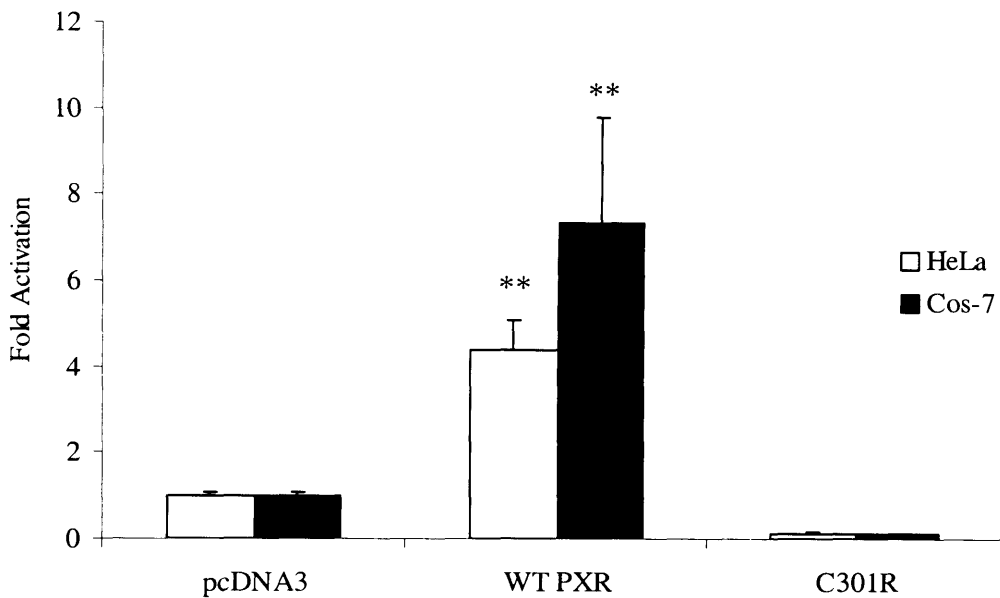


Figure 5.6. Basal activation of human wild type and C301R PXR variants. Co-transfection assay in HeLa (open bars) and Cos-7 (closed bars) cell with an ER6-response element reporter gene. Data represents mean fold activation (n=3) normalized against the empty vector (pcDNA3) control. Error bars represent \pm SD. Statistical significance is indicated as ** (p<0.01) compared to the no treatment pcDNA3 control as determined by a one-way ANOVA.

5.3.2 Confirmation of expression of transfected wild type and C301R variant PXR in a HeLa cell system.

Of concern was the apparent baseline response of the C301R variant which actually demonstrated basal activation lower than that of wild-type PXR and even the empty pcDNA3.1 vector transfected into both HeLa and Cos-7 cells in the absence of ligand (Figure 5.6). Though the cDNA clone of C301R was shown to translate to the correct size protein within an *in vitro* translation reaction, it was necessary to confirm that, within the HeLa cell system, transfected C301R was being expressed at levels equivalent to those of the wild type receptor.

RT-PCR of duplicate lysates of transfected HeLa cells (Figure 5.7) detected a 166bp product corresponding to PXR at equivalent levels in the cells transfected with wild type PXR and the C301R variant. No PXR mRNA was detected in HeLa cells transfected with empty vector only. Detection of an 88bp B-Actin cDNA product in equal abundance in all the lysates confirms the validity of the PXR mRNA expression levels.

Western blot analysis of PXR protein expression in duplicate HeLa cell lysates (Figure 5.7B) does not appear to show the same differential expression between the empty vector control and those cells transfected with either of the PXR receptors.

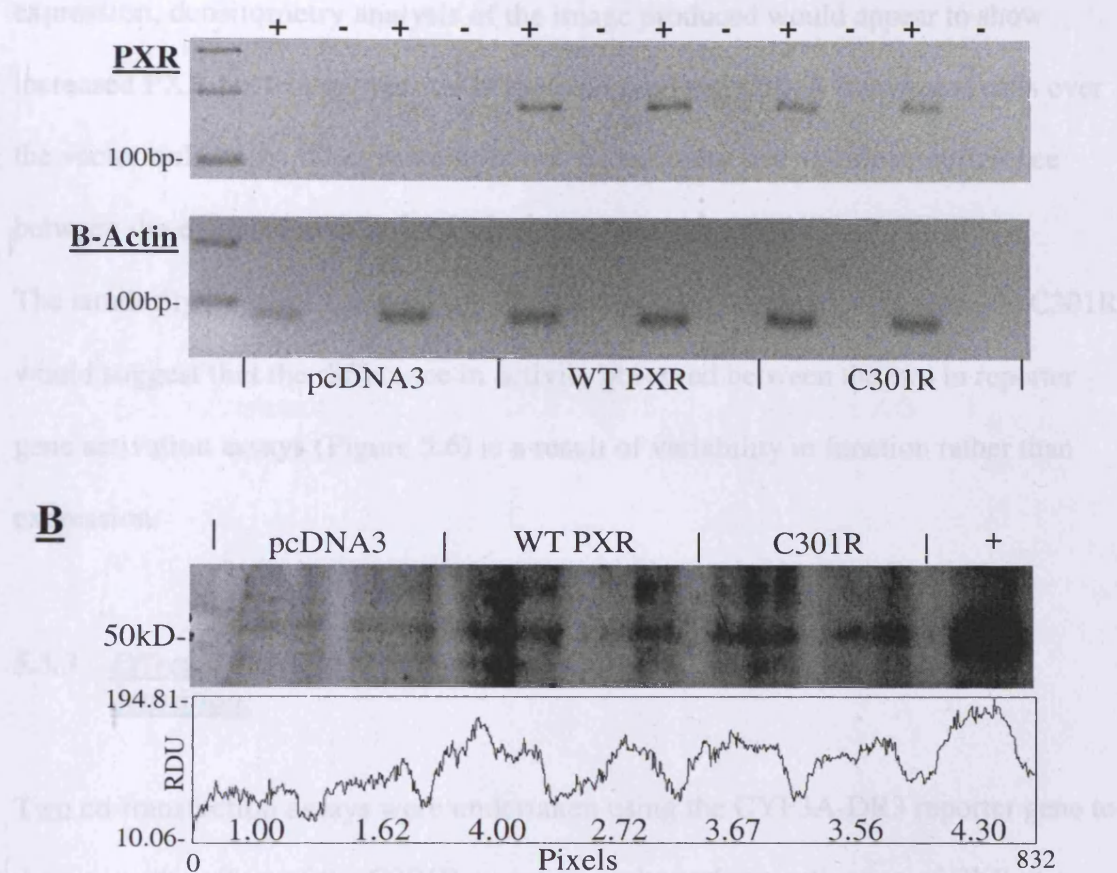


Figure 5.7. mRNA and protein expression levels of human PXR in HeLa cells transfected with PXR cDNA clones. **A** represents shows RT-PCR of mRNA isolated from transfected HeLa cells. For each transfected plasmid (pcDNA3 (empty vector), wild-type PXR and C301R, 2 cDNA samples were synthesised (+) with a corresponding negative control (-). Results for PCR targeting PXR and B-Actin from the cDNA are shown resolved on a 3% ethidium-stained agarose gel.

B represents a western blot of HeLa cell lysates (2 samples/transfected plasmid) with 2 μ l in vitro transcribed/translated wild-type PXR as a positive control. Below is a densitometry trace of the image produced where RDU represents relative densitometric units of the image with the area under the curve for each lane (normalised to the first lane) indicated by the red text.

Whilst the blot itself does not show a substantial increase over background expression, densitometry analysis of the image produced would appear to show increased PXR protein expression in the wild type and C301R transfected cells over the vector only cells. There also does not appear to be any significant difference between the expression of wild type protein over C301R.

The similarity in mRNA and protein expression levels between wild type and C301R would suggest that the difference in activity observed between the two in reporter gene activation assays (Figure 5.6) is a result of variability in function rather than expression.

5.3.3 Effect of the C301R protein variation on hyperforin-induced PXR activation.

Two co-transfection assays were undertaken using the CYP3A-DR3 reporter gene to determine the effect of the C301R variation on hyperforin activation of PXR at a range of concentrations up to 1 μ M in the first instance (Figure 5.8A) and 3 μ M in a subsequent assay (Figure 5.8B).

In both assays the basal fold-activation over the vector only control of the wild-type receptor (6.45 ± 0.09 and 9.45 ± 0.77) was markedly higher than that observed for C301R (0.72 ± 0.21 and 0.94 ± 0.04). In both instances a significant hyperforin-induced effect on wild type activation was observed at the lowest concentration of 0.01 μ M with increases of 1.38 and 1.93-fold over the wild type no treatment controls. A dose-dependant response was then observed up to 1 μ M hyperforin where fold activation compared to the empty vector no treatment control reached 25.77 ± 3.44 and 27.53 ± 3.50 . This equates to a drug -induced fold-activation for the wild-type PXR of 3.99 and 2.91-fold respectively. In the one example given a hyperforin concentration

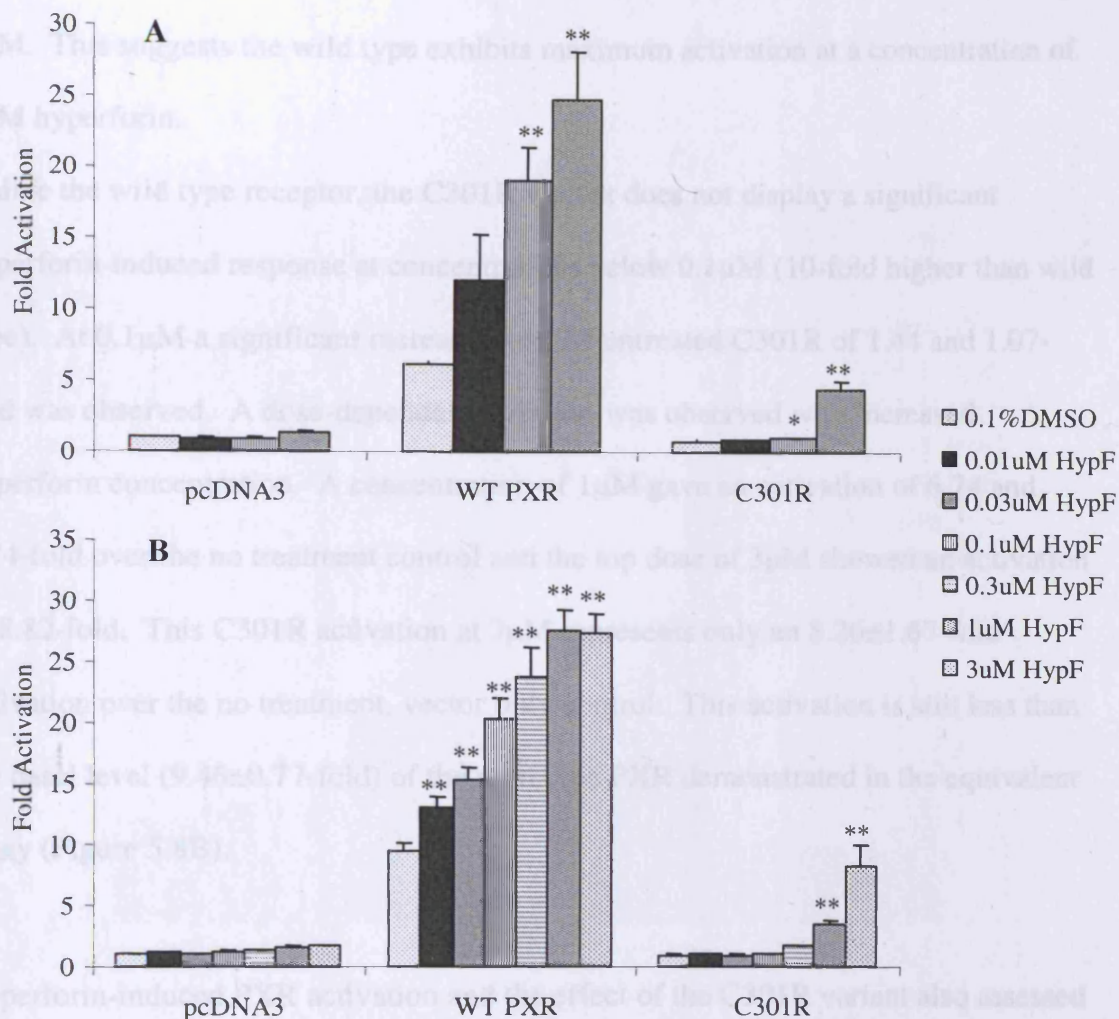


Figure 5.8. Hyperforin-induced activation of wild type and C301R PXR variants in a HeLa cell co-transfection assay with a DR3-response element reporter gene. **A** and **B** are duplicate experiments using differing concentration ranges of Hyperforin as indicated. Data represents mean fold activation (n=3) normalized against the empty vector (pcDNA3), no treatment (0.1% DMSO) control. Error bars represent \pm SD. Statistical significance is indicated as * (p<0.05) and ** (p<0.01) compared to the no treatment control for that receptor as determined by a step-down one-way ANOVA

of 3 μ M showed a nominal decrease in fold-activation (27.36 ± 0.95) in comparison to 1 μ M. This suggests the wild type exhibits maximum activation at a concentration of 1 μ M hyperforin.

Unlike the wild type receptor, the C301R variant does not display a significant hyperforin-induced response at concentrations below 0.1 μ M (10-fold higher than wild type). At 0.1 μ M a significant increase over the untreated C301R of 1.44 and 1.07-fold was observed. A dose-dependant response was observed with increased hyperforin concentration. A concentration of 1 μ M gave an activation of 6.74 and 3.74-fold over the no treatment control and the top dose of 3 μ M showed an activation of 8.82-fold. This C301R activation at 3 μ M represents only an 8.26 ± 1.67 -fold activation over the no treatment, vector only control. This activation is still less than the basal level (9.46 ± 0.77 -fold) of the wild type PXR demonstrated in the equivalent assay (Figure 5.8B).

Hyperforin-induced PXR activation and the effect of the C301R variant also assessed in a HeLa cell co-transfection assay using a CYP3A ER6 luciferase reporter gene construct (Figure 5.9). In this assay a cloned cDNA of the rat PXR protein coding region was also used as a comparison.

Basal activity of both the wild type human and rat PXR were comparable with each other yet considerably lower than with basal PXR activity observed using the DR3 reporter construct (1.48 ± 0.02 and 1.95 ± 0.01 -fold activation respectively compared to the empty vector, no treatment control). Equivalent basal activation of the C301R was demonstrated to be even lower at 1.03 ± 0.03 -fold.

Both wild type and rat PXR activation were significant increased by hyperforin treatment at 0.01 μ M (1.75 and 1.35-fold increase respectively over basal activation).

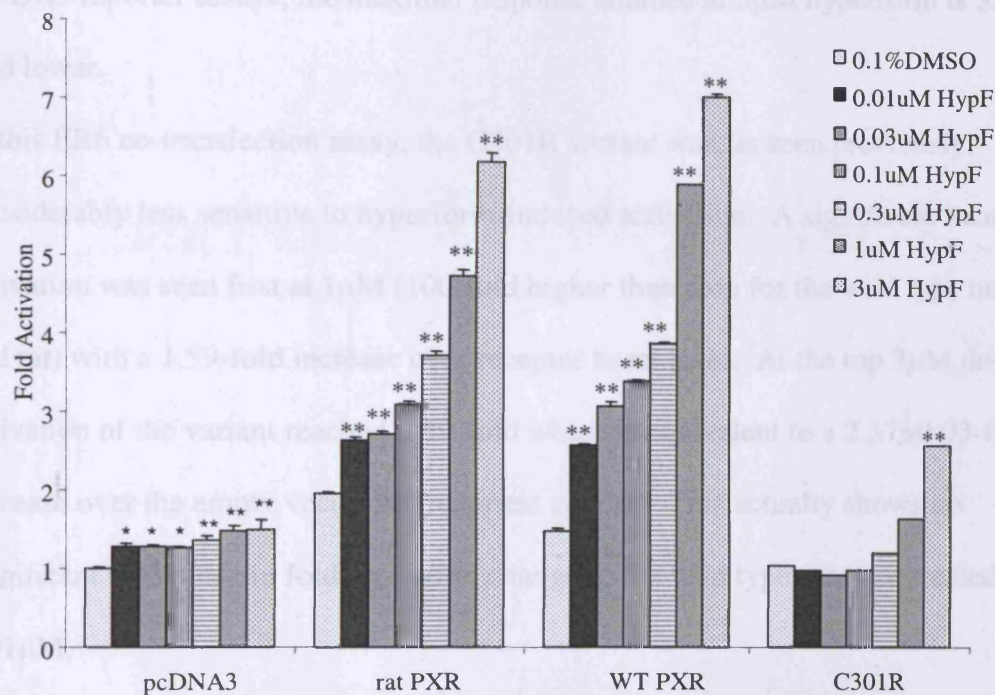


Figure 5.9. Hyperforin-induced activation of human wild type and C301R PXR variants in HeLa cell co-transfection assay with an ER6-response element reporter gene. Data represents mean fold activation (n=3) normalized against the empty vector (pcDNA3), no treatment (0.1% DMSO) control. Error bars represent \pm SD. Statistical significance is indicated as * (p<0.05) and ** (p<0.01) compared to the no treatment control for that receptor as determined by a step-down one-way ANOVA.

Both rat and wild type human receptors demonstrated a dose dependant response of activation up to the 3 μ M peak concentration where 4.76 and 3.18-fold increases over receptor basal activity were observed. These equate to 7.04 \pm 0.12 and 6.20 \pm 0.12-fold increases over the empty vector no treatment control (Figure 5.9). In comparison to the DR3 reporter assays, the maximal response attained at 3 μ M hyperforin is 3.88-fold lower.

In this ER6 co-transfection assay, the C301R variant was, as seen previously, considerably less sensitive to hyperforin-induced activation. A significant increase in activation was seen first at 1 μ M (100-fold higher than seen for the wild type human and rat) with a 1.59-fold increase over receptor basal level. At the top 3 μ M dose, activation of the variant reached 2.49-fold which is equivalent to a 2.57 \pm 0.03-fold increase over the empty vector no treatment control. This actually shows no significant difference in fold activation change to the wild type receptor treated with 0.01 μ M.

5.3.4 **Effect of the C301R protein variation on rifampicin--induced PXR activation.**

The effect of the C301R variant was also examined on ligand-mediated activation by rifampicin using both the DR3 and ER6 reporter constructs (Figure 5.10). As previously observed, basal activation of the wild type receptor was considerably higher with the DR3 reporter compared to the ER6 construct (6.83 \pm 0.87-fold against 1.53 \pm 0.02-fold). In both instances, a dose response effect of rifampicin in the activation of wild type PXR is demonstrable with both DR3 and ER6. The latter is considerably less pronounced with a maximal increase over basal-activation of just

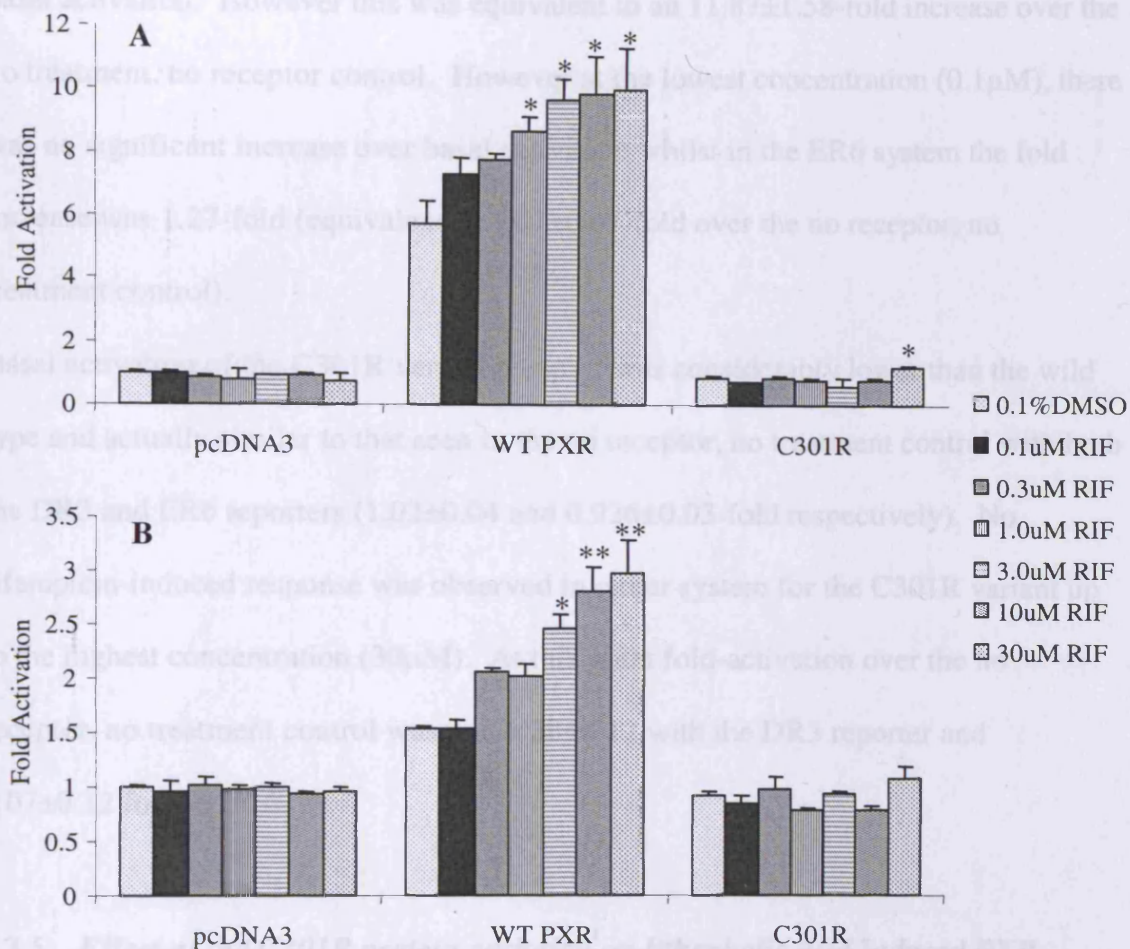


Figure 5.10. Rifampicin-induced activation of human wild type and C301R PXR variants in a HeLa cell co-transfection assay with a DR3 (A) and ER6 (B)-response element reporter gene. Data represents mean fold activation (n=3) normalized against the empty vector (pcDNA3), no treatment (0.1% DMSO) control. Error bars represent \pm SD. Statistical significance is indicated as * (p<0.05) and ** (p<0.01) compared to the no treatment control for that receptor as determined by a step-down one-way ANOVA

1.98-fold at 30 μ M. This is equivalent to 2.98 \pm 0.31-fold increase over the no receptor, no treatment control. The DR3 reporter system gave rise to a 1.74-fold increase over basal activation. However this was equivalent to an 11.87 \pm 1.58-fold increase over the no treatment, no receptor control. However at the lowest concentration (0.1 μ M), there was no significant increase over basal activation whilst in the ER6 system the fold increase was 1.27-fold (equivalent to 8.67 \pm 0.61-fold over the no receptor, no treatment control).

Basal activation of the C301R variant receptor was considerably lower than the wild type and actually similar to that seen in the no receptor, no treatment control with both the DR3 and ER6 reporters (1.02 \pm 0.04 and 0.926 \pm 0.03-fold respectively). No rifampicin-induced response was observed in either system for the C301R variant up to the highest concentration (30 μ M). At this point fold-activation over the no receptor, no treatment control was just 1.38 \pm 0.12 with the DR3 reporter and 1.07 \pm 0.12 for the ER6.

5.3.5 **Effect of the C301R protein variation on lithocholic acid-induced PXR activation.**

The effect of lithocholic acid on the activation of the wild type and C301R PXR was assessed in the DR3 and ER6 reporter co-transfection system (Figure 5.11).

Basal activation of the wild type receptor was again considerably increased in both assays at 10.64 \pm 0.90 and 8.25 \pm 1.23-fold for the DR3 and ER6 reporter assays respectively, compared to the no receptor, no treatment control. Basal activation of the C301R variant was, as previously observed, comparable to that of the no vector control at 0.77 \pm 0.02-fold (DR3) and 0.78 \pm 0.03-fold (ER6). An apparent dose-response effect of lithocholic acid (LCA) was for activation of the wild type response

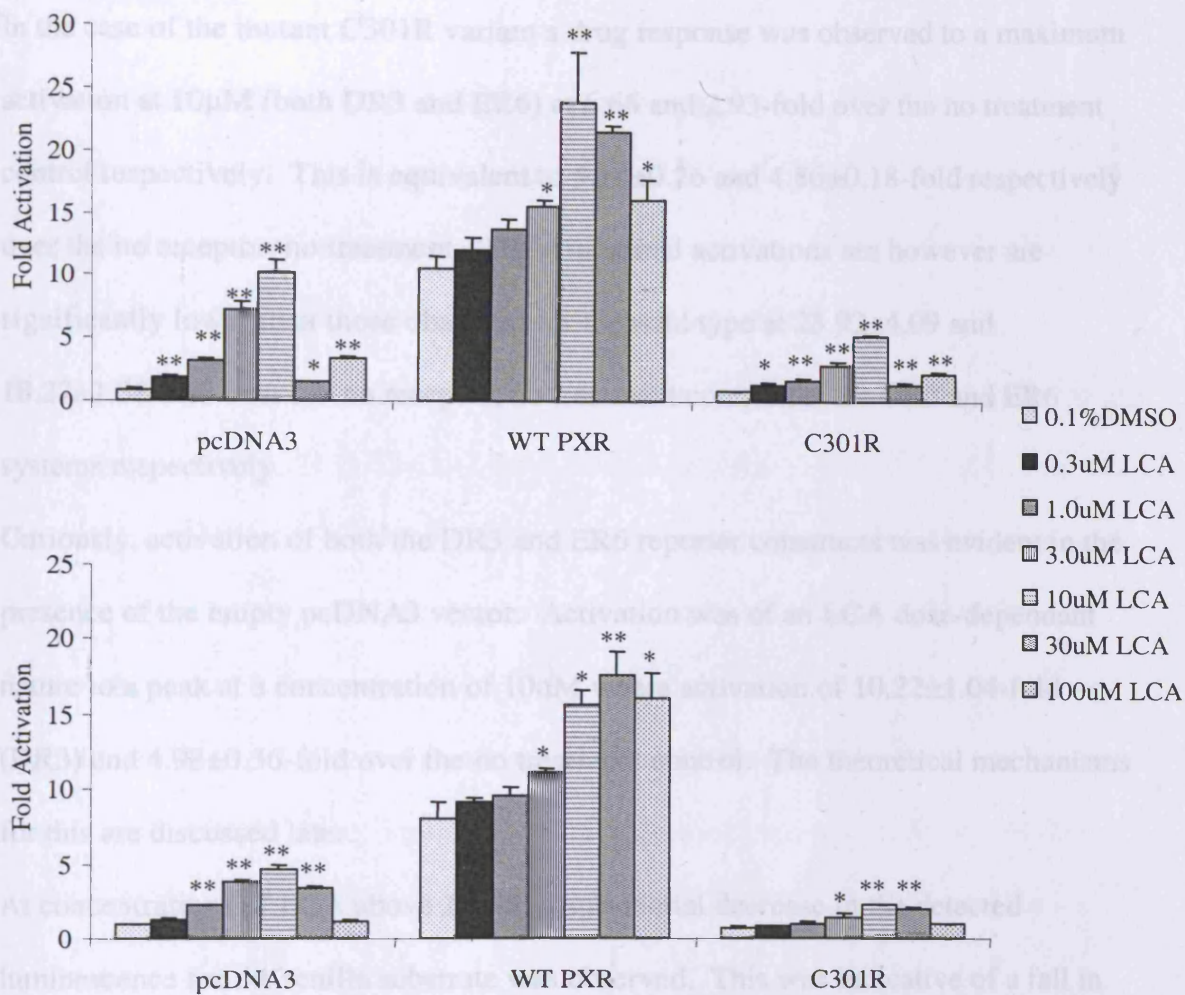


Figure 5.11. Lithocholic Acid-induced activation of human wild type and C301R PXR variants in a HeLa cell co-transfection assay with a DR3 (A) and ER6 (B)-response element reporter gene. Data represents mean fold activation (n=3) normalized against the empty vector (pcDNA3), no treatment (0.1% DMSO) control. Error bars represent \pm SD. Statistical significance is indicated as * (p<0.05) and ** (p<0.01) compared to the no treatment control for that receptor as determined by a one-way ANOVA.

to a peak at 10 μ M LCA in the DR3 system (2.25-fold over the no treatment control) and 30 μ M LCA in the ER6 system (2.21-fold over the no treatment control).

In the case of the mutant C301R variant a drug response was observed to a maximum activation at 10 μ M (both DR3 and ER6) at 6.66 and 2.93-fold over the no treatment control respectively. This is equivalent to 5.14 ± 0.26 and 4.86 ± 0.18 -fold respectively over the no receptor, no treatment. These maximal activations are however are significantly lower than those observed for the wild type at 23.92 ± 4.09 and 18.27 ± 1.58 -fold over the no receptor, no treatment control for the DR3 and ER6 systems respectively.

Curiously, activation of both the DR3 and ER6 reporter constructs was evident in the presence of the empty pcDNA3 vector. Activation was of an LCA dose-dependant nature to a peak at a concentration of 10 μ M where activation of 10.22 ± 1.04 -fold (DR3) and 4.98 ± 0.36 -fold over the no treatment control. The theoretical mechanisms for this are discussed later.

At concentrations of LCA above 10 μ M, a substantial decrease in the detected luminescence for the renilla substrate was observed. This was indicative of a fall in cell viability at these higher LCA concentrations (data not shown).

5.4 Does the C301R variant confer human PXR with rodent PXR-like ligand-binding and activation properties?

Co-transfection activation assays done to this point suggest that the C301R has considerably altered ligand activation properties to the wild type when exposed to classic human PXR ligands. Rodent PXR-specific ligands dexamethasone and pregnenolone-16 α carbonitrile were used to determine whether the C301R variant is able to confer human PXR with ligand activation properties more akin to the rodent PXR protein.

5.4.1 Effect of the C301R protein variation on dexamethasone-induced PXR activation.

A co-transfection assay in order to determine dexamethasone (DEX) activation was undertaken using the ER6 reporter construct only (Figure 5.12).

In those cells transfected with the empty vector, activation of 3.15 ± 0.24 -fold over the no treatment control was observed at the lowest concentration ($0.3 \mu\text{M}$) of dexamethasone. However, this activation was not significantly increased up to the top concentration of $100 \mu\text{M}$ (3.57 ± 0.42 -fold). Basal activation of the C301R variant was determined at 0.63 ± 0.07 -fold compared to the no vector control. No DEX-dependant increase in activation was evident up to a concentration of $100 \mu\text{M}$ (1.69 ± 0.30).

In the case of rat PXR, basal activation was measured at 8.55 ± 0.70 -fold over the no vector control. A significant dose-response effect on activation by DEX was observed from $0.3 \mu\text{M}$ (1.26 -fold over basal activation) to a maximum at $100 \mu\text{M}$ of 3.41 -fold over basal activation. This is equivalent to 29.17 ± 1.70 -fold activation over the no vector, no treatment control.

Basal activation of the wild type was considerably lower than that observed for rat PXR (4.18 ± 0.53 -fold) but is again considerably higher than that observed for the C301R variant. No significant DEX-induced activation of the wild type was observed up to $30 \mu\text{M}$. However a significant activation (1.88 -fold over the basal level) is observed at $100 \mu\text{M}$ DEX equivalent to 7.84 ± 1.53 -fold over the no vector, no treatment control.

5.4.2 Effect of the C301R protein variation on PCN-induced PXR activation.

Activation of the rat PXR by PCN was of a dose-dependant manner and was significantly increased at the lowest concentration ($0.3 \mu\text{M}$) (Figure 5.13). At this

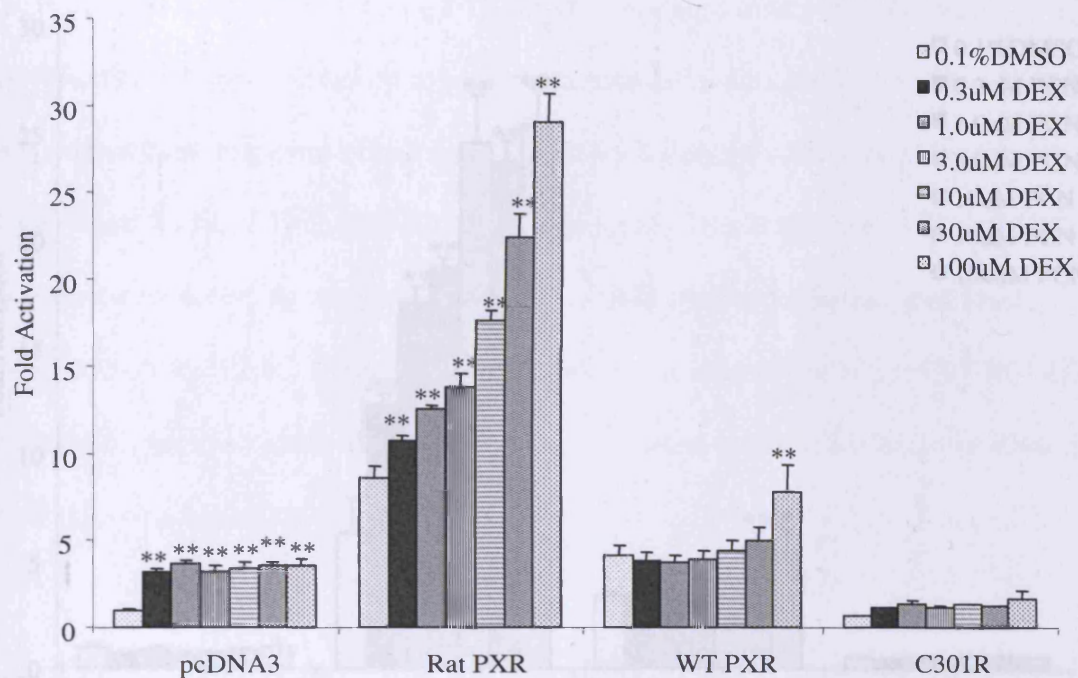


Figure 5.12. Dexamethasone-induced activation of rat PXR and human wild type and C301R PXR variants in a HeLa cell co-transfection assay. Data represents mean fold activation of co-transfected ER6 reporter gene construct (n=3) normalized against the empty vector (pcDNA3), no treatment (0.1% DMSO) control. Error bars represent \pm SD. Statistical significance is indicated as * (p<0.05) and ** (p<0.01) compared to the no treatment control for that receptor as determined by a step-down one-way ANOVA.

concentration, a 1.93-fold increase over the basal activation was observed. At the top dose (300µM), a 3.97-fold activation was observed over the basal level. This equates to a 25.56±1.72-fold increase in activation over the no receptor, no treatment control.

The wild type PXR showed no significant PCN-induced effect over the basal

activation of 0.52±0.03-fold up to a concentration of 3µM. Above this concentration, a dose-responsive effect was observed with a significant peak at 10µM of 1.68-fold over the basal level. This is equivalent to a 2.5-fold increase in activation over the no receptor, no treatment control.

Co-transfection with rat PXR, C301R, and WT PXR variants was recorded at 0.52±0.03-fold of the no receptor, no treatment control. PCN induced activation was observed at 0.1% DMSO, 0.3µM, 1.0µM, 3.0µM, 10µM, 30µM, and 100µM PCN.

Figure 5.13 is a bar chart showing PCN-induced activation of rat PXR and human wild type and C301R PXR variants in a HeLa cell co-transfection assay. The y-axis is labeled 'Fold Activation' and ranges from 0 to 30. The x-axis shows four receptor variants: pcDNA3, Rat PXR, WT PXR, and C301R. For each variant, seven bars represent different treatments: 0.1% DMSO (white), 0.3µM PCN (black), 1.0µM PCN (light gray), 3.0µM PCN (medium gray), 10µM PCN (dark gray), 30µM PCN (horizontal lines), and 100µM PCN (vertical lines). Error bars represent ±SD. Statistical significance is indicated by asterisks (* for p<0.05, ** for p<0.01) above the bars. Rat PXR shows the highest activation, reaching approximately 25.56-fold at 100µM PCN. WT PXR shows a peak at 10µM PCN (1.68-fold). C301R shows minimal activation across all treatments.

Figure 5.13 PCN-induced activation of rat PXR and human wild type and C301R PXR variants in a HeLa cell co-transfection assay. Data represents mean fold activation (n=3) normalized against the empty vector (pcDNA3), no treatment (0.1% DMSO) control. Error bars represent ±SD. Statistical significance is indicated as * (p<0.05) and ** (p<0.01) compared to the no treatment control for that receptor as determined by a step-down one-way ANOVA.

replicating an ER6 response element with a 3' biotin label (Figure 3-14). Chemiluminescent detection of complex formation gave rise to a number of detectable products. In the presence and absence of unlabelled ER6 probe, no variability in the number of products and the quantity in which they are detected is apparent. This suggested that the use of a biotin detection system for assessing the complex formation was not specific enough and indeed a number of unbound products were visible which may mask the genuine complex signal.

concentration, a 1.93-fold increase over the basal activation was observed. At the top dose (100 μ M), a 3.97-fold activation was observed over the basal level. This equates to a 25.56 \pm 1.72-fold increase in activation over the no receptor, no treatment control. The wild type PXR showed no significant PCN-induced effect over the basal activation of 0.52 \pm 0.03-fold up to a concentration of 3 μ M. Above this dose, however, an apparent dose-response effect was evident with a significant peak activation observed at 30 μ M of 1.68-fold over the basal level. This is equates to 5.85 \pm 0.57-fold over the no receptor, no treatment control which is equivalent to the basal level observed with rat PXR. C301R basal activation was recorded at 0.52 \pm 0.03-fold of the no receptor, no treatment control and no PCN induced activation effect was observed up the top concentration of 100 μ M.

5.5 Effect of C301R variation on PXR heterodimerisation with RXR and subsequent ER6 and DR3 response element.

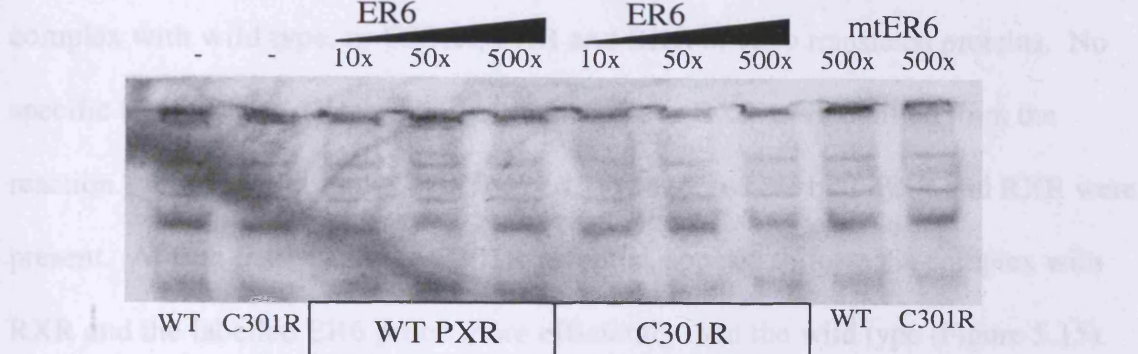
The ability of the C301R variant to bind, as a heterodimer with RXR, to response elements of the proximal promoter region of CYP3A4 was assessed by way of an electrophoretic mobility shift assay (EMSA).

Initial experiments were undertaken using a double stranded oligonucleotide replicating an ER6 response element with a 5' biotin label (Figure 5.14).

Chemiluminescent detection of complex formation gave rise to a number of detectable products. In the presence and absence of unlabelled ER6 probe, no variability in the number of products and the quantity in which they are detected is apparent. This suggested that the use of a biotin detection system for assessing the complex formation was not specific enough and indeed a number of undetermined products were visible which may mask the genuine complex signal.

In order to overcome the specificity problems seen with biotin labelled probes ³²P-labelled double-stranded oligonucleotides representative of DR3 and ER6 response elements were used. In biotin labelled EMSA experiments the size of the PXR/RXR/ER6 probe complex was not apparent. Therefore initial radio labelled EMSA experiments were undertaken to determine the formation of the complex and assess the size and retardation of acrylamide gel mobility (Figure 5.15).

A simple EMSA was carried out where a radiolabelled ER6 probe was bound in



A competition assay, again using the radiolabelled ER6 probe, was undertaken

Figure 5.14. Electrophoretic mobility shift assay of PXR/RXR/ER6 CYP3A4 response element by wild type and C301R PXR variants. Biotin-labelled ER6 oligonucleotide was incubated with and without wild type or C301R PXR and RXR in the absence (-) and presence of unlabelled ER6 or mtER6 (10-500-fold molar excess). Chemiluminescent complex formation was detected on HyperFilm™.

both PXR

At first inspection the C301R receptor, appears to form the complex with RXR and the labelled ER6 probe more efficiently than the wild type (Figure 5.15).

A repeat EMSA, again using the radiolabelled ER6 probe, was undertaken (Figure 5.16A). In this instance the PXR/RXR/ER6 complex was formed in the presence and absence of molar excess of unlabelled ER6 and mutated ER6 probe. In the absence of

In order to overcome the specificity problems seen with biotin labelled probes ³²P-labelled double-stranded oligonucleotides representative of DR3 and ER6 response elements were used. In biotin labelled EMSA experiments the size of the PXR/RXR/ER6 probe complex was not apparent. Therefore initial radio labelled EMSA experiments were undertaken to determine the formation of the complex and assess its size and retardation of acrylamide gel mobility (Figure 5.15).

A simple EMSA was carried out where a radiolabelled ER6 probe was bound in complex with wild type, or C301R, PXR and RXR *in vitro* translated proteins. No specific binding was detected when either PXR or RXR were omitted from the reaction. A specific complex was formed, however, where both PXR and RXR were present. At first inspection the C301R receptor, appears to form the complex with RXR and the labelled ER6 probe more efficiently than the wild type (Figure 5.15).

A competition assay, again using the radiolabelled ER6 probe, was undertaken (Figure 5.15). In this instance the PXR/RXR/ER6 complex was formed in the presence and absence of molar excess of unlabelled ER6 and mutated ER6 probe. In the absence of competitor probe, the binding efficiency of the C301R PXR again appeared to be marginally higher than that observed for the wild type receptor. With both PXR

At first inspection the C301R receptor, appears to form the complex with RXR and the labelled ER6 probe more efficiently than the wild type (Figure 5.15).

A repeat EMSA, again using the radiolabelled ER6 probe, was undertaken (Figure 5.16A). In this instance the PXR/RXR/ER6 complex was formed in the presence and absence of molar excess of unlabelled ER6 and mutated ER6 probe. In the absence of

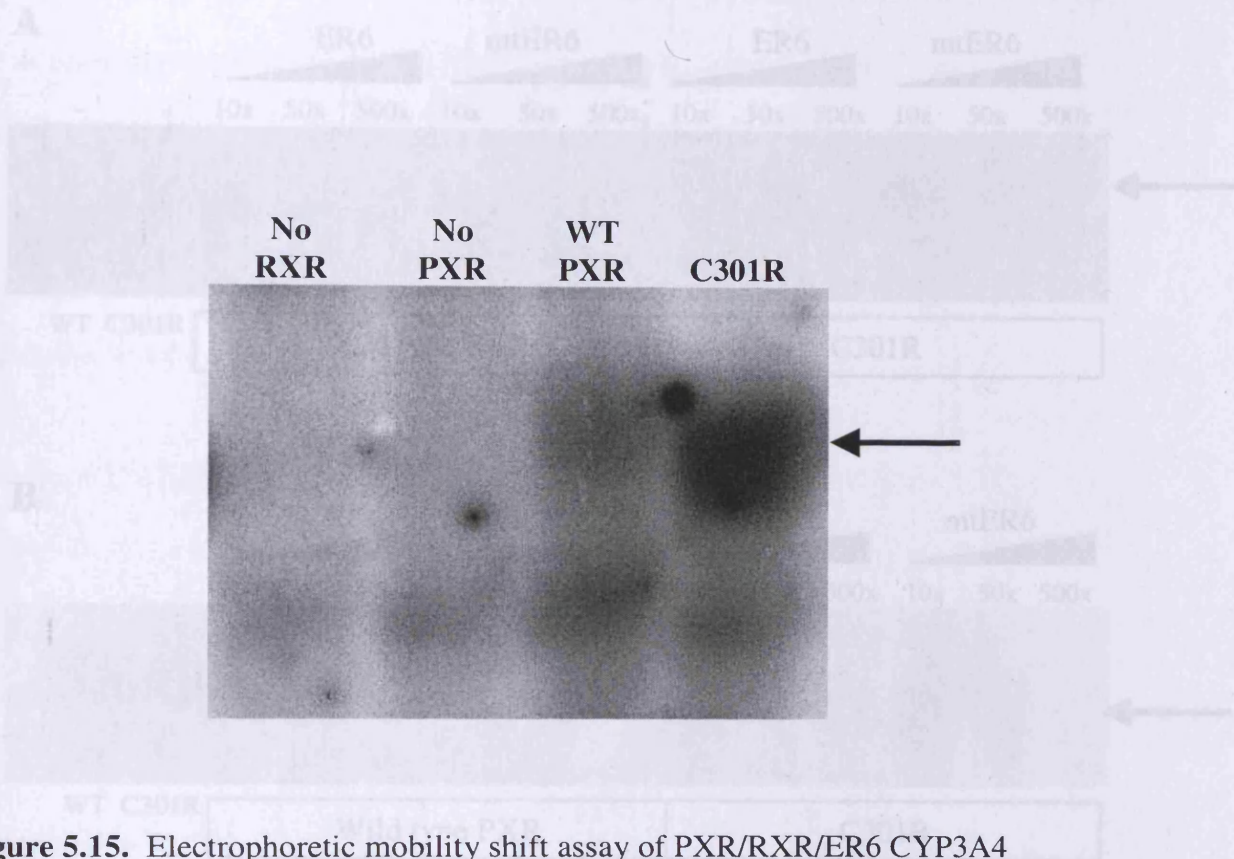


Figure 5.15. Electrophoretic mobility shift assay of PXR/RXR/ER6 CYP3A4 response element by wild type and C301R PXR variants. 32 P-labelled ER6 oligonucleotide was incubated with and without wild type or C301R PXR and RXR in the absence (-) and presence of unlabelled ER6 or mtER6 (10-500-fold molar excess). Complex formation (indicated by arrow) was assessed by detection on x-ray film.

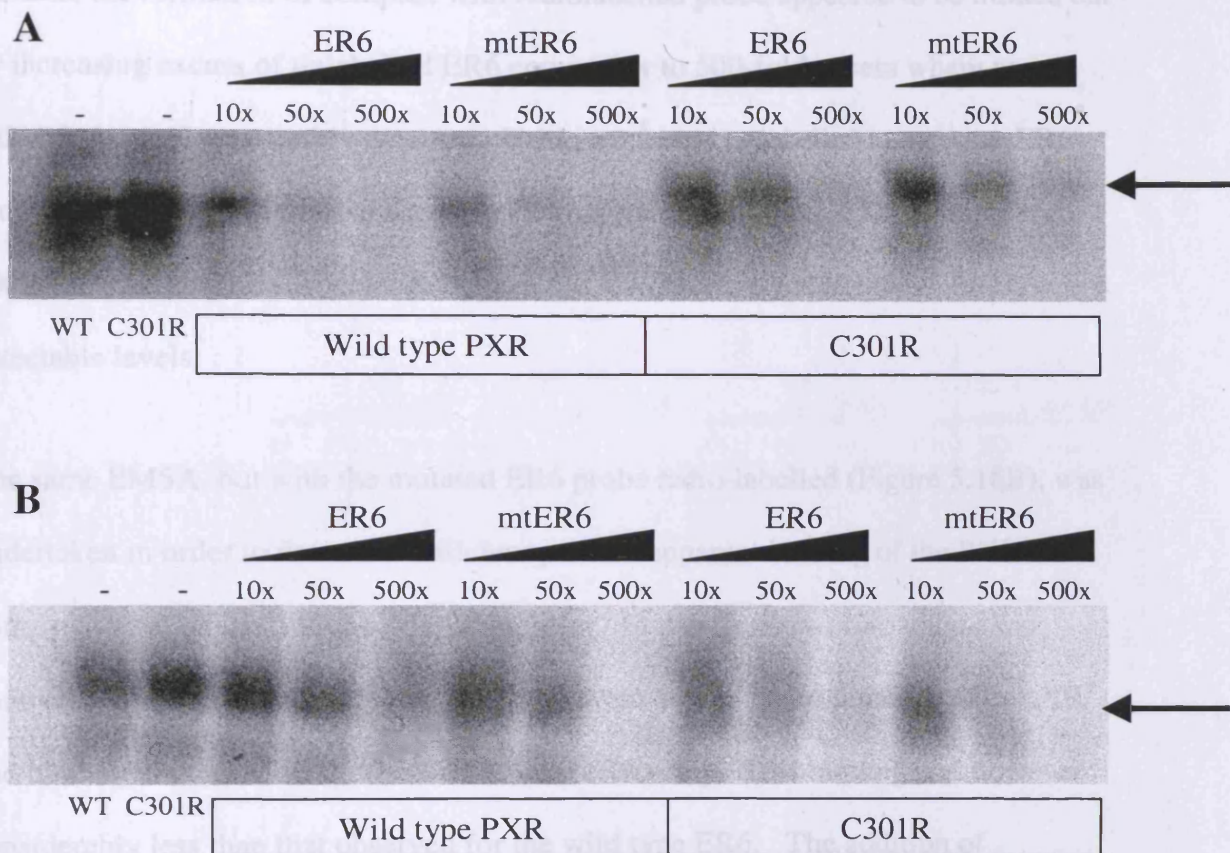


Figure 5.16. Electrophoretic mobility shift assay of PXR/RXR/ER6 CYP3A4 response element by wild type and C301R PXR variants. 32 P-labelled ER6 (**A**) and mutated ER6 (**B**) oligonucleotide was incubated with wild type or C301R PXR and RXR in the absence (-) and presence of unlabelled ER6 or mtER6 (10-500-fold molar excess). Complex formation was assessed by detection on x-ray film.

competitor probe, the binding efficiency of the C301R PXR again appeared to be marginally higher than that observed for the wild type receptor. With both PXR variants, the formation of complex with radiolabelled probe appeared to be titrated out by increasing excess of unlabelled ER6 competitor to 500-fold excess where no radiolabel signal was visibly detected. Using a mutated unlabelled competitor ER6 probe the same titrating out of the signal was apparent with both PXR variants with 500-fold excess again sufficient to deplete the radiolabel signal to below visibly detectable levels.

The same EMSA, but with the mutated ER6 probe radio-labelled (Figure 5.16B), was undertaken in order to determine efficiency of the apparent binding of the PXR/RXR complex to the mutated ER6 response element. In the presence of no unlabelled competitor probe, both wild type and C301R were able to heterodimerise with RXR and bind the mutated ER6 probe with similar efficiency. This binding was however considerably less than that observed for the wild type ER6. The addition of increasing excess of unlabelled wild type ER6 probe competed out the radiolabel signal in an excess-dependant manner with 500-fold again sufficient to compete out the radiolabel completely. Increasing excess of unlabelled mutated ER6 competitor was also able to compete out the signal with 500-fold mutant ER6 enough to completely compete out the labelled mutant ER6 signal.

The apparent, albeit lower than wild type, binding of the PXR/RXR heterodimer to the mutated ER6 was of concern and so an EMSA using a wild type and mutated DR3 response element double-stranded oligonucleotide probe was undertaken (Figure 5.17). As seen with the ER6 probe, C301R appears to form the PXR/RXR/DR3 complex more efficiently than wild type PXR in the absence of any unlabelled competitor probe. Addition of unlabelled DR3 competitor titrates out the labelled

probe signal in the complex in the case of both the wild type and C301R PXR. This is again in a competitor excess-dependant manner. The ³²P signal was competed out to a level not visibly detectable at 500-fold molar excess. Use of an unlabeled mutated DR3 probe, as a competitor was also able to compete out the radiolabelled DR3. This titration effect was similar to that observed for wild-type DR3 with 500-fold excess able to compete out the entire radiolabelled probe signal.

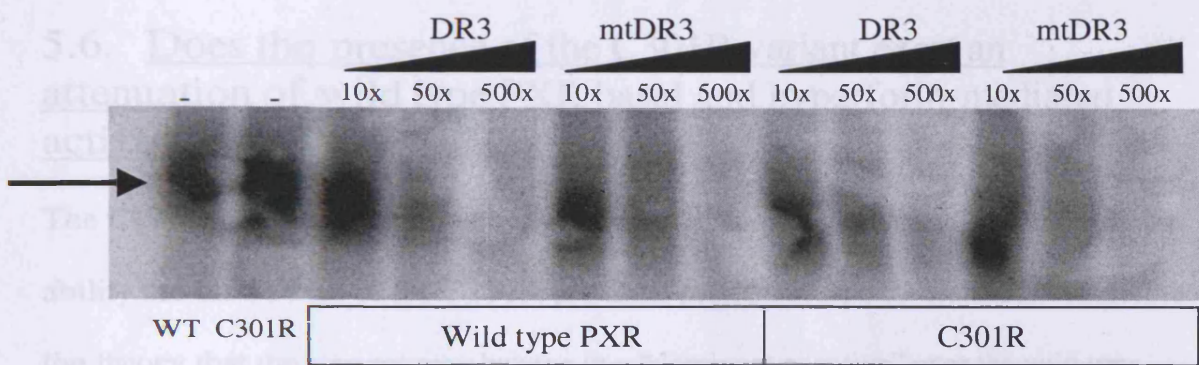


Figure 5.17. Electrophoretic mobility shift assay of PXR/RXR/DR3 CYP3A4 response element by wild type and C301R PXR variants. ³²P-labelled DR3 oligonucleotide was incubated with wild type or C301R PXR and RXR in the absence (-) and presence of unlabelled DR3 or mtDR3 (10-500-fold molar excess). Complex formation was assessed by detection on x-ray film.

probe signal in the complex in the case of both the wild type and C301R PXR. This is again in a competitor excess-dependant manner. The ^{32}P signal was competed out to a level not visibly detectable at 500-fold molar excess. Use of an unlabelled mutated DR3 probe, as a competitor was also able to titrate out the radiolabelled DR3. This titration effect was similar to that observed for wild type DR3 with 500-fold excess able to compete out the entire radiolabelled probe signal.

5.6. Does the presence of the C301R variant exert an attenuation of wild type PXR basal and hyperforin-mediated activation?

The C301R variant displays a highly impaired ligand activation profile but retains the ability to bind DNA of the CYP3A proximal promoter response elements. Therefore the theory that the variant may behave in a “dominant negative” over the wild type receptor was investigated

To determine the effect of the presence of the variant protein on wild type PXR activation, both were transfected along with the DR3 or ER6 reporter. The C301R variant was transfected at equal and increasing excess quantities over the wild type receptor (Figure 5.18). The effect was also assessed in the presence of $0.1\mu\text{M}$ hyperforin, which appears to be the highest concentration at which wild type, but not C301R exerts an effect on activation (Figures 5.8 and 5.9).

In the DR3 reporter assay (Figure 5.18A), activation of the wild type PXR alone was 3.41 ± 0.07 -fold over the no PXR control. In the presence of $0.1\mu\text{M}$ hyperforin this activation was 4.80 ± 0.3 -fold. The introduction of an equal quantity of the C301R variant decreases the activation of wild type by 11.7% and in the presence of $0.1\mu\text{M}$ hyperforin this decrease was 15.5% over wild type PXR only. A 5-fold excess of

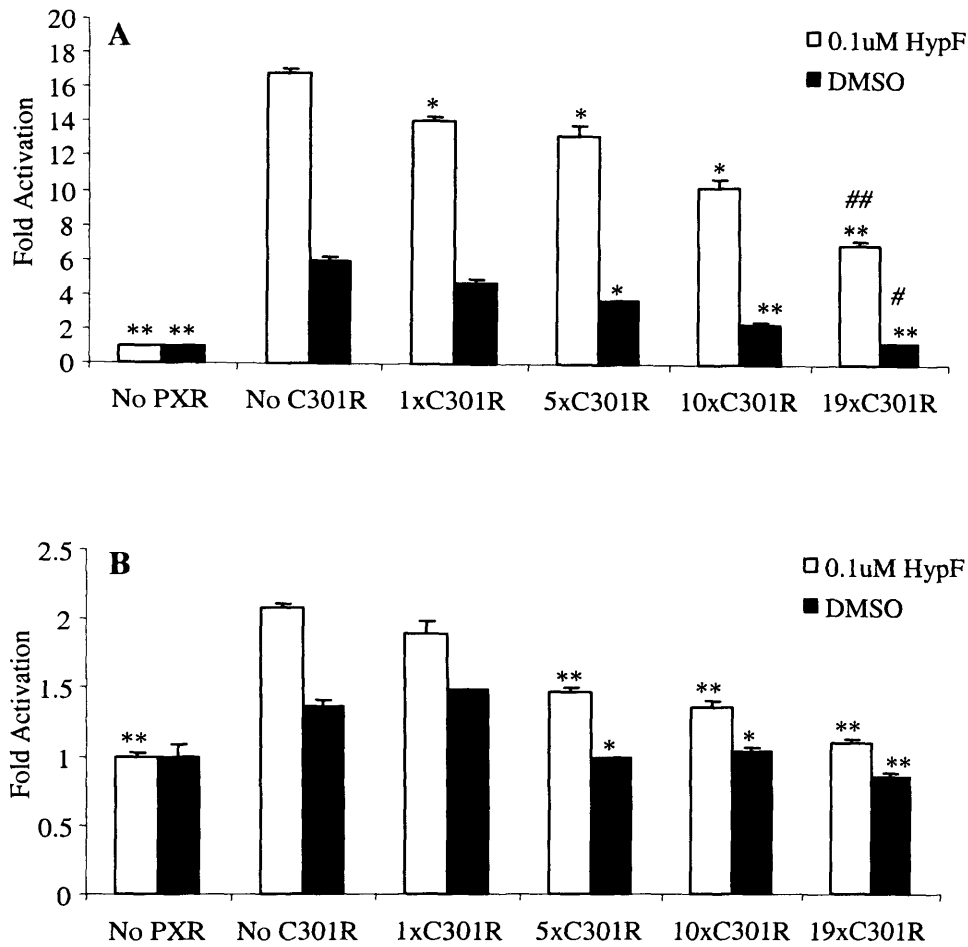


Figure 5.18. Effect of C301R co-transfection on wild type PXR basal and hyperforin activation. **A** represents data for transfection with DR3 RE reporter construct and **B**, with the ER6 RE. Open bars are indicative of transfected cells treated with 0.1µM hyperforin and closed bars, 0.1% DMSO only. Data represents mean fold activation (n=3) normalized against the empty vector respective no PXR control. Error bars represent \pm SD. Statistical significance is indicated as * concentration a ($p < 0.05$) and ** ($p < 0.01$) compared to the wild type PXR only (no C301R) control for that treatment as determined by a step-down one-way ANOVA. # and ## denote statistical significance ($p < 0.05$ and $p < 0.01$ respectively) compared to the no PXR control.

C301R brought about a reduction of 41.1% in the absence of, and 37.1% in the presence of, 0.1 μ M hyperforin over wild type PXR only. At 10-fold excess of C301R, activation rose to 33.6% of PXR only in the presence of the hyperforin but continued to decrease in its absence with a decrease of 46.2% over PXR only.

At the highest excess, DR3 reporter activation by wild type PXR was attenuated to 36.5% in the presence of hyperforin and 46.0% in its absence. The activation at this excess of C301R is equivalent to just 1.77 ± 0.08 -fold over the no PXR control with 0.1 μ M hyperforin and 1.56 ± 0.04 -fold without.

Using the ER6 reporter gene (Figure 5.18B), activation of the wild type alone was lower than that observed with the DR3 reporter. In the presence of 0.1 μ M hyperforin, 2.07 ± 0.03 -fold activation over the no PXR control was observed, and in its absence a 1.36 ± 0.05 -fold increase was seen. With an equal amount of C301R competing with the wild type, mean activation was reduced in the presence of Hyperforin by 9% whilst with no hyperforin; an increase in activation to 1.48 ± 0.01 -fold over the no PXR control was observed. At C301R excesses from 5-fold to 19-fold a decrease in wild type PXR activation was evident with and without 0.1 μ M hyperforin. At 19-fold excess C301R, wild type PXR activation is reduced to 48.8% with hyperforin and 62.9% without. This equates to 1.10 ± 0.03 and 0.86 ± 0.03 -fold, respectively, over the no PXR control.

5.7 Hepatic histology of the two C301R positive ADR cases

Reassessment of the liver histology, post-case selection, of cases 4 and 10, who demonstrated heterozygosity for the C301R allele, showed the hepatic morphology of the two to be quite different (Figures 5.19 and 5.20). Case 4 was at this point classified as moderate steatohepatitis with some biliary duct injury whilst case 10 showed fatty change but again with some biliary duct injury.

The histology of patient 4 is characterised by the presence of a number of isolated necrotic cells and moderate fat deposition of within the tissue (Figure 5.19A). Larger areas of necrosis with considerable inflammatory infiltration are also present (Figure 5.19B). Patient 10 displays a similar pattern of fatty change (Figure 5.20A) and evidence of biliary duct injury with inflammatory infiltration (Figure 5.20B). Unlike patient 4 however, no large areas of necrosis, associated with hepatitis were observed.

5.8 Discussion

5.8.1 Identification of the C301R variant allele.

Given that the variant PXR codon 301 was initially identified, as a heterozygote, from DNA extracted from a formalin-fixed tissue biopsy and amplified by two rounds of PCR amplification, two concerns instantly come to mind. Since the starting DNA sample is so small (<5ng), the possibility that a sequence artefact, albeit present in both forward and reverse sequencing reactions, has been incorporated. The second possibility is that, despite the use of a high fidelity Taq polymerase, in the course of the two PCR amplification reactions an erroneous base has been introduced.

In both cases, these events are spontaneous and, in the case of formalin-fixation artefacts, is unlikely to occur in DNA samples from more than 300 cells (Williams *et al.*, 1999) as is the case with these hepatic biopsy sections.

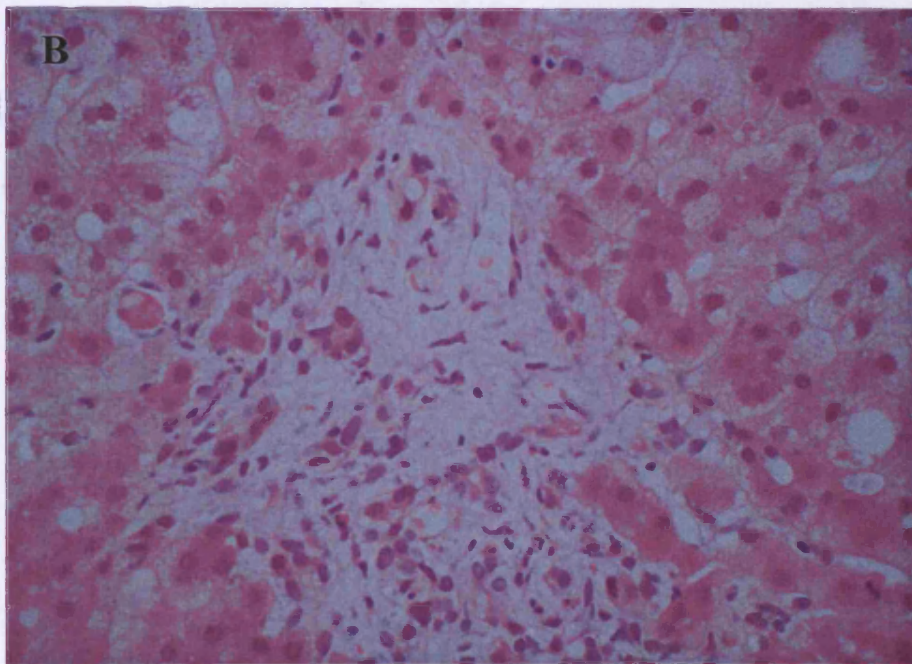
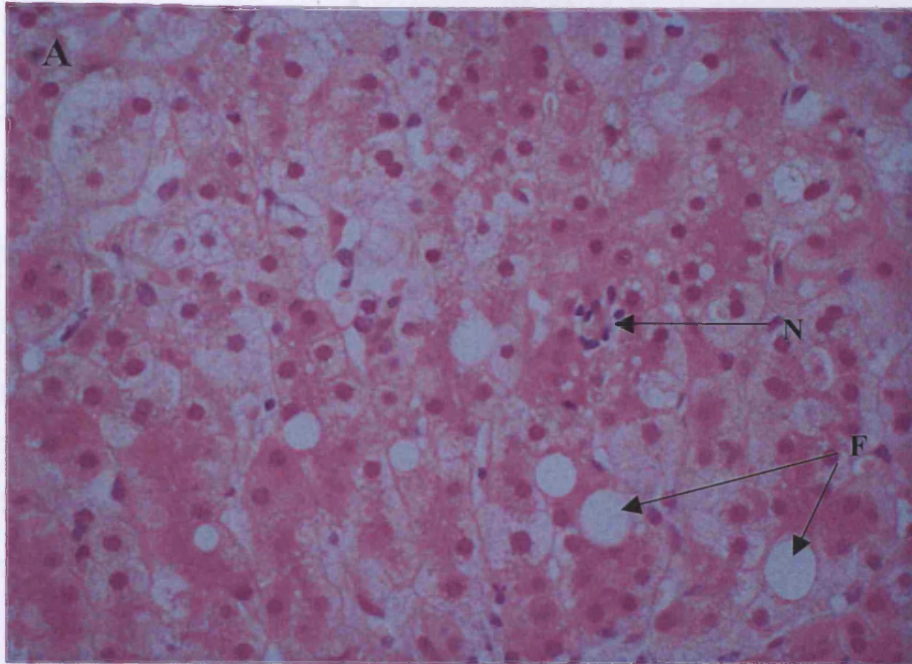


Figure 5.19. Liver Histology of ADR patient number 4, a PXR C301R positive patient. **A** shows the pattern of fatty change (F) with isolated necrotic hepatocytes (N). **B** shows larger areas of severe necrosis with inflammatory infiltrate. High power (400x) magnification.

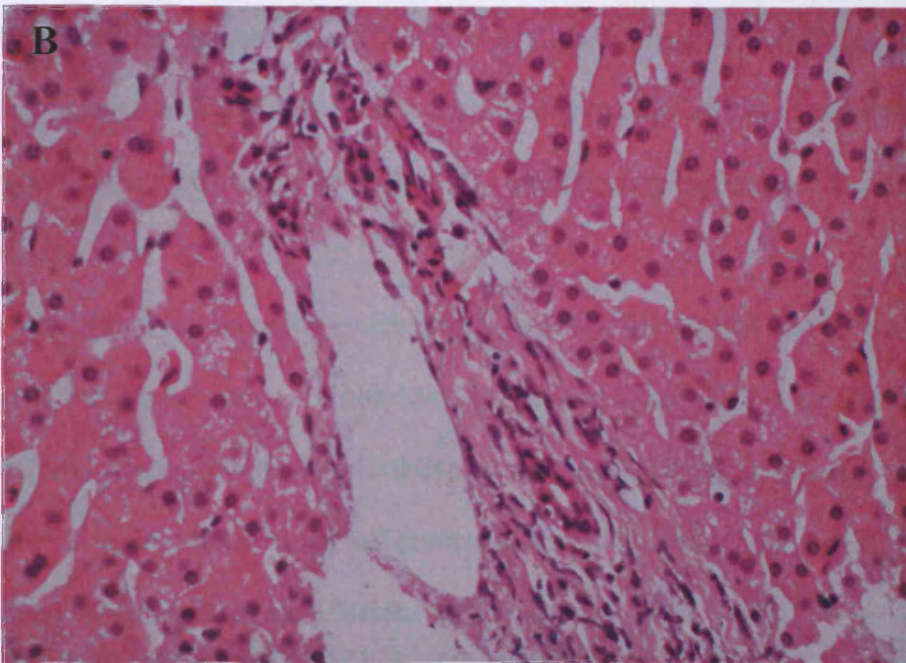
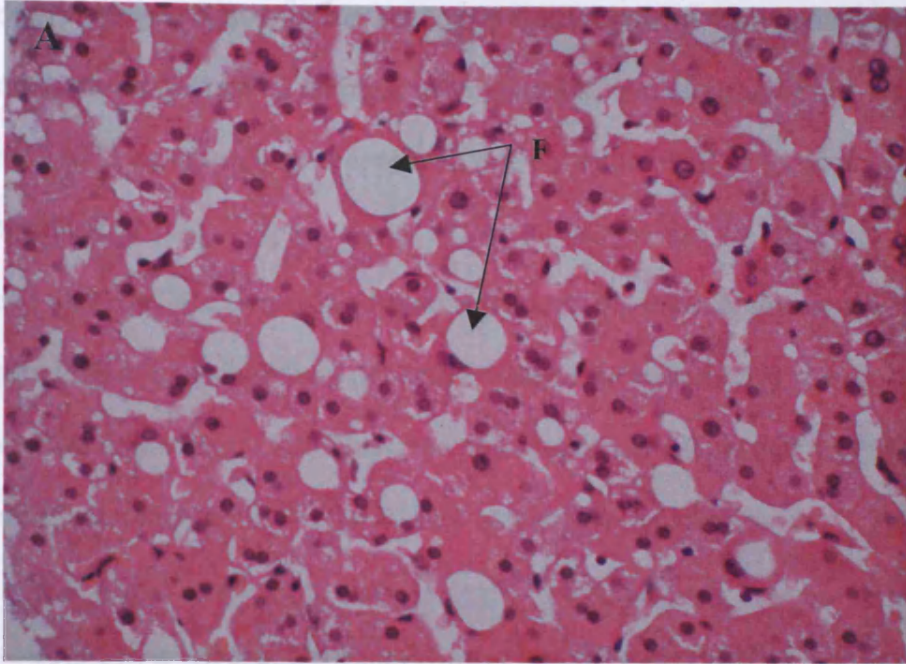


Figure 5.20. Liver Histology of ADR patient number 10, a PXR C301R positive patient. A shows a demonstration of the moderate fatty change (F) observed. B shows a representative bile duct exhibiting injury with inflammatory infiltration. High power (400x) magnification.

Returning to the biopsy tissue for the one initial C301R positive case and repeating the extraction, multiplex nested amplification reactions and sequencing, the presence of the same T to C variation would appear to rule out either PCR or formalin sequence artefact introduction.

Screening of all 53 ADR cases using MwoI restriction digestion of the exon 6 PCR products provided a far quicker and definitive method for determining the presence of the variant allele and indeed highlighted the presence of C301R, as heterozygote in a second individual which seem to give further credence to its validity.

5.8.2 Frequency of C301R in ADR and control populations.

Having determined the frequency of C301R as 2 heterozygotes in 53 ADR patients, it was necessary to determine the frequency within control populations in order to ascertain whether the occurrence of C301R was significantly increased within the ADR population.

In the 100 formalin-fixed biopsies which were histologically normal and 100 determined as metastatic cases, no individuals with the variant allele were identified. The panel of 108 normal DNAs supplied by AstraZeneca also gave rise to no variant alleles. This meant that, as a combined control cohort, 308 individuals (616 chromosomes) were negative for C301R.

Statistical comparison of the ADR cohort (2/53) with the combined control group (0/308) using a Fisher's Exact Test suggests the increase in the ADR cohort is statistically significant to the 95% confidence level ($p=0.023$). This would seem to indicate that the presence of the variant allele is linked to the ADR disease state.

Other PXR variant studies would seem to add further weight to the idea of a relationship between ADR population enrichment and the increase in C301R frequency.

Zhang, *et al.*, (2001) used a shotgun sequencing approach to analyse sequence variation in 75 Caucasians and 11 African American. The C301R variant was not reported as apparent in any of these. Hustert *et al.*, (2001) also used a general PXR sequencing strategy and they too found no individuals exhibiting the C301R variant in a total of 209 Caucasians and 37 Africans. In a Japanese cohort of 205 (Koyano *et al.*, 2002) again using a shotgun sequencing approach, C301R was not identified.

This means that in studies published where a sequencing strategy for identifying novel SNPs in the PXR gene was used, a total of 537 individuals or 1074 chromosomes were analysed and C301R was not found to be present in a single individual. Coupled with the 616 chromosomes analysed as controls for this study, the total number of individuals screened equates to 0/1690 chromosomes which are negative for C301R compared to the ADR cohort where 2/106 or 0.0189 was the frequency of incidence.

5.8.3 Creation of C301R mutant PXR cDNA clone.

Creating a PXR clone incorporating the TGT to CGT variation of codon 301R proved to be difficult for reasons that could only be put down to inefficient priming of the linear PCR reaction of the in vitro mutagenesis kit (Figure 5.3). Ultimately an AGA codon was introduced which, though strictly speaking was not the exact variation observed in the two ADR cases, still introduced the same cysteine to arginine amino acid change. However there was some concern that the difference in frequency of codon usage between CGT and AGA may cause variability in protein translation. In vitro translation, using a coupled transcription/ translation rabbit reticulocyte kit, was

able to yield the correct 51kD protein product from both the wild type and C301R (AGA codon 301) cDNA clones. This suggested that with an arginine encoding AGA codon at residue 301, the protein could be synthesised, from the T7 promoter of the pcDNA3 plasmid, with efficiency equal to that of the wild type.

When independently transfected into a cell-line (HeLa), both wild type and C301R PXR expression were detected, at the mRNA level, at similar levels (Figure 5.7). The same was true at the protein level, though the expression above empty vector transfected cells was not so apparent. Protein detection by immunolabelling does not appear to be particularly efficient in this case; with the primary anti-human PXR antibody and shortcomings in the protein extraction technique the possible sources of this. However, in summary, there does appear to be equal cellular protein expression for both the wild type and C301R PXR variants. The levels of detection are only moderately higher than the empty vector transfected cells and considerably lower than the positive control (*in vitro* synthesised PXR protein).

5.8.4 C301R induces a significant attenuation of PXR activation.

Using the reporter gene co-transfection assay to assess ligand-modulated activation of PXR, it is very apparent that the C301R variant receptor exhibits considerably impaired function in the presence of high efficacy human PXR ligands, hyperforin and rifampicin.

Basal activation of C301R is apparently comparable with the presence of no transfected PXR and in order to achieve reporter gene activation equivalent to the basal level of wild type receptor, a concentration of as much as 3 μ M hyperforin was required. In the presence of rifampicin, activation of both DR3 and ER6 RE reporter

genes was not observed above wild type basal levels up to a concentration of 30 μ M with C301R. At this dose, rifampicin has been reported to exert maximal activation of human PXR (Lehmann *et al.*, 1998).

Within similar reporter gene systems, a number of other functional protein variants of human PXR have been characterised. (Zhang *et al.*, 2001) and (Hustert *et al.*, 2001) both reported DBD variants with attenuated basal and ligand-induced activation of a DR3 RE. In the case of the latter, the activation of one variant D163G was dependant on the presence of an ER6 rather than DR3 RE reporter construct. The most dramatic loss of functionality was observed by (Koyano *et al.*, 2004), where an R98C variant showed basal and clotrimazole induction, which were hugely attenuated and comparable to activation in the absence of any transfected PXR.

Though other ligand-binding domain variants have been identified the dramatic attenuation of basal and ligand activation of C301R is more akin to a DBD variation than that of an LBD variant. This would suggest that the specific amino acid substitution at residue 301 is, compared to other LBD variants, particularly damaging to the protein functionality and indeed the arginine at this position of the protein is crucial to the specificity and compound efficacy of the ligand binding domain.

Lithocholic-induced activation of human PXR did appear to be attenuated by the introduction of C301R (Figure 5.11). However, in the presence of both DR3 and ER6 response elements, there appeared to be endogenous reporter gene activation up to a concentration of 10 μ M. This endogenous activation of a CYP3A4 reporter gene was not observed by (Staudinger *et al.*, 2001) in similar studies carried out in primary rat hepatocyte cultures. This may mean that the mechanism of endogenous activation is specific to HeLa cells rather than primary rodent hepatocytes. One theory of this activation is possible involvement of the vitamin D receptor (VDR). (Makishima *et*

al., 2002) reported VDR functions as a sensor for LCA within the intestine and (Jurutka *et al.*, 2004) described the modulation of LCA induced CYP3A4 by VDR. Derivatives of LCA have also been demonstrated to activate VDR with 30-fold lower concentration than PXR (Adachi *et al.*, 2005). VDR, heterodimerised with RXR, is well known to bind the DR3 DNA sequence that PXR competes for binding to (Shaffer and Gewirth, 2004). The cause of the activation in the absence of PXR may simply be due to the activation of endogenous VDR in HeLa cells by LCA and subsequent binding to DR3. This is likely to be the case for endogenous ER6 activation also. Therefore in future assays it may be necessary to adopt a reporter gene with a more PXR-specific response element or use a cell-line with a low VDR expression phenotype.

5.8.5 Mutation of residue 301 does not confer PXR “rodent-like” activation properties upon wild-type human PXR.

Previous studies have demonstrated that key hydrophilic amino acid residues are critical within the ligand-binding pocket for species specific and constitutive activation (Ostberg *et al.*, 2002). The theory was that rather than displaying attenuated activation, C301R in fact changed the specificity of the ligand binding pocket to something more akin to the rodent PXR compound activation spectrum. This has been demonstrated to occur by introducing residue changes at human PXR codons 285 and 407 in previous studies (Ostberg *et al.*, 2002). Tirona *et al.*, (2004) also described the leucine residue 308 as critical for human PXR activation specificity.

The results appear to suggest that this is not the case. Figures 5.12 and 5.13 clearly demonstrate that the introduction C301R does not alter specificity for dexamethasone and PCN within the ligand-binding pocket of human PXR. This would suggest that residue 301 is not critical for species specification within the ligand-binding pocket.

This would seem to be supported by the highly conserved nature of residue 301 in species as diverse as fish and chickens (Tirona *et al.*, 2004). However it appears critical for efficacy and specificity of classic human PXR ligands.

5.8.6 C301R exhibits no alteration in the DNA binding activity of human PXR

In the case of PXR DBD variants previously reported with attenuated reporter gene activation properties, it is likely that this effect is due a decrease in DNA binding activity. In these instances PXR heterodimerisation with RXR and binding to an ER6 RE was dramatically reduced compared to wild type. In the case of C301R, this DNA binding activity was comparable to that of the wild type receptor in the presence of both ER6 (Figure 5.16) and DR3 (Figure 5.17) REs. This adds weight to the idea that basal and ligand-mediated activation of C301R is reduced as result of altered ligand binding specificity.

Of concern, in interpreting the information provided by the EMSA experiments, is the apparent lack of response element binding specificity exhibited by the PXR/RXR protein heterodimer (Figure 5.16). It would seem that, though more efficacious than the standard ER6 RE, the mutated ER6 (containing 3 point mutations) shows significant binding ability with the PXR/RXR complex, both with wild type and C301R PXR. This is something that was not observed in the studies of Zhang *et al.*, (2001) who were able to observe non-competitor-like binding to the standard ER6 with a 500-fold excess of mutated probe. The same mutated probe binding is apparent using a DR3 RE sequence (Figure 5.17) where 500-fold excess of mutated probe was able to titrate out the radio labelled standard DR3 binding signal.

5.8.7 Wild type PXR activation, in the presence of the C301R variant is significantly impaired.

Co-transfection with wild type PXR in increasing excess suggests that C301R exerts an apparent “dominant negative” inhibitory effect on both basal and hyperforin-induced activation (Figure 5.18). The data seem to suggest that while PXR mediated gene transcription within individuals possessing the variant allele may be considerably impaired by the attenuated activation of C301R; the effect is not likely to be lethal and may only present itself physically in extreme cases of toxic insult such as ADRs. However PXR variation is highly unlikely to be the sole explanation for these or any other ADR cases.

5.8.8 Concurrence of C301R functionality with liver histology and LFT data.

Both of the C301R positive cases have characteristics of cholestatic injury. This injury however, does not appear to be hepatocanalicular in origin. Case 10 appears to be a cholangiolytic (ductular) cholestasis (Levy and Lindor, 2003) with associated scattered steatosis and minimal hepatocellular damage. Though sharing steatosis and bile duct injury, case 4 appears to be, primarily, hepatic injury caused by drug-induced hepatitis.

PXR-humanised animal models of bile duct ligation (Stedman *et al.* 2004) demonstrated that CYP3A4 induction was a significant *in vivo* adaptive response to cholestasis. This was a response to conjugated bile acids in general and not an LCA-specific effect. As such it appears that impaired CYP3A induction in conjunction with bile duct ligation/ injury may exacerbate the toxic effects of bile acids.

It seems that, rather than being a consequence of impaired bile acid homeostasis at the hepatocanalicular level, the C301R impairment of PXR is likely to induce an adverse effect via attenuation of drug/ bile transporter protein and metabolizing enzyme

expression and thus altered pharmacokinetics. Altered xenobiotic distribution and metabolism could, therefore, be one explanation for the pathology observed in these two cases.

5.8.9 Conclusions

A novel variant allele of the human PXR has been identified in two individuals, as a heterozygote, from the ADR cohort of 53. The frequency of incidence in the ADR cohort is significantly higher than a control population, where it did not occur. The variant encodes for a cysteine to arginine amino acid substitution C301R within the PXR LBD. The result of this is an apparent attenuation of basal and ligand-induced (hyperforin and rifampicin) activation of the wild-type receptor response. It did not however appear to alter the ability of the receptor to bind, as a heterodimer with RXR, to the downstream CYP3A response element.

The two individuals possessing the C301R variant allele did not display histology suggestive of hepatocanalicular injury. However it is possible that the bile duct injury observed in both cases may be exacerbated by the C301R variant proteins dysfunctional induction of bile acid homeostatic mechanisms (CYP3A4 principally). This could lead to the primary drug-induced liver injury observed in the two cases (steatosis and steatohepatitis respectively). However PXR dysfunction is unlikely to represent a single predisposing factor in the aetiology of the injury.

Chapter 6: General Discussion

6. General Discussion

6.1 Identification and characterisation of an ADR cohort.

In principal, the concept of identifying a patient cohort retrospectively is good one.

The ability to enrich a population for a clinical manifestation as rare as hepatic ADRs, using archival records and tissue, is clearly advantageous over a retrospective accumulation of cases. Were the 53 cases identified in this study collected upon presentation, it would take in excess of 9 years within an NHS hospital trust of equivalent size to Leicester.

Whilst there are clear advantages to utilizing a clinical biopsy archive, there are also limitations to this approach. The selection of the cases in this study was undertaken using information supplied within the pathology report compiled from observation of the tissue histology. Some basic information of age, sex, the serum liver function test data and suspicious drug use was available but this was not available for all 53 cases. Other studies (Aithal and Day, 1999), though retrospective were able to call upon extensive clinical notes, from within a gastroenterology department detailing comprehensive records of suspicious drugs and follow-up information following therapy withdrawal. Such information would be beneficial to a study, such as this one, but clearly without the means, or even ability given the time elapsed, to do so is simply not possible.

One other clear possibility, should clinical support be available would have been the collection of blood samples from not only retrospective ADR individuals but also from some of the 53 members identified. This would have clearly aided the genotypic analysis by providing a source of high yield, low degradation DNA not found in formalin-fixed archival tissue.

For the purpose of this study, the cohort demonstrates enrichment of the population for hepatic ADRs. Whilst not homologous in nature, the 53 ADR cases demonstrate common features, both histological and biochemical, suspicious of drug-induced hepatotoxicity. The high incidence of cholestatic injury within the cohort coupled with the consensus of the LFT data would suggest that the origin of the injury in the majority of the cases is hepatocanalicular. This could suggest that dysfunctional drug-mediated PXR transcriptional regulation and/or downstream target gene functionality may be a factor in the predisposition of these individuals.

The cohort selection process seems to have yielded a comparably sized cohort with characteristics which suggest ADR predominantly hepatocanalicular in origin and a possible link to PXR mediated drug metabolism and bile homeostatic pathway dysfunction. However given greater clinical support, further information and more user friendly sources of DNA could have both enhanced the study and allowed for wider scope in terms genotypic analysis of other candidate genes.

6.2 Use of DNA preamplification in genotypic analysis of formalin-fixed archival tissue.

Given the limited yield (<5ng) and degradation of DNA extracted from formalin fixed biopsy tissue demonstrated in this study, standard extraction and amplification techniques would have been very limiting. Indeed, using a single round of PCR amplification, it would only have been possible to analyse the sequence of <300 bases from the hepatic tissue of each member of the cohort. By utilizing the multiplex nested amplification approach, sequence data for the entire protein coding region of the PXR gene could be obtained from the <5ng DNA yielded from a large proportion of the formalin-fixed specimens.

Of consideration, for future similar studies, is the use of the “Rapid” DNA extraction protocol where the ability to simultaneously extract total RNA is sacrificed but where the DNA yield from formalin-fixed tissue and subsequent PCR success across a number of samples is considerably higher. Use of a non-nested PCR method would have eliminated all of the inherent risks associated with use and handling of pre-amplified DNA.

One of the objectives of this study, however, was to develop a means of analysing the mRNA expression levels with the intention of determining a possible correlation between dysfunctional PXR genotypes with variability to the downstream PXR target transcriptome. The dual extraction methodology, despite DNA extraction efficiency and handling difficulties does appear to meet the initial objective set out for this study.

The need for internal controls against cross-sample contamination is a key requisite in ensuring that sample population DNA sequence data acquired is truly representative when using a preamplification-based technique. The work of this study (Figure 4.13) would seem to suggest that a comparison of a previously described SNP’s frequency with the frequency determined from the cohort whose DNA is subjected to a two-step amplification provides a simple and clear assessment of possible cross-contamination. In this study, the control SNP in question was within one of the PCR products amplified as part of the PXR screening program and gave a clear indication that the allelic frequency of the SNP within ADR cohort was not influenced by cross-contamination. Such a control would prove useful in further studies base on small formalin-fixed tissue samples where mRNA analysis was desired and thus DNA preamplification was a necessity.

6.3 PXR protein variant C301R demonstrates significantly increased frequency in an ADR cohort and attenuated functionality.

Within the identified and characterised ADR cohort the C301R variant PXR was evident at an allelic frequency of 1.8%. Screening of control populations did not detect any individuals possessing the variant allele and as such the increased frequency in the ADR cohort was determined as statistically significant. The analysis of C301R in non-ADR controls would need to be undertaken on a far larger “normal” population in order to ascertain the true allelic frequency within the population as a whole. The C301R PXR variant may be associated with genetic predisposition to a specific hepatic ADR whose occurrence is at a frequency of one in several thousand. By using the retrospective case selection and genotyping techniques employed in this project, a variant allele of a key xenobiotic metabolism and bile acid homeostatic regulatory gene which may yield a predisposition to an ADR has been identified in 2 individuals in a cohort of just 53. To discover this very same variant in the general population would require the screening of potentially tens of thousands of individuals.

Functionally, the C301R variant appears to exert its effect on PXR mediated gene transcription as a result of alteration to the ligand binding pocket. Reporter gene assays clearly demonstrated that the introduction of arginine at residue 301 resulted in dramatic attenuation of ligand-mediated PXR activation and down stream target transcription in the presence of human PXR ligands. The distinct difference in the alteration of hyperforin and rifampicin-induced activation would suggest that C301R introduces a change in binding efficiency to the LBD which is compound specific. Of interest may be the ability to bind and activate C301R, of SR12813 which in studies has been shown to bind PXR in three distinct orientations (Watkins *et al.* 2001). The

altered LBD of C301R may decrease the effect of SR12813 activation slightly less dramatically than is the case with hyperforin which binds in one single orientation. In other words C301R may only prevent efficient binding of SR12813 in one of its three orientations thus an intermediate attenuated activation state may be apparent.

Gel shift assays appeared to confirm that the effect is solely a result of ligand binding dysfunction, since variant PXR binding to CYP3A response elements does not appear to be affected. This would appear to be as expected since there is no legitimate reason to suggest residue 301 variation, given its location within the ligand-binding pocket, would affect the ability of PXR to heterodimerise with RXR and bind to target response element sequence.

It is also likely that the mutation affects transcriptional activation to similar degree.

The ability of C301R to abolish any basal activity within the HeLa cell system may be due to a number of reasons though it is likely that altered activation properties of an undetermined endogenous ligand binding may play a role in this. The fact that PXR expression was consistent, for both wild-type and C301R, would suggest that any functional alteration of PXR expression modulation can be discounted. 3-dimensional analysis of the C301R variant protein could however identify a possible structural conformation alteration to the protein which introduces altered transcriptional regulation. This is likely to be independent of DNA response element binding given the data for EMSA assays shown.

The histology and biochemistry data available for the ADR cohort would seem to fit with the dysfunction associated with the C301R PXR. The observed cholestatic liver injury of a hepatocanalicular origin would fit with the disruption of bile acid homeostasis and metabolism that are the likely impact of C301R. However the two cases (numbers 4 and 10) where C301R heterogeneity was observed, do not display

the classic bland cholestasis that might be predicted for dysfunctional PXR (Figures 5.19 and 5.20).

ADR number patient 4 appears to display histology consistent with steatohepatitis with some biliary duct injury. ADR patient number 10 also displays features of bile duct injury and steatosis. However no presence of any hepatitis was recorded.

It is conceivable that the bile duct injury observed in these two cases may not be of a drug-induced origin. Such ductal injury is often observed in cholestatic liver disease such primary biliary cirrhosis (PBC) or primary sclerosing cholangitis (PSC).

However it is widely accepted that both these diseases have an autoimmune component to their aetiology (Abraham *et al.*, 2004). The case selection process adopted for this study discriminated against cases where clinical data suggested the presence of serum autoantibodies. As such it would seem that this is a suitable way of excluding cases of both PBC and PSC. The cases observed, therefore, are far more likely to have a drug-induced rather than an autoimmune aetiology.

Another consideration is the possibility that these cases of apparent ductopenia may in fact possess the characteristics of vanishing bile duct syndrome (VBDS). Among the drugs known to cause VBDS are flucloxacillin (Davies *et al.*, 1994; Eckstein *et al.*, 1993) and carbamazepine (Ramos *et al.*, 2002). However since the drug of suspicion cannot be identified in either C301R case the likelihood of VBDS cannot be determined. The presence of steatosis in both cases would suggest that it would not be the only mechanism of pathogenesis.

The type of hepatic injury seen in cases 4 and 10 is unlikely to be as result of the hypothesised disruption of PXR bile acid homeostasis. It is possible that the observed dysfunctional characteristics of C301R could in some part be responsible for the manifestation of the histological features. Hepatitis, steatosis and bile duct injury are

histological features that could arise as a result of altered xenobiotic metabolism and distribution. Given the role PXR plays in the regulation of expression of so many phase I (CYP3A and 2B6), phase II (GST and UGT) and phase III transporter (MDR1 and OATP-C), it is possible that the presence of a C301R allele may alter the expression of one or more of these clearance mechanisms. This could lead to the build up of toxic metabolites within hepatic tissue leading the manifestation of the injury observed.

It is impossible to say whether the C301R PXR variant is solely responsible, for the ADR pathology of the two cases. As originally hypothesised, disrupted PXR function should, in theory, alter bile acid homeostatic pathway regulation and cause some degree of cholestatic injury. However, two ADR cases displaying a PXR allele demonstrated to be dramatically impaired as a ligand-mediated transcription factor have shown no evidence of cholestasis. This would suggest that despite disruption of those hepatocanicular clearance mechanisms regulated by PXR, FXR, the primary regulatory mechanism of bile acid clearance and cholesterol catabolism is able to cope with bile acid clearance without the need to “fall back” on the conceived secondary mechanism which PXR represents.

Recent PXR knockout animal model studies have alluded to the protective role that PXR plays against cholestatic liver disease (Sonoda et al., 2005; Stedman et al., 2005). The loss of PXR results in hepatic damage due to bile acid accumulation and can induce lethality associated with severe hepatorenal failure (Sonoda et al., 2005). The pattern of liver injury however is consistent with cholestatic liver injury and does not appear to resemble that observed in the two C301R cases found in this study.

Whilst the knockout may offer an insight into the clinical manifestation of PXR dysfunction, it cannot be assumed to be entirely representative.

6.4 Possible future work.

The DNA preamplification protocol adopted for the sequence analysis was designed specifically for the protein coding region of the PXR gene, the main candidate gene of this study. This means that future genotypic analysis of other genes, associated with xenobiotic metabolism and bile acid homeostasis, from the ADR cohort hepatic tissue is not possible. Further ethical permission would be required to retrospectively obtain biological specimens (blood) in order to pursue sequence variation analysis of a wider range of candidate genes.

Expression analysis of the ADR cohort hepatic tissue using the total RNA extracted alongside DNA could provide a correlation altered target gene expression with the dysfunction exhibited by the C301R PXR variant observed in the two individuals. However a more beneficial outcome of such an exercise may be to determine altered expression levels of transcripts associated with other hepatic metabolism and bile homeostatic pathways such as those regulated by FXR and SHP-1. This could identify further candidate genes where a dysfunctional genotype may manifest as a hepatic injury, histologically or biochemically, akin to those observed within the ADR cohort.

Given the size of the RNA yield from the ADR biopsies, a sensitive RT-PCR protocol is required for detection of mRNA transcripts. A semi-quantitative method has already been valuated (Figure 4.14) but the use of a fully quantitative protocol, such a TaqMan™ real-time PCR may address the sensitivity issue and provide good meaningful expression data. Due to nature of the mRNA isolation procedure, the

expression levels determined would need to be compared to the expression of a house-keeping gene (GAPDH, Beta-Actin) rather than the 18S ribosomal RNA control commonly adopted for TaqMan™ analysis.

Another option in gene expression analysis in relation to the C301R PXR variant is to adopt a cell-line based system. The reporter gene assays undertaken in this study involved the transfection of the wild-type and variant PXR into non-human liver derived cell-lines (Cos-7 and HeLa). In order to recreate a system representative of the hepatic environment within which PXR exerts its transcriptional regulation, it would be necessary to undertake drug-induced expression studies where cloned PXR is transfected into human liver derived cell lines such as HepG2 or HuH7.

In undertaking functional studies using cells transfected with cDNA clones, the fact that the mRNA expression level of the gene in question is often considerably higher than the endogenous level exhibited by a given cell-line. In the case of transcription factors, such as PXR, this endogenous expression is very low. In order obtain an accurate representation of the drug-induced gene expression profile created by the introduction the C301R variation; the cellular expression level of transfected variant clone could be controlled to mimic the endogenous level of the wild type PXR.

In order to replicate near-endogenous levels of PXR with a transfected C301R variant clone a doxycycline-regulated transgene activator could be utilised (Urlinger et al., 2000). This would allow for fine-tuning of C301R PXR protein expression by treating the post-transfected cells with a range of doxycycline concentrations. This system has recently been evaluated in HepG2 and HuH7 for protein expression regulation of, among other proteins, CYP2E1 and GST P1-1 (Goldring et al., 2004). By adopting this system with the C301R ligated into the plasmid construct, variant

PXR levels could be limited to near endogenous levels allowing for drug-induced gene expression variability to be assessed.

The dysfunctional effect exerted by the C301R variant PXR is clearly as a result of alteration of the structure of the receptor ligand binding domain and more specifically the ligand-binding pocket. Studies relating to the crystalline structure of the human PXR LBD (Watkins *et al.*, 2003) and the binding of ligands, such as hyperforin (Watkins *et al.*, 2001) have identified the key hydrophilic binding amino acid residues. The ligand-binding pocket has also shown considerable promiscuity with some specific ligands ligand binding in a number of different orientations. In the case of the C301R variant, it would seem that the binding ability, and thus the promiscuity of PXR is attenuated. Use of an x-ray crystallography technique could help to understand the structural changes to the ligand-binding pocket, which occur as a result of the residue substitution at codon 301. This would also represent a novel approach to understanding functional alteration of the LBD since other residue changes in this region, as identified by Koyano *et al* (2002), have not been characterised to this degree.

6.5 Conclusions.

The original objective of this study was to identify an ADR cohort from a collection of archival liver biopsies in order to identify possible functional variants of the PXR gene which may predispose individuals to ADR. On face value this objective would seem to have been achieved. The retrospectively accrued ADR cohort appears to be a good population and genetic enrichment for hepatic ADR, a series of pathologies whose occurrence within the population is 1 in several thousand.

The protocols developed for nucleic acid extraction and amplification have, as intended, allowed for simultaneous DNA and RNA analysis from single core-needle hepatic biopsies. This however was only possible with a single candidate gene, PXR. For sequence analysis, a nested PCR approach was developed with a suitable internal inter-sample contamination control included. This allowed sequencing of the protein-coding region in the 53 ADR cases identified.

The identification of a novel, and clearly dysfunctional variant PXR allele within the cohort at a significantly increased frequency than the general population would tend to suggest that the intention of ADR predisposition genetic enrichment may have been successful in this instance. However, the fact that within such a highly enriched ADR population, only 3.6% of cases actually possessed the C301R allele, would suggest that it is by no means the only predisposing factor to hepatic ADR within this cohort. The development of the methodologies, within this study, and utilisation of formalin-fixed hepatic biopsy tissue provide a means for future investigation of the pharmacogenetics of similar cohorts. This could shed further light on the mechanisms underlying genetic predisposition to the spectrum of pathologies observed as hepatic ADRs.

References

- Abraham, S., Begum, S., and Isenberg, D. (2004). Hepatic manifestations of autoimmune rheumatic diseases. *Ann Rheum Dis* 63, 123-129.
- Adachi, R., Honma, Y., Masuno, H., Kawana, K., Shimomura, I., Yamada, S., and Makishima, M. (2005). Selective activation of vitamin D receptor by lithocholic acid acetate, a bile acid derivative. *J. Lipid. Res.* 46(1), 6-57.
- Aithal, G.P., and Day, C. (1999). The natural history of histologically proved drug induced liver disease. *Gut* 44, 731-735.
- Aithal, G. P., Day, C. P., Kesteven, P. J., and Daly, A. K. (1999). Association of polymorphisms in the cytochrome P450 CYP2C9 with warfarin dose requirement and risk of bleeding complications. *Lancet* 353, 717-719.
- Aithal, G. P., Day, C. P., Leathart, J. B., and Daly, A. K. (2000). Relationship of polymorphism in CYP2C9 to genetic susceptibility to diclofenac-induced hepatitis. *Pharmacogenetics* 10, 511-518.
- Aithal, G. P., Ramsay, L., Daly, A. K., Sonchit, N., Leathart, J. B., Alexander, G., Kenna, J. G., Caldwell, J., and Day, C. P. (2004). Hepatic adducts, circulating antibodies, and cytokine polymorphisms in patients with diclofenac hepatotoxicity. *Hepatology* 39, 1430-1440.
- Aithal, G. P., Rawlins, M. D., and Day, C. P. (1999). Accuracy of hepatic adverse drug reaction reporting in one English health region. *BMJ* 319, 1541.
- Aithal, G. P., Rawlins, M. D., and Day, C. P. (2000). Clinical diagnostic scale: a useful tool in the evaluation of suspected hepatotoxic adverse drug reactions. *J Hepatol* 33, 949-952.
- Al-Taher, A., Bahein, A., Nolan, T., Hollingsworth, M., and Brady, G. (2000). Global cDNA amplification combined with real-time RT-PCR: accurate quantification of multiple human potassium channel genes at the single cell level. *Yeast* 17, 201-210.
- Ananthanarayanan, M., Balasubramanian, N., Makishima, M., Mangelsdorf, D. J., and Suchy, F. J. (2001). Human bile salt export pump promoter is transactivated by the farnesoid X receptor/bile acid receptor. *J Biol Chem* 276, 28857-28865.

- Applied-Biosystems (2001). AmpF/STR SGM Plus PCR Amplification Kit: User's Manual).
- Benichou, C. (1990). Criteria of drug-induced liver disorders. Report of an international consensus meeting. *J Hepatol* 11, 272-276.
- Berson, A., Freneaux, E., Larrey, D., Lepage, V., Douay, C., Mallet, C., Fromenty, B., Benhamou, J. P., and Pessayre, D. (1994). Possible role of HLA in hepatotoxicity. An exploratory study in 71 patients with drug-induced idiosyncratic hepatitis. *J Hepatol* 20, 336-342.
- Bertilsson, G., Heidrich, J., Svensson, K., Asman, M., Jendeberg, L., Sydow-Backman, M., Ohlsson, R., Postlind, H., Blomquist, P., and Berkenstam, A. (1998). Identification of a human nuclear receptor defines a new signaling pathway for CYP3A induction. *Proc Natl Acad Sci U S A* 95, 12208-12213.
- Bissell, D. M., Gores, G. J., Laskin, D. L., and Hoofnagle, J. H. (2001). Drug-induced liver injury: mechanisms and test systems. *Hepatology* 33, 1009-1013.
- Blumberg, B., Sabbagh, W., Juguilon, H., Bolado, J., van Meter, C. M., Ong, E. S., and Evans, R. M. (1998). SXR, a novel steroid and xenobiotic-sensing receptor. *Genes Dev* 12, 3195-3205.
- Bull, L. N. (2002). Hereditary forms of intrahepatic cholestasis. *Curr Opin Genet Dev* 12, 336-342.
- Bull, L. N., van Eijk, M. J., Pawlikowska, L., DeYoung, J. A., Juijn, J. A., Liao, M., Klomp, L. W., Lomri, N., Berger, R., Scharschmidt, B. F., et al. (1998). A gene encoding a P-type ATPase mutated in two forms of hereditary cholestasis. *Nat Genet* 18, 219-224.
- Cao, H., and Hegele, R. A. (2002). Identification of polymorphisms in the human SHP1 gene. *J Hum Genet* 47, 445-447.
- Capon, F., Allen, M.H., Ameen, M., Burden, A.D., Tillman, D., Barker, J.N., and Trembath, R.C. (2004). A synonymous SNP of the corneodesmosin gene leads to increased mRNA stability and demonstrates association with psoriasis across diverse ethnic groups. *Hum Mol Genet* 13(20), 2361-2368.
- Carlton, V. E., Knisely, A. S., and Freimer, N. B. (1995). Mapping of a locus for progressive familial intrahepatic cholestasis (Byler disease) to 18q21-q22, the benign recurrent intrahepatic cholestasis region. *Hum Mol Genet* 4, 1049-1053.

- Cartegni, L., Chew, S.L., and Krainer, A.R. (2002). Listening to silence and understanding nonsense: exonic mutations that affect splicing. *Nat Rev Genet.* 3(4), 285-298.
- Chang, T. K., Bandiera, S. M., and Chen, J. (2003). Constitutive androstane receptor and pregnane X receptor gene expression in human liver: interindividual variability and correlation with CYP2B6 mRNA levels. *Drug Metab Dispos* 31, 7-10.
- Chen, C., Staudinger, J. L., and Klaassen, C. D. (2003). Nuclear receptor, pregnane X receptor, is required for induction of UDP-glucuronosyltransferases in mouse liver by pregnenolone-16 alpha-carbonitrile. *Drug Metab Dispos* 31, 908-915.
- Chiang, J. Y., Miller, W. F., and Lin, G. M. (1990). Regulation of cholesterol 7 alpha-hydroxylase in the liver. Purification of cholesterol 7 alpha-hydroxylase and the immunochemical evidence for the induction of cholesterol 7 alpha-hydroxylase by cholestyramine and circadian rhythm. *J Biol Chem* 265, 3889-3897.
- Coombs, N. J., Gough, A. C., and Primrose, J. N. (1999). Optimisation of DNA and RNA extraction from archival formalin-fixed tissue. *Nucleic Acids Res* 27, e12.
- Cui, J., Heard, T. S., Yu, J., Lo, J. L., Huang, L., Li, Y., Schaeffer, J. M., and Wright, S. D. (2002). The amino acid residues asparagine 354 and isoleucine 372 of human farnesoid X receptor confer the receptor with high sensitivity to chenodeoxycholate. *J Biol Chem* 277, 25963-25969.
- Danan, G. (1988). Causality assessment of drug-induced liver injury. Hepatology Working Group. *J Hepatol* 7, 132-136.
- Danielian, P.S., White, R., Lees, J.A. and Parker, M.G. 1992. Identification of a conserved region required for hormone dependant transcriptional activation by steroid hormone receptors. *EMBO J.* 11, 1025-1033.
- Davies, M. H., Harrison, R. F., Elias, E., and Hubscher, S. G. (1994). Antibiotic-associated acute vanishing bile duct syndrome: a pattern associated with severe, prolonged, intrahepatic cholestasis. *J Hepatol* 20, 112-116.

- del Castillo-Olivares, A., and Gil, G. (2001). Suppression of sterol 12 α -hydroxylase transcription by the short heterodimer partner: insights into the repression mechanism. *Nucleic Acids Res* 29, 4035-4042.
- Deleuze, J. F., Jacquemin, E., Dubuisson, C., Cresteil, D., Dumont, M., Erlinger, S., Bernard, O., and Hadchouel, M. (1996). Defect of multidrug-resistance 3 gene expression in a subtype of progressive familial intrahepatic cholestasis. *Hepatology* 23, 904-908.
- Denson, L. A., Sturm, E., Echevarria, W., Zimmerman, T. L., Makishima, M., Mangelsdorf, D. J., and Karpen, S. J. (2001). The orphan nuclear receptor, shp, mediates bile acid-induced inhibition of the rat bile acid transporter, ntcp. *Gastroenterology* 121, 140-147.
- Desai, P. B., Nallani, S. C., Sane, R. S., Moore, L. B., Goodwin, B. J., Buckley, D. J., and Buckley, A. R. (2002). Induction of cytochrome P450 3A4 in primary human hepatocytes and activation of the human pregnane X receptor by tamoxifen and 4- hydroxytamoxifen. *Drug Metab Dispos* 30, 608-612.
- de Vree, J. M., Jacquemin, E., Sturm, E., Cresteil, D., Bosma, P. J., Aten, J., Deleuze, J. F., Desrochers, M., Burdelski, M., Bernard, O., et al. (1998). Mutations in the MDR3 gene cause progressive familial intrahepatic cholestasis. *Proc Natl Acad Sci U S A* 95, 282-287.
- Dietmaier, W., Hartmann, A., Wallinger, S., Heinmoller, E., Kerner, T., Endl, E., Jauch, K. W., Hofstadter, F., and Ruschoff, J. (1999). Multiple mutation analyses in single tumor cells with improved whole genome amplification. *Am J Pathol* 154, 83-95.
- Dixon, P. H., Weerasekera, N., Linton, K. J., Donaldson, O., Chambers, J., Egginton, E., Weaver, J., Nelson-Piercy, C., de Swiet, M., Warnes, G., et al. (2000). Heterozygous MDR3 missense mutation associated with intrahepatic cholestasis of pregnancy: evidence for a defect in protein trafficking. *Hum Mol Genet* 9, 1209-1217.
- Dotzlaw, H., Leygue, E., Watson, P., and Murphy, L. C. (1999). The human orphan receptor PXR messenger RNA is expressed in both normal and neoplastic breast tissue. *Clin Cancer Res* 5, 2103-2107.

- Drocourt, L., Pascussi, J. M., Assenat, E., Fabre, J. M., Maurel, P., and Vilarem, M. J. (2001). Calcium channel modulators of the dihydropyridine family are human pregnane x receptor activators and inducers of cyp3a, cyp2b, and cyp2c in human hepatocytes. *Drug Metab Dispos* 29, 1325-1331.
- Dussault, I., Yoo, H. D., Lin, M., Wang, E., Fan, M., Batta, A. K., Salen, G., Erickson, S. K., and Forman, B. M. (2003). Identification of an endogenous ligand that activates pregnane X receptor-mediated sterol clearance. *Proc Natl Acad Sci U S A* 100, 833-838.
- Echchgadda I., Song C.S., Oh T.S., Cho S.H., Rivera O.J., and Chatterjee B. (2004). Gene regulation for the senescence marker protein DHEA-sulfotransferase by the xenobiotic-activated nuclear pregnane X receptor (PXR). *Mech Ageing Dev.* 125(10-11), 733-745.
- Eckstein, R. P., Dowsett, J. F., and Lunzer, M. R. (1993). Flucloxacillin induced liver disease: histopathological findings at biopsy and autopsy. *Pathology* 25, 223-228.
- Ekins, S., and Erickson, J. A. (2002). A pharmacophore for human pregnane X receptor ligands. *Drug Metab Dispos* 30, 96-99.
- Falkner, K. C., Pinaire, J. A., Xiao, G. H., Geoghegan, T. E., and Prough, R. A. (2001). Regulation of the rat glutathione S-transferase A2 gene by glucocorticoids: involvement of both the glucocorticoid and pregnane X receptors. *Molecular Pharmacology* 60, 611-619.
- Forman, B. M., Goode, E., Chen, J., Oro, A. E., Bradley, D. J., Perlmann, T., Noonan, D. J., Burka, L. T., McMorris, T., Lamph, W. W., and et al. (1995). Identification of a nuclear receptor that is activated by farnesol metabolites. *Cell* 81, 687-693.
- Fregeau, C. J., Tan-Siew, W. F., Yap, K. H., Carmody, G. R., Chow, S. T., and Fourney, R. M. (1998). Population genetic characteristics of the STR Loci D21S11 and FGA in eight diverse human populations. *Hum Biol* 70, 813-844.
- Friis, H., and Andreasen, P. B. (1992). Drug-induced hepatic injury: an analysis of 1100 cases reported to the Danish Committee on Adverse Drug Reactions between 1978 and 1987. *J Intern Med* 232, 133-138.

- Fukuen, S., Fukuda, T., Matsuda, H., Sumida, A., Yamamoto, I., Inaba, T., and Azuma, J. (2002). Identification of the novel splicing variants for the hPXR in human livers. *Biochem Biophys Res Commun* 298, 433-438.
- Funk, C., Pantze, M., Jehle, L., Ponelle, C., Scheuermann, G., Lazendic, M., and Gasser, R. (2001a). Troglitazone-induced intrahepatic cholestasis by an interference with the hepatobiliary export of bile acids in male and female rats. Correlation with the gender difference in troglitazone sulfate formation and the inhibition of the canalicular bile salt export pump (Bsep) by troglitazone and troglitazone sulfate. *Toxicology* 167, 83-98.
- Funk, C., Ponelle, C., Scheuermann, G., and Pantze, M. (2001b). Cholestatic potential of troglitazone as a possible factor contributing to troglitazone-induced hepatotoxicity: in vivo and in vitro interaction at the canalicular bile salt export pump (Bsep) in the rat. *Mol Pharmacol* 59, 627-635.
- Geick, A., Eichelbaum, M., and Burk, O. (2001). Nuclear receptor response elements mediate induction of intestinal MDR1 by rifampin. *J Biol Chem* 276(18), 14581-14587.
- Gerloff, T., Stieger, B., Hagenbuch, B., Madon, J., Landmann, L., Roth, J., Hofmann, A. F., and Meier, P. J. (1998). The sister of P-glycoprotein represents the canalicular bile salt export pump of mammalian liver. *J Biol Chem* 273, 10046-10050.
- Gillam, E. M. (2001). The PXR ligand-binding domain: how to be picky and promiscuous at the same time. *Trends Pharmacol Sci* 22, 448.
- Gillam, E. M. (2002). Coordinating clearance - the many phases of PXR! *Trends Pharmacol Sci* 23, 548-549.
- Goldring, C., Kitteringham, N., Lovat, C., Jenkins, R., Randle, L., Abdullah, A., Owen, A., Liu, X., Berens, C., Hillen, W., and Park, B. (2004). Development of Doxycycline-Regulatable Gene Expression in Hepatoma cells, Poster presented at: Joint BPS/BTS Meeting: Adverse Reactions to Drugs and Chemicals: studies from Molecule to Man (University of Liverpool).
- Goodwin, B., Gauthier, K. C., Umetani, M., Watson, M. A., Lochansky, M. I., Collins, J. L., Leitersdorf, E., Mangelsdorf, D. J., Kliewer, S. A., and Repa, J. J. (2003). Identification of bile acid precursors as endogenous ligands for the

nuclear xenobiotic pregnane X receptor. *Proc Natl Acad Sci U S A* 100, 223-228.

- Goodwin, B., Jones, S. A., Price, R. R., Watson, M. A., McKee, D. D., Moore, L. B., Galardi, C., Wilson, J. G., Lewis, M. C., Roth, M. E., et al. (2000). A regulatory cascade of the nuclear receptors FXR, SHP-1, and LRH-1 represses bile acid biosynthesis. *Mol Cell* 6, 517-526.
- Goodwin, B., and Kliewer, S. (2002). Nuclear Receptors. I. Nuclear Receptors and bile acid homeostasis. *Am J Physiol Gastrointest Liver Physiol* 282, G926-G931.
- Goodwin, B., Moore, L. B., Stoltz, C. M., McKee, D. D., and Kliewer, S. A. (2001). Regulation of the human CYP2B6 gene by the nuclear pregnane X receptor. *Molecular Pharmacology* 60, 427-431.
- Goodwin, B., Redinbo, M. R., and Kliewer, S. A. (2002). Regulation of cyp3a gene transcription by the pregnane x receptor. *Annu Rev Pharmacol Toxicol* 42, 1-23.
- Greiner, B., Eichelbaum, M., Fritz, P., Kreichgauer, H. P., von Richter, O., Zundler, J., and Kroemer, H. K. (1999). The role of intestinal P-glycoprotein in the interaction of digoxin and rifampin. *J Clin Invest* 104, 147-153.
- Hartleb, M., Biernat, U., and Kochel, A. (2002). Drug-induced liver damage - a three-year study of patients from one gastroenterological department. *Med Sci Monit* 8, CR292-296.
- Hautekeete, M. L., Horsmans, Y., Van Waeyenberge, C., Demanet, C., Henrion, J., Verbist, L., Brenard, R., Sempoux, C., Michielsen, P. P., Yap, P. S., et al. (1999). HLA association of amoxicillin-clavulanate--induced hepatitis. *Gastroenterology* 117, 1181-1186.
- Hendrickson, B. C., Leclair, B., Forrest, S., Ryan, J., Ward, B. E., Petersen, D., Kupferschmid, T. D., and Scholl, T. (2004). Accurate STR allele designations at the FGA and vWA loci despite primer site polymorphisms. *J Forensic Sci* 49, 250-254.
- Hesse, L. M., and Court, M. H. (2003). Quantitation of CYP2B6, constitutive androstane receptor, and pregnane X receptor mRNA levels. *Drug Metab Dispos* 31, 685; author reply 686.

- Hofmann, A. F. (2002). Rifampicin and treatment of cholestatic pruritus. *Gut* 51, 756-757.
- Honkakoski, P. and Negishi, M. (2000). Regulation of cytochrome P450 (CYP) genes by nuclear receptors. *Biochem. J.* 347, 321-337.
- Houwen, R. H., Baharloo, S., Blankenship, K., Raeymaekers, P., Juyn, J., Sandkuijl, L. A., and Freimer, N. B. (1994). Genome screening by searching for shared segments: mapping a gene for benign recurrent intrahepatic cholestasis. *Nat Genet* 8, 380-386.
- Huang, Y. S., Chern, H. D., Su, W. J., Wu, J. C., Chang, S. C., Chiang, C. H., Chang, F. Y., and Lee, S. D. (2003). Cytochrome P450 2E1 genotype and the susceptibility to antituberculosis drug-induced hepatitis. *Hepatology* 37, 924-930.
- Huang, Y. S., Chern, H. D., Su, W. J., Wu, J. C., Lai, S. L., Yang, S. Y., Chang, F. Y., and Lee, S. D. (2002). Polymorphism of the N-acetyltransferase 2 gene as a susceptibility risk factor for antituberculosis drug-induced hepatitis. *Hepatology* 35, 883-889.
- Hustert, E., Zibat, A., Presecan-Siedel, E., Eiselt, R., Mueller, R., Fuß, C., Brehm, I., Brinkmann, U., Eichelbaum, M., Wojnowski, L., and Burk, O. (2001). Natural Protein Variants of Pregnane X Receptor with altered transactivation activity toward CYP3A4. *Drug Metab Dispos* 29, 1454-1459.
- Jacquemin, E., Cresteil, D., Manouvrier, S., Boute, O., and Hadchouel, M. (1999). Heterozygous non-sense mutation of the MDR3 gene in familial intrahepatic cholestasis of pregnancy. *Lancet* 353, 210-211.
- Jansen, P. L., Muller, M., and Sturm, E. (2001). Genes and cholestasis. *Hepatology* 34, 1067-1074.
- Jansen, P. L., Strautnieks, S. S., Jacquemin, E., Hadchouel, M., Sokal, E. M., Hooiveld, G. J., Koning, J. H., De Jager-Krikken, A., Kuipers, F., Stellaard, F., et al. (1999). Hepatocanicular bile salt export pump deficiency in patients with progressive familial intrahepatic cholestasis. *Gastroenterology* 117, 1370-1379.
- Jones, S. A., Moore, L. B., Shenk, J. L., Wisely, G. B., Hamilton, G. A., McKee, D. D., Tomkinson, N. C., LeCluyse, E. L., Lambert, M. H., Willson,

- T. M., et al. (2000). The pregnane X receptor: a promiscuous xenobiotic receptor that has diverged during evolution. *Mol Endocrinol* 14, 27-39.
- Jurutka, P.W., Thompson, P.D., Whitfield, G.K., Eichhorst, K.R., Hall, N., Dominguez, C.E., Hsieh, J.C., Haussler, C.A., and Haussler, M.R. (2004). Molecular and functional comparison of 1,25-dihydroxyvitamin D(3) and the novel vitamin D receptor ligand, lithocholic acid, in activating transcription of cytochrome P450 3A4. *J. Cell Biochem.* 2004 Dec 2, (epub ahead of print).
 - Kittler, R., Stoneking, M., and Kayser, M. (2002). A whole genome amplification method to generate long fragments from low quantities of genomic DNA. *Anal Biochem* 300, 237-244.
 - Kliewer, S. A., Moore, J. T., Wade, L., Staudinger, J. L., Watson, M. A., Jones, S. A., McKee, D. D., Oliver, B. B., Willson, T. M., Zetterstrom, R. H., et al. (1998). An orphan nuclear receptor activated by pregnanes defines a novel steroid signaling pathway. *Cell* 92, 73-82.
 - Kohlroser, J., Mathai, J., Reichheld, J., Banner, B. F., and Bonkovsky, H. L. (2000). Hepatotoxicity due to troglitazone: report of two cases and review of adverse events reported to the United States Food and Drug Administration. *Am J Gastroenterol* 95, 272-276.
 - Kolars, J. C., Schmiedlin-Ren, P., Schuetz, J. D., Fang, C., and Watkins, P. B. (1992). Identification of rifampin-inducible P450III A4 (CYP3A4) in human small bowel enterocytes. *J Clin Invest* 90, 1871-1878.
 - Koyano, S., Kurose, K., Ozawa, S., M. Saeki, M., Nakajima, Y., Hasegawa, R., Komamura, K., Ueno, K., Kamakura, S., Nakajima, T., et al. (2002). Eleven novel single nucleotide polymorphisms in the NR1I2 (PXR) gene, four of which induce non-synonymous amino acid alterations. *Drug Metab Pharmacokinet* 17, 561-565.
 - Koyano, S., Kurose, K., Saito, Y., Ozawa, S., Hasegawa, R., Komamura, K., Ueno, K., Kamakura, S., Kitakaze, M., Nakajima, T., et al. (2004). Functional characterization of four naturally occurring variants of human pregnane X receptor (PXR): one variant causes dramatic loss of both DNA binding activity and the transactivation of the CYP3A4 promoter/enhancer region. *Drug Metab Dispos* 32, 149-154.

- Kullak-Ublick, G. A., Jung, D., Hagenbuch, B., and Meier, P. J. (2002). Organic anion transporting polypeptides, cholestasis, and nuclear receptors. *Hepatology* 35, 732-734.
- Larrey, D., Hadengue, A., Pessayre, D., Choudat, L., DeGott, C., and Benhamou, J. P. (1987). Carbamazepine-induced acute cholangitis. *Dig Dis Sci* 32, 554-557.
- Lee, Y. K., Dell, H., Dowhan, D. H., Hadzopoulou-Cladaras, M., and Moore, D. D. (2000). The orphan nuclear receptor SHP inhibits hepatocyte nuclear factor 4 and retinoid X receptor transactivation: two mechanisms for repression. *Mol Cell Biol* 20, 187-195.
- Lee, Y. K., and Moore, D. D. (2002). Dual mechanisms for repression of the monomeric orphan receptor liver receptor homologous protein-1 by the orphan small heterodimer partner. *J Biol Chem* 277, 2463-2467.
- Lehmann, J. M., McKee, D. D., Watson, M. A., Willson, T. M., Moore, J. T., and Kliewer, S. A. (1998). The human orphan nuclear receptor PXR is activated by compounds that regulate CYP3A4 gene expression and cause drug interactions. *Journal of Clinical Investigation* 102, 1016-1023.
- Levy, C., and Lindor, K. D. (2003). Drug-induced cholestasis. *Clin Liver Dis* 7, 311-330.
- Lewis, F., Maughan, N. J., Smith, V., Hillan, K., and Quirke, P. (2001). Unlocking the archive--gene expression in paraffin-embedded tissue. *J Pathol* 195, 66-71.
- Lewis, J. H., and Zimmerman, H. J. (1999). Drug- and chemical-induced cholestasis. *Clin Liver Dis* 3, 433-464, vii.
- Maglich, J. M., Stoltz, C. M., Goodwin, B., Hawkins-Brown, D., Moore, J. T., and Kliewer, S. A. (2002). Nuclear pregnane x receptor and constitutive androstane receptor regulate overlapping but distinct sets of genes involved in xenobiotic detoxification. *Mol Pharmacol* 62, 638-646.
- Makishima, M., Okamoto, A. Y., Repa, J. J., Tu, H., Learned, R. M., Luk, A., Hull, M. V., Lustig, K. D., Mangelsdorf, D. J., and Shan, B. (1999). Identification of a nuclear receptor for bile acids. *Science* 284, 1362-1365.
- Mangelsdorf, D. J., and Evans, R. M. (1995). The RXR heterodimers and orphan receptors. *Cell* 83, 841-850.

- Mangelsdorf, D.J., Thummel, C., Beato, M., et al. (1995). The nuclear receptor superfamily: the second decade. *Cell* 83, 835-839.
- Maria, V. A., and Victorino, R. M. (1997). Development and validation of a clinical scale for the diagnosis of drug-induced hepatitis. *Hepatology* 26, 664-669.
- Masuda, N., Ohnishi, T., Kawamoto, S., Monden, M., and Okubo, K. (1999). Analysis of chemical modification of RNA from formalin-fixed samples and optimization of molecular biology applications for such samples. *Nucleic Acids Res* 27, 4436-4443.
- McCarthy, J. J., and Hilfiker, R. (2000). The use of single-nucleotide polymorphism maps in pharmacogenomics. *Nat Biotechnol* 18, 505-508.
- Mela, M., Mancuso, A., and Burroughs, A. K. (2003). Review article: pruritus in cholestatic and other liver diseases. *Aliment Pharmacol Ther* 17, 857-870.
- Mills, K. A., Even, D., and Murray, J. C. (1992). Tetranucleotide repeat polymorphism at the human alpha fibrinogen locus (FGA). *Hum Mol Genet* 1, 779.
- Moore, J. T., and Kliewer, S. A. (2000). Use of the nuclear receptor PXR to predict drug interactions. *Toxicology* 153, 1-10.
- Moore, L. B., Goodwin, B., Jones, S. A., Wisely, G. B., Serabjit-Singh, C. J., Willson, T. M., Collins, J. L., and Kliewer, S. A. (2000a). St. John's wort induces hepatic drug metabolism through activation of the pregnane X receptor. *Proc Natl Acad Sci U S A* 97, 7500-7502.
- Moore, L. B., Parks, D. J., Jones, S. A., Bledsoe, R. K., Consler, T. G., Stimmel, J. B., Goodwin, B., Liddle, C., Blanchard, S. G., Willson, T. M., et al. (2000b). Orphan nuclear receptors constitutive androstane receptor and pregnane X receptor share xenobiotic and steroid ligands. *J Biol Chem* 275, 15122-15127.
- Murphy, E. J., Davern, T. J., Shakil, A. O., Shick, L., Masharani, U., Chow, H., Freise, C., Lee, W. M., and Bass, N. M. (2000). Troglitazone-induced fulminant hepatic failure. Acute Liver Failure Study Group. *Dig Dis Sci* 45, 549-553.

- O'Donohue, J., Oien, K. A., Donaldson, P., Underhill, J., Clare, M., MacSween, R. N., and Mills, P. R. (2000). Co-amoxiclav jaundice: clinical and histological features and HLA class II association. *Gut* 47, 717-720.
- Ourlin, J. C., Lasserre, F., Pineau, T., Fabre, J. M., Sa-Cunha, A., Maurel, P., Vilarem, M. J., and Pascussi, J. M. (2003). The small heterodimer partner interacts with the pregnane X receptor and represses its transcriptional activity. *Mol Endocrinol* 17, 1693-1703.
- Parks, D. J., Blanchard, S. G., Bledsoe, R. K., Chandra, G., Consler, T. G., Kliewer, S. A., Stimmel, J. B., Willson, T. M., Zavacki, A. M., Moore, D. D., and Lehmann, J. M. (1999). Bile acids: natural ligands for an orphan nuclear receptor. *Science* 284, 1365-1368.
- Pessayre, D., Larrey, D., and Biour, M. (1999). Drug-induced liver injury, In *Oxford Textbook of Clinical Hepatology*, J. Bircher, J.-P. Benhamou, N. McIntyre, and J. Rodes, eds. (Oxford: Oxford University Press), pp. 1261-1315.
- Przygodzki, R. M., Goodman, Z. D., Rabin, L., Centeno, J. A., Liu, Y., Hubbs, A. E., and O'Leary, T. J. (2001). Hemochromatosis (HFE) gene sequence analysis of formalin-fixed, paraffin-embedded liver biopsy specimens. *Mol Diagn* 6, 227-232.
- Ramensky, V., Bork, P., and Sunyaev, S. (2002). Human non-synonymous SNPs: server and survey. *Nucleic Acids Res* 30, 3894-3900.
- Ramos, A. M., Gayotto, L. C., Clemente, C. M., Mello, E. S., Luz, K. G., and Freitas, M. L. (2002). Reversible vanishing bile duct syndrome induced by carbamazepine. *Eur J Gastroenterol Hepatol* 14, 1019-1022.
- Rosmorduc, O., Poupon, R., Nion, I., Wendum, D., Feder, J., Bereziat, G., and Hermelin, B. (2000). Differential HFE allele expression in hemochromatosis heterozygotes. *Gastroenterology* 119, 1075-1086.
- Schrenk, D., Gant, T. W., Preisegger, K. H., Silverman, J. A., Marino, P. A., and Thorgeirsson, S. S. (1993). Induction of multidrug resistance gene expression during cholestasis in rats and nonhuman primates. *Hepatology* 17, 854-860.

- Schuetz, E. G., Beck, W. T., and Schuetz, J. D. (1996). Modulators and substrates of P-glycoprotein and cytochrome P4503A coordinately up-regulate these proteins in human colon carcinoma cells. *Mol Pharmacol* 49, 311-318.
- Serth, J., Kuczyk, M. A., Paeslack, U., Lichtinghagen, R., and Jonas, U. (2000). Quantitation of DNA extracted after micropreparation of cells from frozen and formalin-fixed tissue sections. *Am J Pathol* 156, 1189-1196.
- Shaffer, P.L., and Gewirth, D.T. (2004). Structural analysis of RXR-VDR interactions on DR3 DNA. *J. Steroid Biochem Mol. Biol.* 89-90(1-5), 215-219.
- Sgro, C., Clinard, F., Ouazir, K., Chanay, H., Allard, C., Guilleminet, C., Lenoir, C., Lemoine, A., and Hillon, P. (2002). Incidence of drug-induced hepatic injuries: a French population-based study. *Hepatology* 36, 451-455.
- Sharma, S. K., Balamurugan, A., Saha, P. K., Pandey, R. M., and Mehra, N. K. (2002). Evaluation of clinical and immunogenetic risk factors for the development of hepatotoxicity during antituberculosis treatment. *Am J Respir Crit Care Med* 166, 916-919.
- Shneider, B. L., Fox, V. L., Schwarz, K. B., Watson, C. L., Ananthanarayanan, M., Thevananther, S., Christie, D. M., Hardikar, W., Setchell, K. D., Mieli-Vergani, G., et al. (1997). Hepatic basolateral sodium-dependent-bile acid transporter expression in two unusual cases of hypercholanemia and in extrahepatic biliary atresia. *Hepatology* 25, 1176-1183.
- Simon, T., Becquemont, L., Mary-Krause, M., de Waziers, I., Beaune, P., Funck-Brentano, C., and Jaillon, P. (2000). Combined glutathione-S-transferase M1 and T1 genetic polymorphism and tacrine hepatotoxicity. *Clin Pharmacol Ther* 67, 432-437.
- Sinal, C. J., Tohkin, M., Miyata, M., Ward, J. M., Lambert, G., and Gonzalez, F. J. (2000). Targeted disruption of the nuclear receptor FXR/BAR impairs bile acid and lipid homeostasis. *Cell* 102, 731-744.
- Smit, J. J., Schinkel, A. H., Oude Elferink, R. P., Groen, A. K., Wagenaar, E., van Deemter, L., Mol, C. A., Ottenhoff, R., van der Lugt, N. M., van Roon, M. A., and et al. (1993). Homozygous disruption of the murine mdr2 P-

glycoprotein gene leads to a complete absence of phospholipid from bile and to liver disease. *Cell* 75, 451-462.

- Sonoda, J., Chong, L. W., Downes, M., Barish, G. D., Coulter, S., Liddle, C., Lee, C. H., and Evans, R. M. (2005). Pregnane X receptor prevents hepatorenal toxicity from cholesterol metabolites. *Proc Natl Acad Sci U S A* 102, 2198-2203.
- Sonoda, J., Xie, W., Rosenfeld, J. M., Barwick, J. L., Guzelian, P. S., and Evans, R. M. (2002). Regulation of a xenobiotic sulfonation cascade by nuclear pregnane X receptor (PXR). *Proc Natl Acad Sci U S A* 99, 13801-13806.
- Specht, K., Richter, T., Muller, U., Walch, A., Werner, M., and Hofler, H. (2001). Quantitative gene expression analysis in microdissected archival formalin-fixed and paraffin-embedded tumor tissue. *Am J Pathol* 158, 419-429.
- Srinivasan, M., Sedmak, D., and Jewell, S. (2002). Effect of fixatives and tissue processing on the content and integrity of nucleic acids. *Am J Pathol* 161, 1961-1971.
- Staudinger, J., Liu, Y., Madan, A., Habeebu, S., and Klaassen, C. D. (2001a). Coordinate regulation of xenobiotic and bile acid homeostasis by pregnane x receptor. *Drug Metab Dispos* 29, 1467-1472.
- Staudinger, J. L., Goodwin, B., Jones, S. A., Hawkins-Brown, D., MacKenzie, K. I., LaTour, A., Liu, Y., Klaassen, C. D., Brown, K. K., Reinhard, J., et al. (2001b). The nuclear receptor PXR is a lithocholic acid sensor that protects against liver toxicity. *Proc Natl Acad Sci U S A* 98, 3369-3374.
- Stedman, C. A., Liddle, C., Coulter, S. A., Sonoda, J., Alvarez, J. G., Moore, D. D., Evans, R. M., and Downes, M. (2005). Nuclear receptors constitutive androstane receptor and pregnane X receptor ameliorate cholestatic liver injury. *Proc Natl Acad Sci U S A* 102, 2063-2068.
- Stedman, C., Robertson, G., Coulter, S., and Liddle, C. (2004). Feed-forward Regulation of Bile Acid Detoxification by CYP3A4: Studies in Humanized Transgenic Mice. *J. Biol. Chem.* 279(12), 11336-11343.
- Stieger, B., Fattinger, K., Madon, J., Kullak-Ublick, G. A., and Meier, P. J. (2000). Drug- and estrogen-induced cholestasis through inhibition of the

hepatocellular bile salt export pump (Bsep) of rat liver. *Gastroenterology* 118, 422-430.

- Stoecklein, N. H., Erbersdobler, A., Schmidt-Kittler, O., Diebold, J., Schardt, J. A., Izbicki, J. R., and Klein, C. A. (2002). SCOMP is superior to degenerated oligonucleotide primed-polymerase chain reaction for global amplification of minute amounts of DNA from microdissected archival tissue samples. *Am J Pathol* 161, 43-51.
- Strautnieks, S. S., Kagalwalla, A. F., Tanner, M. S., Knisely, A. S., Bull, L., Freimer, N., Kocoshis, S. A., Gardiner, R. M., and Thompson, R. J. (1997). Identification of a locus for progressive familial intrahepatic cholestasis PFIC2 on chromosome 2q24. *Am J Hum Genet* 61, 630-633.
- Thompson, R., and Strautnieks, S. (2001). BSEP: function and role in progressive familial intrahepatic cholestasis. *Semin Liver Dis* 21, 545-550.
- Tirona, R.G., Leake, B.F., Podust, L.M., and Kim, R.B. (2004). Identification of Amino Acids in Rat Pregnane X Receptor that Determine Species-Specific Activation. *Molecular Pharmacology* 65, 36-44.
- Urlinger, S., Baron, U., Thellmann, M., Hasan, M. T., Bujard, H., and Hillen, W. (2000). Exploring the sequence space for tetracycline-dependent transcriptional activators: novel mutations yield expanded range and sensitivity. *Proc Natl Acad Sci U S A* 97, 7963-7968.
- Uno, Y., Sakamoto, Y., Kenici, Y., Hasegawa, T., Hasegawa, Y., Koshino, T., and Inoue, I. (2003). Characterisation of six base pair deletion in the putative HNF1-binding site of human PXR promoter. *J Hum Genet* 48, 594-597.
- Vavricka, S. R., Van Montfoort, J., Ha, H. R., Meier, P. J., and Fattinger, K. (2002). Interactions of rifamycin SV and rifampicin with organic anion uptake systems of human liver. *Hepatology* 36, 164-172.
- Wang, H., Chen, J., Hollister, K., Sowers, L. C., and Forman, B. M. (1999). Endogenous bile acids are ligands for the nuclear receptor FXR/BAR. *Mol Cell* 3, 543-553.
- Watanabe, I., Tomita, A., Shimizu, M., Sugawara, M., Yasumo, H., Koishi, R., Takahashi, T., Miyoshi, K., Nakamura, K., Izumi, T., et al. (2003). A study to survey susceptible genetic factors responsible for troglitazone-associated

- hepatotoxicity in Japanese patients with type 2 diabetes mellitus. *Clin Pharmacol Ther* 73, 435-455.
- Watkins, P. B., Murray, S. A., Winkelman, L. G., Heuman, D. M., Wrighton, S. A., and Guzelian, P. S. (1989). Erythromycin breath test as an assay of glucocorticoid-inducible liver cytochromes P-450. *Studies in rats and patients. J Clin Invest* 83, 688-697.
 - Watkins, R. E., Maglich, J. M., Moore, L. B., Wisely, G. B., Noble, S. M., Davis-Searles, P. R., Lambert, M. H., Kliewer, S. A., and Redinbo, M. R. (2003). 2.1 A crystal structure of human PXR in complex with the St. John's wort compound hyperforin. *Biochemistry* 42, 1430-1438.
 - Watkins, R. E., Wisely, G. B., Moore, L. B., Collins, J. L., Lambert, M. H., Williams, S. P., Willson, T. M., Kliewer, S. A., and Redinbo, M. R. (2001). The human nuclear xenobiotic receptor PXR: structural determinants of directed promiscuity. *Science* 292, 2329-2333.
 - Whitehead, M. W., Hainsworth, I., and Kingham, J. G. (2001). The causes of obvious jaundice in South West Wales: perceptions versus reality. *Gut* 48, 409-413.
 - Williams, C., Ponten, F., Moberg, C., Soderkvist, P., Uhlen, M., Ponten, J., Sitbon, G., and Lundeberg, J. (1999). A high frequency of sequence alterations is due to formalin fixation of archival specimens. *Am J Pathol* 155, 1467-1471.
 - Willson, T. M., Jones, S. A., Moore, J. T., and Kliewer, S. A. (2001). Chemical genomics: Functional analysis of orphan nuclear receptors in the regulation of bile acid metabolism. *Med Res Rev* 21, 513-522.
 - Xie W., Barwick J.L., Downes M., Blumberg B., Simon C.M., Nelson M.C., Neuschwander-Tetri B.A., Brunt E.M., Guzelian P.S., Evans R.M. (2000) Humanized xenobiotic response in mice expressing nuclear receptor SXR. *Nature* 27: 406(6794), 435-439.
 - Xie, W., Radominska-Pandya, A., Shi, Y., Simon, C. M., Nelson, M. C., Ong, E. S., Waxman, D. J., and Evans, R. M. (2001). An essential role for nuclear receptors SXR/PXR in detoxification of cholestatic bile acids. *Proc Natl Acad Sci U S A* 98, 3375-3380.

- Zhang, J., Kuehl, P., Green, E. D., Touchman, J. W., Watkins, P. B., Daly, A., Hall, S. D., Maurel, P., Relling, M., Brimer, C., et al. (2001). The human pregnane X receptor: genomic structure and identification and functional characterization of natural allelic variants. *Pharmacogenetics* 11, 555-572.
- Zhang, L., Cui, X., Schmitt, K., Hubert, R., Navidi, W., and Arnheim, N. (1992). Whole genome amplification from a single cell: Implications for genetic analysis. *Proc Natl Acad Sci U S A* 89, 5847-5851.
- Zhang, M., and Chiang, J. Y. (2001). Transcriptional regulation of the human sterol 12alpha-hydroxylase gene (CYP8B1): roles of hepatocyte nuclear factor 4alpha in mediating bile acid repression. *J Biol Chem* 276, 41690-41699.
- Zollner, G., Fickert, P., Zenz, R., Fuchsbichler, A., Stumptner, C., Kenner, L., Ferenci, P., Stauber, R. E., Krejs, G. J., Denk, H., et al. (2001). Hepatobiliary transporter expression in percutaneous liver biopsies of patients with cholestatic liver diseases. *Hepatology* 33, 633-646.

Appendices

Appendices

A. Multiplex Nested PCR Primers

<u>PXR</u> <u>Exon</u>	<u>Primer</u>	<u>Sequence</u>	<u>NT_005994</u> <u>Position</u>
1A	F	5'-CATGAGTTACCACAAGTCACA-3'	2488
	M13F	5'- ACTGTA AAAACGACGGCCAGT CATACA ACCAGCTCCCTGTT-3'	2510
	SF	5'-CTGGGGACTATGGGAACTG-3'	2583
	SM13F	5'- ACTGTA AAAACGACGGCCAGT ATGGGAACTGGGATCA ACTC-3'	2592
	SM13R	5'- CAGGAA ACAGCT ATGAC CGGTTTGAAGCCA ACTCAGC -3'	2750
	SR	5'-GGGCTGTAAAGTGGAGAGAAG-3'	2773
	M13R	5'- CAGGAA ACAGCT ATGAC CATGCAGGCAAGACTCG-3'	2836
	R	5'-GGGCTGTAAAGTGGAGAGAAG-3'	2858
2	F	5'-AGGTCAGCTCCCGAGTTC-3'	27036
	M13F	5'- ACTGTA AAAACGACGGCCAGT AGTTCACAGGCCCA ATGT-3'	27055
	SF	5'-TAGTCCAAGAGGCCCAGAA-3'	27144
	SM13F	5'- ACTGTA AAAACGACGGCCAGT CAAACCTGGAGGTGAG ACC-3'	27164
	SM13R	5'- CAGGAA ACAGCT ATGAC CGATAGCCAGTGGCCTTGTC-3'	27322
	SR	5'-TCATGACATTGAAGTGATAGCC-3'	27337
	M13R	5'- CAGGAA ACAGCT ATGAC CCAGCCCACACTCTGAACC-3'	27428
	R	5'-CAGCCCACACTCTGAACC-3'	27460
3	F	5'-GACTCCCACCTACACCCTTC-3'	29809
	M13F	5'- ACTGTA AAAACGACGGCCAGT GACGCAAAGGCTAGTGTCC -3'	29851
	SF	5'-CTTCTGCTCCCCATTCTCTC-3'	29955
	SM13F	5'- ACTGTA AAAACGACGGCCAGT CCCCATTCTCTCACAGG AG-3'	29963
	SM13R	5'- CAGGAA ACAGCT ATGAC CGTCTTCCGGGTGATCTCG-3'	30050
	SR	5'-GTCTTCCGGGTGATCTCG-3'	30050
	M13R	5'- CAGGAA ACAGCT ATGAC CACGGCACGTCCTTACTCAG-3'	30176
	R	5'-ACACAAGCATGCCACAC-3'	30196
4	F	5'-GAGTCCAGACAGGGGAGAAT-3'	31306
	M13F	5'- ACTGTA AAAACGACGGCCAGT AGAGGGTTACACAGTGGCTCT - 3'	31375
	SF	5'-AGTGATCATGTCCGACGAG-3'	31455
	SM13F	5'- ACTGTA AAAACGACGGCCAGT AGTGATCATGTCCGACGAG -3'	31455
	SM13R	5'- CAGGAA ACAGCT ATGAC CGTTTTTCATCTGAGCGTCCAT-3'	31607
	SR	5'-GGGAGAAGGTAGTGTCAAAGG-3'	31627

	M13R	5'-CAGGAAACAGCTATGACCTATGTGAGAATGAAGATGGCAG-3'	31687
	R	5'-GGGAACCTCAGTTTCTATGTGA-3'	31695
5	F	5'-TGCATTTGTGCATCCTCTC-3'	32480
	M13F	5'-ACTGTAAAACGACGGCCAGTAACTGTGGCTGTGCATGTTT-3'	32506
	SF	5'-CTGCGAGTTGCCAGAGTC-3'	32618
	SM13F	5'-ACTGTAAAACGACGGCCAGTCTGCGAGTTGCCAGAGTC-3'	32627
	SM13R	5'-CAGGAAACAGCTATGACCTGGGGGTTTGTAGTTCAG-3'	32768
	SR	5'-AGATCTCTTCCCGCCACT-3'	32793
	M13R	5'-CAGGAAACAGCTATGACCCACCCAGTCTCCATGTCCTA-3'	32899
	R	5'-CCACTTCCAGTTCTTTTCCA-3'	32927
6	F	5'-ATCCTCCCTCTCCTCTCG-3'	34786
	M13F	5'-ACTGTAAAACGACGGCCAGTAACTTCTGGATTATGGGATGG-3'	34810
	SF	5'-CATCGAGGACCAGATCTCC-3'	34906
	SM13F	5'-ACTGTAAAACGACGGCCAGTCCAGATCTCCCTGCTGAAG-3'	34915
	SM13R	5'-CAGGAAACAGCTATGACCACACTCCCAGTTCCAGTCT-3'	35005
	SR	5'-CTTCCAAGCAGTAGGACAGC-3'	35030
	M13R	5'-CAGGAAACAGCTATGACCGCATATCCTGGCGTAGCTC-3'	35121
	R	5'-TCCACCATTCCATCTTCCT-3'	35160
7	F	5'-GATATGCAGGTTCTGGGATG-3'	35115
	M13F	5'-ACTGTAAAACGACGGCCAGTAGGAAGATGGAATGGTGGGA-3'	35142
	SF	5'-TTCTACTGGAGCCCATGCT-3'	35256
	SM13F	5'-ACTGTAAAACGACGGCCAGTCCATGCTGAAATTCCACTACA-3'	35268
	SM13R	5'-CAGGAAACAGCTATGACCTGGGGAGGGCAGATAAG-3'	35377
	SR	5'-CTGGGGAGGGCAGATAAG-3'	35414
	M13R	5'-CAGGAAACAGCTATGACCATGAGGAGCAAGGCCATAG-3'	35446
	R	5'-CAGGAGAAACCAGCGAGAG-3'	35488
8	F	5'-CCTGGTCTTCCTTCACTTCC-3'	35479
	M13F	5'-ACTGTAAAACGACGGCCAGTTTCACTTCCCTGCCTGG-3'	35511
	SF	5'-CATGATCTTGACCCACACC-3'	35611
	SM13F	5'-ACTGTAAAACGACGGCCAGTCTCCCTCCCCTCCAGAC-3'	35629
	SM13R	5'-CAGGAAACAGCTATGACCAGTAATGGCGAATTGCTCCT-3'	35705
	SR	5'-GGACTTCAGAGTAATGGCGA-3'	35714
	M13R	5'-CAGGAAACAGCTATGACCCATGAAGTCTTGGGCAATTT-3'	35792
	R	5'-CTCCAGATGCCACCCTCT-3'	35828

9	F	5'-GTCTCTTGGCTGACCTGAAA-3'	36889
	M13F	5'- ACTGTAAAACGACGGCCAGT ATTATGCTTGTGCAGCCTCA-3'	36889
	SF	5'-GCATGCAGGTTCTTGTTC-3'	36978
	SM13F	5'- ACTGTAAAACGACGGCCAGT AAGATCATGGCTATGCTCACC-3'	36999
	SM13R	5'- CAGGAAACAGCTATGACC GGGGTGTATGTCCTGGATG-3'	37082
	SR	5'-GTAGCAAAGGGGTGTATGTCC-3'	37090
	M13R	5'- CAGGAAACAGCTATGACC CTCAGAGGGCTCTGGGTCT-3'	37185
	R	5'-TGGCAGTGTCCATCTGTCT-3'	37221

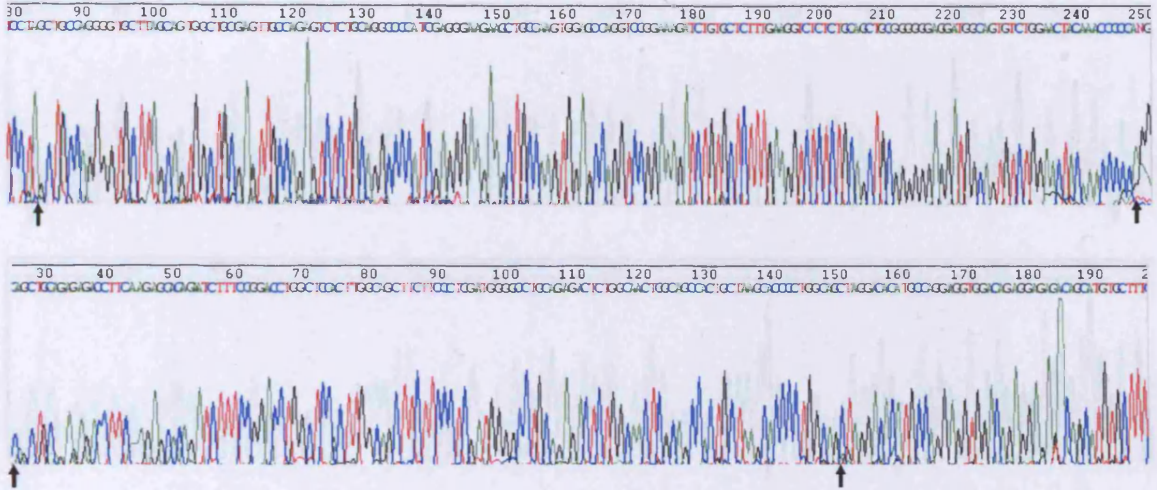
Red text denotes the M13 forward of reverse tag sequence. The position of the 5' nucleotide of the PXR specific primer sequence is stated with reference to a chromosome 13q11 contig sequence (Accession no: NT_005594). The annealing temperature for all is 58°C.

B. RT-PCR Primers.

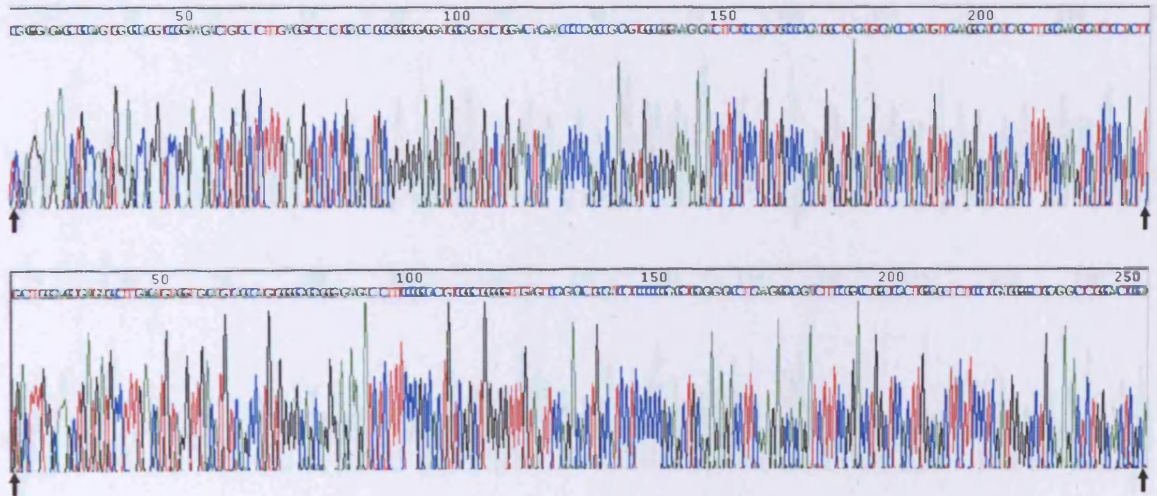
<u>Gene</u>	<u>Reference</u>		<u>Sequence</u>	<u>Position</u>
	<u>(Accession No.)</u>	<u>Primer</u>		<u>(in reference mRNA)</u>
<u>B2M</u>	AB_021288	Forward	5'-TGACAGGATTATTGGAAATTTGT-3'	776-798
		Reverse	5'-CCACAACCATGCCTTACTTT-3'	876-856
<u>PXR</u>	XM_016768.2	Forward	5'-GTGCCTGCCTTGTTTATAGC-3'	4253-4272
		Reverse	5'-GGGCTACATTTCCCAAAACT-3'	4364-4345
<u>CYP3A4</u>	NM_017460.3	Forward	5'-TCAGCCCATCTCCTTTCATA-3'	2644-2663
		Reverse	5'-TGTTTCATTGCATCGAGACAG-3'	2743-2722
<u>MDR1</u>	XM_029059.2	Forward	5'-GACATCATCAAGTGGAGAGAAATC-3'	4339-4362
		Reverse	5'-CAGTTACAGTCCAAATGGGAAA-3'	4463-4442

All RT-PCR primers designed with an annealing temperature of 58°C.

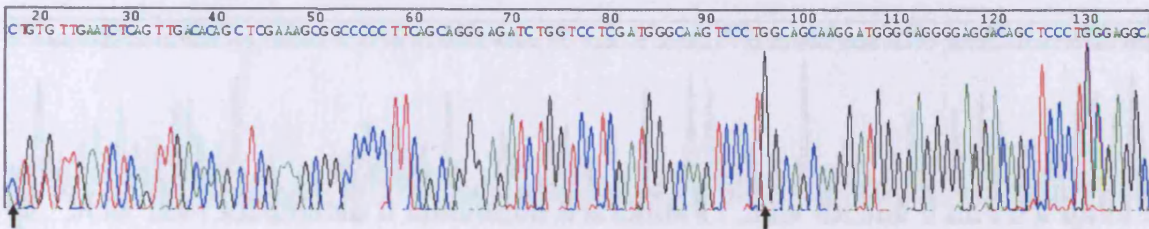
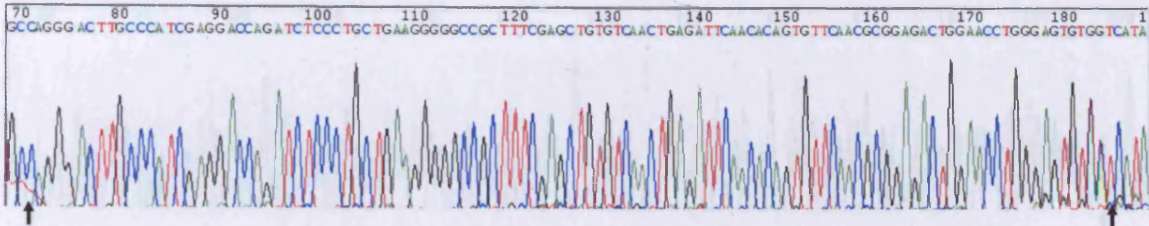
Exon 5: Amplicon A



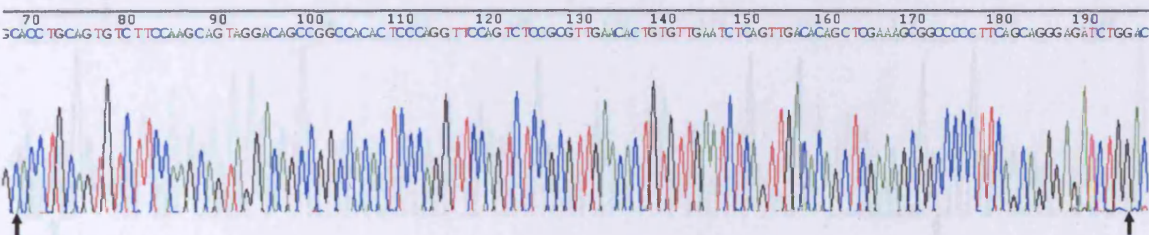
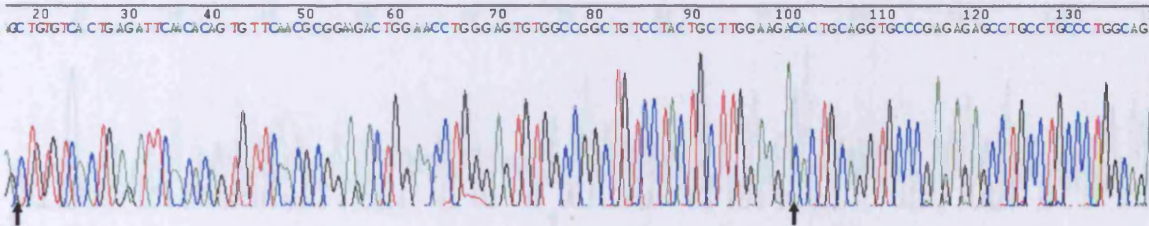
Exon 5: Amplicon B



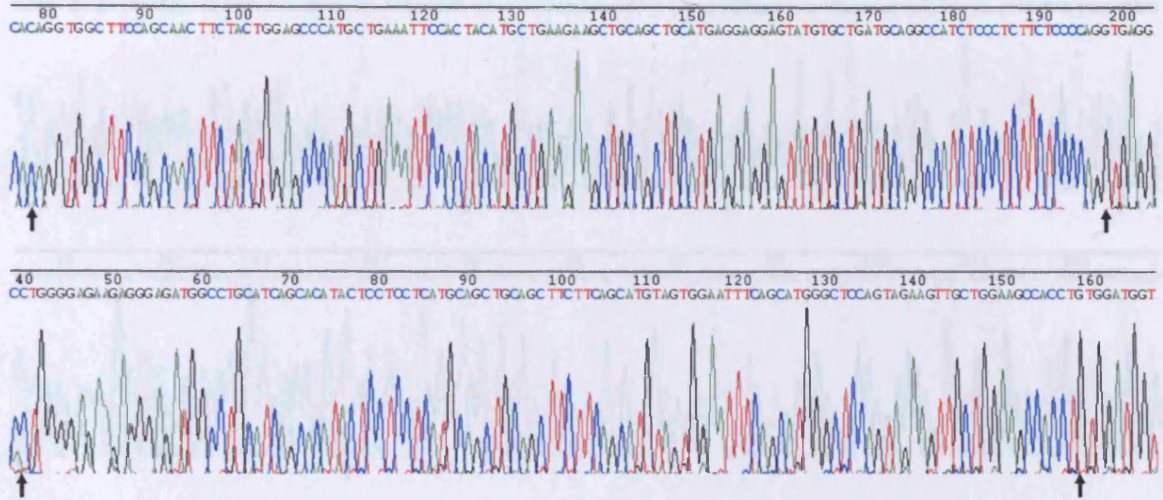
Exon 6: Amplicon A



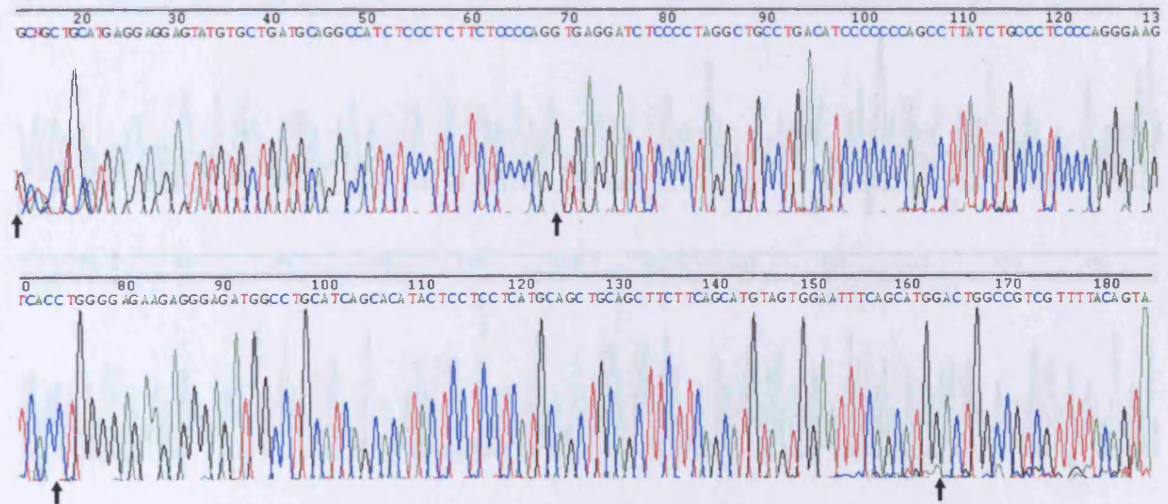
Exon 6: Amplicon B



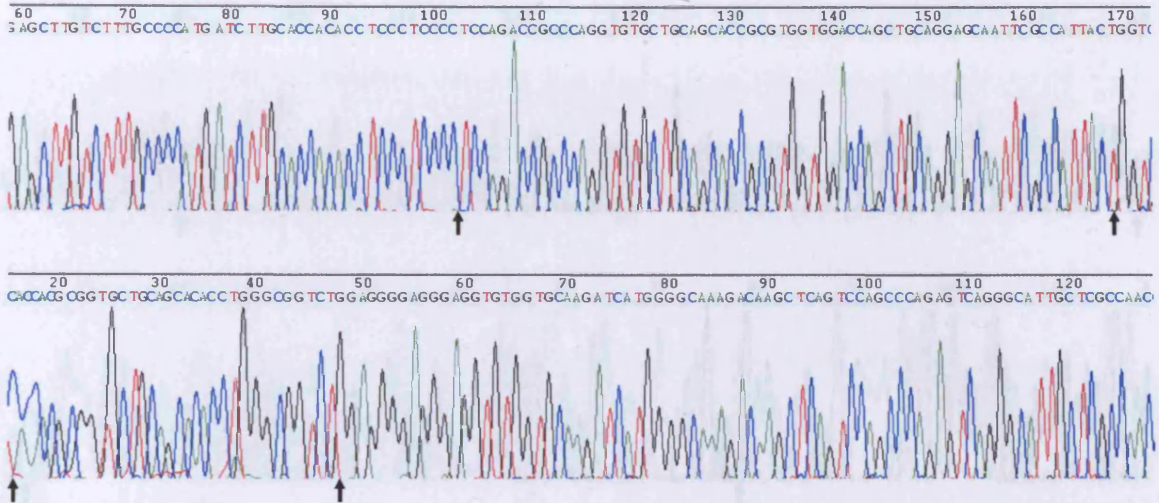
Exon 7: Amplicon A



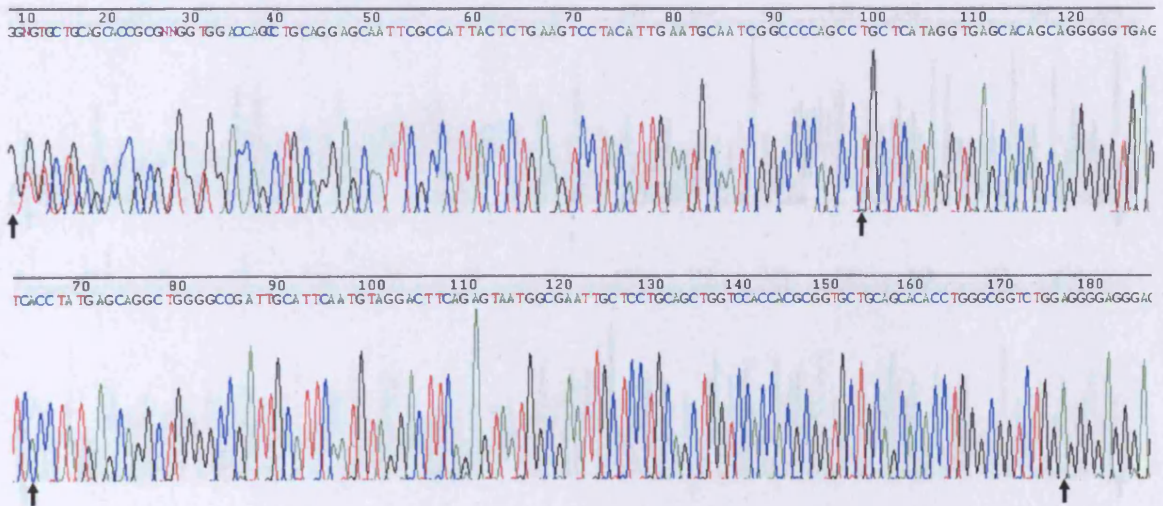
Exon 7: Amplicon B



Exon 8: Amplicon A



Exon 8: Amplicon B



D. Presentation of work.

Work contained within this thesis has been presented at the following forums:

Poster presentation:

- AstraZeneca, Safety Assessment UK Local Science Day. January 2003.
Alderley Park, Cheshire, UK.
- Joint British Toxicology Society/ British Pharmacology Meeting: Adverse Reactions to Drugs and Chemicals: Studies from Molecule to Man.
September 2004. Liverpool, UK.
- Society of Toxicology 44th Annual Meeting. March 2005. New Orleans, USA.

Oral Presentation:

- AstraZeneca, Safety Assessment UK Local Science Day. February 2004.
Alderley Park, Cheshire, UK.

Work is currently ongoing with regard to a manuscript intended for submission to the Journal of Biological Chemistry shortly.